

Die approbierte Originalversion dieser Dissertation ist an der Hauptbibliothek der Technischen Universität Wien aufgestellt (<http://www.ub.tuwien.ac.at>).

The approved original version of this thesis is available at the main library of the Vienna University of Technology (<http://www.ub.tuwien.ac.at/englweb/>).



TECHNISCHE  
UNIVERSITÄT  
WIEN

VIENNA  
UNIVERSITY OF  
TECHNOLOGY

DISSERTATION

**Development and Implementation of Novel Interfaces for  
Miniaturized Analysis Systems  
with Vibrational Spectroscopic Detection**

ausgeführt zum Zwecke der Erlangung des akademischen Grades eines  
Doktors der technischen Wissenschaften

unter der Leitung von

Ao. Univ. Prof. Dr. Bernhard **Lendl**

E164-AC

Institut für Chemische Technologien und Analytik

eingereicht an der Technischen Universität Wien

Fakultät für Technische Naturwissenschaften und Informatik

von

**Dipl. Ing. Michael Haberkorn**

Matr.-Nr. 9325172

Kegelgasse 40/1/15, A-1030 Wien

A handwritten signature in black ink, appearing to read 'Michael Haberkorn', is written over the printed name.

Wien, im Mai 2003

## DEUTSCHE KURZFASSUNG

Ziel dieser Arbeit war die Kombination neuer Techniken mit bereits bestehenden Technologien der Arbeitsgruppe Chemische Analyse und Schwingungsspektroskopie zur Entwicklung von neuartigen Geräten zur Erweiterung der Bandbreite möglicher wissenschaftlicher Anwendungen, Erhöhung des Automationsgrades sowie zur Verbesserung der Leistungsfähigkeit. Die präsentierten Entwicklungen basieren auf den Forschungsschwerpunkten der Arbeitsgruppe, im speziellen Fourier-transform Infrarotspektroskopie, Raman Spektroskopie und automatisierte Fließsysteme. Trotz der zahlreichen Fortschritte welche bereits auf diesen Gebieten erzielt werden konnten, macht es die technologische Weiterentwicklung insbesondere im Bereich der Miniaturisierung von chemischen Analysesystemen (lab-on-a-chip) notwendig neue Funktionseinheiten in die entwickelten Systeme zu implementieren.

Die vorliegende Doktorarbeit beschreibt die Entwicklung und Anwendung zweier Softwarepakete zum computergesteuerten Betrieb der einzelnen Funktionseinheiten der entwickelten Analysesysteme sowie die erstmalige Implementierung von Mikrodispensern, einem automatisierten XY-Tisch, sowie von Quanten-Kaskaden-Laser (QCL) in miniaturisierten chemischen Analysesystemen.

Das Softwarepaket Sagittarius V2 wurde zur Steuerung automatisierter Fließsysteme bestehend aus einer Cavro XP 3000 Spritzenpumpe zusammen mit einem Valco Selektionsventil sowie des Agilent 33120A Signalgenerators als Pulsquelle des unten angeführten Mikrodispensers und eines automatisierten XY-Tisches konzipiert. Das Programm ermöglicht die benutzerdefinierte Erstellung von Ereignissequenzen um eine flexible automatische Gerätesteuerung zu realisieren. Des weiteren besteht die Möglichkeit einer Kommunikation mit der Meßsoftware welche die der Arbeitsgruppe zur Verfügung stehenden IR- und Raman-Spektrometer steuert.

Für Experimente welche die QCL betreffen wurde die Software QCL-Control geschrieben um die Computersteuerung von Laserparametern zur ermöglichen und Meßdaten zu erfassen und darzustellen. Die Anpassung der Einstellungen sowie das Auslesen der Daten erfolgt über das SR245 Computerinterface von Stanford Research Sytems.

Als erste Einheit wurde ein Durchflußmikrodispenser (ein mikrostrukturierter, aus Silizium hergestellter Pikoliter-Tropfengenerator) zur Entwicklung zweier analytischer Interfaces zur Kombination von Fließsystemen mit FT-IR und FT-Raman Spektroskopie implementiert. Die verwendeten Mikrodispenser wurden dazu im Rahmen eines Forschungsaufenthalts am Department of Electrical Measurements an der Lund University in Schweden selbst hergestellt.

Die FT-IR- $\mu$ -Flow-Kopplung zielt auf die Verbesserung der IR-Detektion von Analyten durch Eliminierung der Lösungsmittelinterferenzen in den Messungen ab. Zu diesem Zwecke wurde eine Funktionseinheit basierend auf der schnellen Verdampfung der auf einer infrarottransparenten, festen Oberfläche abgeschiedenen Mikrotropfen entwickelt. Im Falle von wässrigen Lösungen sind aufgrund der kleinen Tropfenvolumina bereits Standardbedingungen (Raumtemperatur und Atmosphärendruck) ausreichend um das Wasser in weniger als 1 Sekunde zu verdampfen. Weiters wird der aufgetragene Analyt im Vergleich zu Spraytechniken auf einer sehr kleinen Fläche konzentriert (üblicherweise 50  $\mu\text{m}$  gegenüber mehr als 300  $\mu\text{m}$ ). Dieser Vorteil führt zu um einen Faktor 100 erhöhten Empfindlichkeit verglichen mit bisher publizierten Forschungsergebnissen. Die praktische Anwendbarkeit der Entwicklung wurde in Verbindung mit einer Hochleistungsflüssigkeitschromatographie-Einheit getestet.

Für die Raman-Kopplung wurde der Mikrodispenser in Kombination mit einem Ultraschall-Levitor verwendet um in levitierten Tröpfchen oberflächenverstärkte Ramanstreuungsexperimente (SERS) durchzuführen. Das levitierte Reaktionsmedium umgeht effizient Probleme wie Memory-Effekte welche von unspezifischer Adsorption an Gefäßwänden resultieren welche große Komplikationen bei der Verwendung von kolloidalen SERS-Substraten darstellen. Für das durchgeführte Experiment wurden die benötigten Reagenzien ( $\text{AgNO}_3$  und Hydroxylamin) mit Hilfe des Mikrodispensers in den Ultraschall-Levitor injiziert um das benötigte SERS-Substrat (Ag-Kolloid) in-situ im levitierten Tropfen herzustellen. Die Funktionsfähigkeit der entwickelten Einheit wurde erfolgreich überprüft und erlaubte Nachweisgrenzen bis in den Femtogrammbereich für den Testanalyten 9-Aminoacridin erzielt.

Als zweiter Ansatz wurde zur Verbesserung der IR spektroskopischen Detektion von wässrigen Proben eine neuartige, alternative Lichtquelle integriert. Durch Einbindung von Quanten-Kaskaden-Lasern (QCL) mit ihrer hohen Emissionleistung (einige zehn mW) in

einem schmalen spektralen Bereich (wenige  $\text{cm}^{-1}$ ) wurde ein Aufbau zur Realisierung von Laserdetektion im mittleren Infrarot entwickelt und getestet.

Bei Verwendung eines FT-IR-Spektrometers muß die optische Weglänge bei Transmissionsmessungen auf wenige  $\mu\text{m}$  (typisch  $< 10 @ 1650 \text{ cm}^{-1}$ ,  $< 50 @ 1080 \text{ cm}^{-1}$ ) reduziert werden. Mit der entwickelten Anordnung unter Verwendung von QCLs konnten mit einer faseroptischen Durchflußzelle deutlich erhöhte Weglängen realisiert werden. Eine quantitative Bestimmung von Xanthosin und Adenin bei den Laserwellenlängen 1080 und  $1650 \text{ cm}^{-1}$  und optischen Weglängen von 150 und 59  $\mu\text{m}$  konnte erfolgreich gezeigt werden.

## ABSTRACT

The aim of this work was to combine novel devices with technology readily available in the workgroup for Chemical Analysis and Vibrational Spectroscopy to form new instrumentation extending the possible range of scientific applications, enhancing the degree of automation and improving system performance. The presented developments are based on the key topics of the workgroup, namely Fourier transform infrared (FT-IR) spectroscopy, Raman spectroscopy and automated flow systems. Despite the numerous successful cutting edge advances already achieved in these fields, progress in technology, especially in the area of miniaturized chemical analysis systems (lab-on-a-chip), drives the need to implement new units in the novel systems.

The presented thesis describes the development and application of two software packages for computer controlled operation of the devices of the newly developed analysis systems as well as the first time implementation of microdispensers, an automated xy-stage and quantum cascade lasers (QCLs) in miniaturized chemical analysis systems.

The software package Sagittarius V2 was designed to operate automated flow systems consisting of a Cavo XP 3000 syringe pump together with a Valco selection valve as well as the Agilent 33120A waveform generator used to drive the microdispenser described below and an automated xy-stage. The program offers the possibility to generate custom device event sequences to allow flexible automated instrument operation. Furthermore it is capable to communicate with the measurement software used to control the IR and Raman spectrometers available in the workgroup.

For experiments concerning quantum cascade lasers (see below) QCL-Control was developed to allow computer control of possible laser parameters and to acquire and display the collected data. The adjustment of settings as well as data readout is achieved via the SR245 computer interface from Stanford Research Systems.

The first device that was implemented is a flow-through microdispenser, a silicon microstructured picoliter droplet generator which led to the development of two analytical interfaces for flow systems in combination with FT-IR and FT-Raman spectroscopy. The dispensers used for the experiments were fabricated during a research stay at the Department of Electrical Measurements at Lund University in Sweden.

The FT-IR-u-flow interface focuses on the improvement of IR detection of analytes by elimination of solvent interferences in the measurement. The developed setup is based on the fast solvent evaporation of the microdroplets deposited on a solid, IR transparent support. For aqueous solutions, already standard conditions (room temperature and atmospheric pressure) allow water evaporation within below one second as a result of the picoliter drop volume. Furthermore, the deposited analyte is concentrated in a relatively small area (around 50  $\mu\text{m}$ ) compared to spraying techniques commonly used for solvent evaporation approaches (above 300  $\mu\text{m}$ ). This advantage reflects in increased sensitivity for measurements with this interface as result of minimized surface spreading of the sample, providing access to picogram amounts of substance. This represents an increase in sensitivity by a factor of 100 compared to previously published research results. The practical applicability of the development was tested coupling the interface to a high performance liquid Chromatographie system.

In the case of the Raman interface, the flow-through microdispenser was combined with an ultrasonic levitator to conduct surface enhanced Raman scattering (SERS) measurements in levitated microdrops. The levitated reaction vessel avoids problems such as memory effects resulting from unspecific adsorption on container walls, which is of crucial significance when working with colloidal SERS substrates. For the conducted experiments the microdispenser was used to inject the reagents ( $\text{AgNO}_3$  and hydroxylamine) into the levitator to prepare the needed SERS substrate (Ag colloid) in-situ in the levitated droplet. The new concept was verified to successfully generate the SERS substrate and subsequently gave access to detection limits down to femtogram amounts of the tested analyte 9-aminoacridine.

As a second approach, improvement of IR spectroscopic detection of aqueous samples was focused on by implementing a novel alternative light source. Applying quantum cascade lasers (QCLs) with their high emission intensity (tens of mWs) in a narrow spectral range (a few  $\text{cm}^{-1}$ ), a setup for laser detection in the mid-IR range was designed and tested.

Using FT-IR spectrometers, the optical pathlength for transmission measurements is limited to a few  $\mu\text{m}$  (typically  $< 10$  @  $1650 \text{ cm}^{-1}$ ,  $< 50$  @  $1080 \text{ cm}^{-1}$ ). With the novel setup consisting of QCLs and a fibre optic flow-through cell significantly larger pathlengths could be realized. The quantitative determination of xanthosine and adenine at laser wavelengths of 1080 and  $1650 \text{ cm}^{-1}$  and optical pathlengths of 150 and 59  $\mu\text{m}$  could be demonstrated.

## ACKNOWLEDGEMENT

I want thank my supervisor *Bernhard Lendl*, especially after four years of working together, for his support and understanding concerning issues not necessarily related to work. Thank you also for the offer of most interesting topics and your encouragement when downtimes and hold-ups were testing my patience.

A major part of my gratitude also goes to my colleagues from the former and recent team of Chemical Analysis and Vibrational Spectroscopy. Especially *Andrea Edelmann*, *Peter Hinsmann* and *Josef Diewok* have to be mentioned here as they have been friends, colleagues and helping hands throughout the whole time of my thesis. Nevertheless, what would this group be without *Josefa Rodríguez Baena*, *Gunta Mazarevica*, *Barbara Muik*, *Maria Jose Ayora Canada*, *Malin Kölhed*, *Almudena Columé Díaz*, *Silvia Ortega Algar*, *Nicolae Leopold* and the recently joined members *Nina Kaun*, *Stephan Kulka*, *Stefan Schaden* and *Johannes Schnöller*? And what would be feasible without the magic hands of *Johannes Frank* having the right focus or *Markus Schaufler*'s electrifying touch to move the electrons in the right direction? Thank you all!!

I am very grateful for the co-operation with the Department of Electrical Measurements at Lund University, namely *Thomas Laurell*, *Johan Nilsson* and *Lars Wallman* who ambitiously supported me during my research stay in Sweden. Furthermore, I would like to acknowledge *Bo Karlberg* from the University of Stockholm for the joint efforts on behalf of quantum cascade laser set-up development.

Financial support for this work provided by the Austrian Science Fund (FWF) within the project P13686 ÖCH is gratefully acknowledged.

Never to be forgotten, my friends outside university without whom my life would be less than half the fun it is. Sorry, for not listing you all, but thanking you all would really fill this thesis and still there would be more to say! Thank you for your company and care!

Just a special one for *Ali Teker*. I'll tell you thanks in Charlie P's!!

*Eva*, I guess there is nothing that would actually express my gratefulness for knowing you: This thesis is dedicated to you! Thank you for being there, for sharing your existence with me!

Finally I want to thank my parents for their patience, their caring and loving support during all the years of my life.

## TABLE OF CONTENTS

Deutsche Kurzfassung	II
Abstract	V
Acknowledgement	VII
Table of Contents	VIII
List of Publications	X
List of Abbreviations	XI
<b>1. INTRODUCTION</b>	<b>1</b>
1.1. Automated Flow Systems	1
1.2. Fourier Transform Infrared Spectroscopy	2
1.3. Raman Spectroscopy	5
1.4. Basis of the Presented Work	7
<b>2. NEW CONCEPTS AND STRATEGIES</b>	<b>8</b>
2.1. Solvent Elimination using Flow-Through Microdispenser	8
2.2. Surface Enhanced Raman Spectroscopy in Levitated Drops	8
2.3. Laser Detection using Quantum Cascade Lasers	9
<b>3. SOFTWARE</b>	<b>11</b>
3.1. Sagittarius V2	11
3.1.1. Startup window	11
3.1.2. Setup dialog	12
3.1.3. Main screen — Manual Control window	15
3.1.4. SLA Run window	19
3.1.5. Automated Run Control window	22
3.1.6. Run Files and Log-Files	23
3.1.7. List of Commands	24
3.1.8. Fields of Application	27

3.2. QCL-Control	27
3.2.1. Setup dialog	28
3.2.2. Main window	29
3.2.3. Readout Chart window	32
3.2.4. Rapid Sampling dialog	33
3.2.5. Time Resolved Measurement dialog	34
3.2.6. File format	34
3.2.7. Fields of Application	35
<b>4. FLOW-THROUGH MICRODISPENSER</b>	<b>37</b>
4.1. Principle of Operation	37
4.2. Fabrication	38
4.3. Instrumental Setup	40
4.4. Solvent Elimination Interface for FT-IR Spectroscopy	41
4.5. Airborne Surface Enhanced Raman Spectroscopy	44
4.6. Conclusion and Outlook	46
<b>5. QUANTUM CASCADE LASERS</b>	<b>48</b>
5.1. Principle of Operation	48
5.2. Instrumental Setup	49
5.3. Measurement of Aqueous Samples	50
5.4. Conclusion and Outlook	51
<b>6. REFERENCES</b>	<b>53</b>
<b>7. APPENDIX</b>	
Publication I	57
Publication II	65
Publication III	72
Curriculum Vitae	80

## LIST OF PUBLICATIONS

- I Haberkorn, M.; Frank, J.; Harasek, M.; Nilsson, J.; Laurell, T.; Lendl, B.  
*"Flow-Through Picoliter Dispenser: A New Approach for Solvent Elimination in FT-IR Spectroscopy"*  
Appl. Spectrosc. **2002**, 56, 902-908
- II Leopold, N.; Haberkorn, M.; Laurell, T.; Nilsson, J.; Baena, J.R.; Frank, J.; Lendl, B.  
*"On-Line Monitoring of Airborne Chemistry in Levitated Nanodroplets: In Situ Synthesis and Application of SERS-Active Ag-Sols for Trace Analysis by FT-Raman Spectroscopy"*  
Anal. Chem. **2003**, 75, 2166-2171
- III Kölhed, M.; Haberkorn, M.; Pustogov, V.; Mizaikoff, B.; Frank, J.; Karlberg, B.; Lendl, B.  
*"Assessment of Quantum Cascade Lasers as Mid Infrared Light Sources for Measurement of Aqueous Samples"*  
Vib. Spectrosc. **2002**, 29, 283-289

## LIST OF ABBREVIATIONS

<b>AAS</b>	atomic absorption spectroscopy
<b>DC</b>	direct current
<b>DDE</b>	dynamic data exchange
<b>FI</b>	flow injection
<b>FIA</b>	flow injection analysis
<b>FT-IR</b>	Fourier transform infrared
<b>FT-Raman</b>	Fourier transform Raman
<b>HPLC</b>	high performance liquid chromatography
<b>I/O</b>	input/output
<b>ICP</b>	inductive coupled plasma
<b>IR</b>	infrared
<b>LC</b>	liquid chromatography
<b>MBE</b>	molecular beam epitaxy
<b>MCT</b>	mercury cadmium telluride
<b>Nd:YAG</b>	Neodymium (3+)-doped Yttrium Aluminium Garnet
<b>PDA</b>	phase Doppler anemometry
<b>QCL</b>	quantum cascade laser
<b>RHEED</b>	reflected high energy electron diffraction
<b>SERS</b>	surface enhanced Raman scattering
<b>SI</b>	sequential injection
<b>SIA</b>	sequential injection analysis
<b>TTL</b>	transistor-transistor logic
<b>UV-Vis</b>	ultraviolet-visible

## 1. INTRODUCTION [1]

### 1.1. Automated Flow Systems

Applying automated analysis systems in chemical analysis helps to minimize solvent and reagent consumption, decrease sample analysis time, increase sample throughput and to minimize the possibility of human errors. Furthermore, these systems generally offer an increased level of reproducibility and precision. That way automation can significantly improve the efficiency of a process.

Flow injection analysis (FIA) [2-5] systems basically consist of a peristaltic pump providing a carrier flow, an injection valve through which the sample is injected into the stream and a detection unit (Figure 1a). While the sample is transported from the place of injection to the detector, it might be passed through different reactors and/or mixed with reagents, allowing modifications of the sample in a way to be able to retrieve the desired information with the coupled detection technique. That way FIA systems already provide numerous possibilities for automated sample analysis.

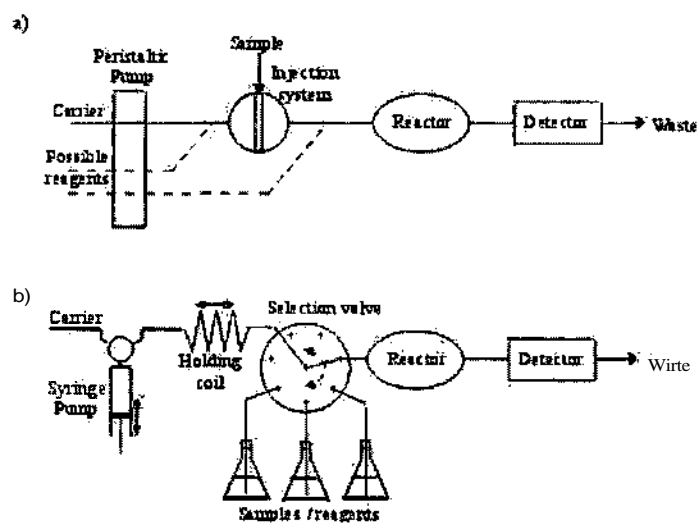


Figure 1: a) Scheme of an FIA system; b) Scheme of an SIA set-up

Sequential injection analysis (SIA) [5,6] systems represent the next level of system automation. Whereas in FIA systems a certain amount of sample defined by the size of the

injection loop is injected into a continuously flowing carrier stream, in SLA a syringe pump in combination with a selection valve is used (Figure 1b). The syringe pump can aspire any desired amount of solution at the selection valve by simple changing the size of the stroke of the syringe highly increasing the flexibility of the setup. As they are being taken up, the aspired solutions are sequentially stacked in the holding coil (a long piece of tubing), before being moved to the reactor unit and/or detector by flow reversal.

As a detector a lot of instruments can be used in combination with FLA and SLA systems, such as an FT-IR or UV-Vis spectrometer, conductivity detectors, LCP, AAS and many others.

Of course, such an automated setup finally requires co-ordination and synchronisation of its components by a computer equipped with dedicated software. This allows full exploitation of an automated system's capability to operate with high precision (especially in respect to processes where timing is crucial, e.g. out of equilibrium measurements of chemical reactions), reproducibility and a minimum of risk of human error.

## 1.2. Fourier Transform Infrared Spectroscopy [7,8]

Infrared (IR) spectroscopy is based on the excitation of vibrational states of molecules by absorbance of radiation in the infrared spectral region, especially the mid-infrared range (wavelength: 2.5 - 25  $\mu\text{m}$ , wavenumbers: 4000 - 400  $\text{cm}^{-1}$ ). Using IR radiation to stimulate a vibrational mode, the transition from one vibrational state to the other has to fulfil the requirement that the vibration causes the molecules dipole momentum to change. Otherwise, the vibrational mode will not be visible in the IR spectrum of the substance. Also IR emission spectra of heated samples can be obtained, but the absorbance technique is the most common.

The vibrational spectrum of a compound is considered a unique physical property comparable to a fingerprint. Therefore, this analytical method presents a powerful tool for substance identification by comparison with reference spectra of known compounds and to provide information on latent variables, such as octane number or secondary structure of proteins, by multivariate data analysis. Furthermore, this detection method allows to draw conclusions about the structure of unknown species by evaluation of presence and/or absence of IR bands in their spectrum. However, not only qualitative information can be

retrieved from IR spectroscopic measurements as the intensities of the absorbance peaks finally allow quantification of analyte concentrations applying Lambert-Bouguer-Beer's law:

$$A = \varepsilon \cdot c \cdot d$$

A ... Absorbance

$\varepsilon$  ... substance-specific molar absorptivity [ $\text{l mol}^{-1} \text{cm}^{-1}$ ]

c ... sample concentration [ $\text{mol/l}$ ]

d ... optical pathlength of the cell [cm]

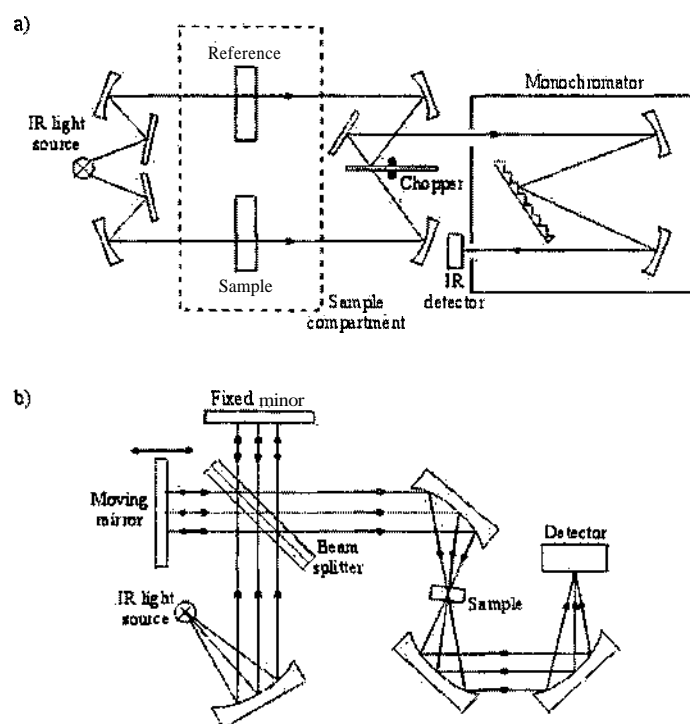


Figure 2: a) Dispersive IR instrument; b) FT-IR instrument

To obtain the wavelength dependent absorbance characteristics of a sample, the continuous IR radiation from the light source (globar) two different instrumental setups are generally used. Dispersive instruments are equipped with monochromators in order to select radiation of a certain wavelength to reach the detector (Figure 2a). By scanning the desired spectral range the final IR spectra is gained. A faster and generally more effective technique is the Fourier transform IR spectroscopy (Figure 2b). The radiation emitted from the light source is directed to a partially reflecting and partially transmitting beamsplitter so that one part shines onto a fixed and the other part onto a moving mirror. From these mirrors the IR

beams reflect back to the beamsplitter where they finally reunite and cause interference on the way to the detector. As the moving mirror alters the optical path difference between the two light beams in the interferometer, the photons at different wavelengths show different degrees of interference depending on mirror displacement. The resulting signal at the detector represents an interference showing intensities versus mirror position (*interferogram*). By calculation of the Fourier transform from the *interferogram*, the final IR spectrum is gained that displays light intensities for the different wavelengths.

Compared to dispersive instruments, Fourier-transform spectrometers have three major advantages:

- Multiplex-Advantage (*Fellgett-advantage*):

FT spectrometer provide higher sensitivity and shorter measurement time due to the simultaneous detection of all spectral frequencies.

- Throughput-Advantage (*Jacquinot-advantage*):

As FT instruments are constructed without any slits (apart from the aperture right after the source of radiation), the intensity reaching the detector is significantly higher than in the case of dispersive spectrometers which require slits to limit the detected wavenumber range in order to achieve the desired spectral resolution

- Calibration-Advantage (*Connes-advantage*):

In contrast to dispersive instruments where a reference material is required to calibrate the frequencies, FT spectrometers do not need to be calibrated in this respect. As the retardation of the mirror is determined with the help of a helium-neon reference laser with an exactly known constant wavelength of 0.632991  $\mu\text{m}$ , the He-Ne-laser acts as an internal standard enabling the determination of all frequencies with a possible spectral resolution below 0.1  $\text{cm}^{-1}$ .

The multiplex- and throughput-advantage of FTIR spectrometers results in an improved signal to noise ratio which is about 100 times better than for dispersive instruments.

It is needless to stress the benefits of this fast technique for direct, non-destructive analyte identification and quantification, but there is a major drawback that set limitations to its applicability. As most compounds are capable of exhibiting vibrations altering the dipole momentum, also most solvents are among them, especially water as non toxic and cheap solvent. This again results in the fact that regions where the used solvent show IR features are not readily accessible for analyte characterisation as the solvent will completely absorbs any radiation in that part of the spectrum. To avoid this effect only very short optical paths

for the sample cell are possible, allowing some fraction of light to pass the cell and that way gain information in that spectral region. In the case of water, with its bending vibration absorbing at  $1640\text{ cm}^{-1}$  and the stretching vibration covering the range from  $3650 - 2930\text{ cm}^{-1}$ , optical pathlengths below  $10\text{ }\mu\text{m}$  are required. This issue is a crucial consideration especially when combining IR spectroscopy with automated flow systems.

### 1.3. Raman Spectroscopy [9]

Raman spectroscopy similar to the IR technique gives information about vibrational characteristics of a molecule. However, the information content of the Raman spectra is limited to vibrations changing the molecule's polarizability. IR and Raman spectra give complimentary information, as IR active vibrations are Raman inactive and vice versa.

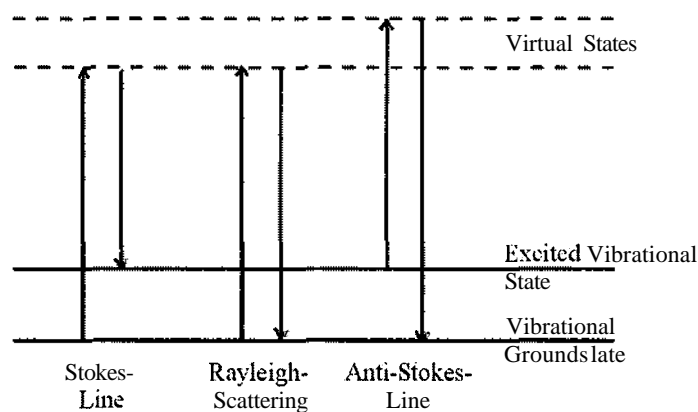


Figure 3: Scheme of Raman scattering processes

Raman spectroscopy is a scattering technique where the sample is irradiated with monochromatic radiation at wavelengths shorter than the mid-IR (e.g. in the visible or near IR region) and the scattered light is collected and analysed. The majority of the scattered light results from an elastic scattering process and has the same wavelength as the exciting radiation (Rayleigh line) containing no useful information about the sample. Only  $10^{-10}$  parts of the incident light are inelastically scattered and show a shifted wavelength as a consequence of excitation or extinction of vibrations of the analyte. The monochromatic radiation excites the analyte from its original vibrational state to virtual level from which it drops back emitting radiation. In the case that the molecule returns to a higher vibrational level than before the interaction, the scattered light has less energy and is therefore shifted to

longer wavelengths as compared to the Rayleigh line (Stokes shift). If the molecule returns to a lower vibrational level during the scattering process the light will gain energy and is shifted to shorter wavelengths (Anti-Stokes shift) (Figure 3). The size of the shift represents the energy difference caused by the excitation or extinction of a vibration and hence, contain the structural information about the analyte. Similar to IR measurements, the intensities of the features in the Raman spectra allow quantitative analysis of samples.

Again, in order to get a spectrum from the scattered light, either dispersive or Fourier transform Raman spectrometers are used. The dispersive instrument are generally more common as most Raman instruments apply radiation in the visible range to benefit from the larger Raman effect and the more sensitive detector available in this spectral range. However, Raman excitation with light in the visible also results in intense emission of fluorescent radiation from the sample which again deteriorates the Raman signal. To avoid this effect, less intense light in the near IR (e.g. Nd:YAG laser @ 1.06  $\mu\text{m}$ ) is used for measurement in combination with FT units to exploit its throughput and multiplex advantage to compensate for the lower yield of Raman signal and the less efficient near IR detectors.

Thinking of the combination of aqueous flow systems, Raman spectroscopy, compared to IR analysis, has the advantage that water shows very weak response and therefore does not mask possible features from the analyte under investigation.

#### *Surface Enhanced Raman Scattering*

A major problem that has to be faced with Raman detection is the fact that the regular Raman signal is very weak. To overcome this drawback, surface enhanced Raman scattering (SERS) [10,11] is a possible approach to achieve highly sensitive, molecular specific detection.

For these measurements the analyte is brought in contact with a rough metal surface (mostly silver, gold or copper) and is then being excited by a laser with an appropriate wavelength to excite the surface plasmon resonance to yield Raman lines enhanced by a factor of around  $10^6$ . The mechanism is mainly considered to be the result of an increased electrical field strength at the surface of the metal which decays rapidly with increasing distance from the metal particle [12,13]. That way only the first molecular layers of the analyte adsorbed on the metal surface provide the described signal enhancement.

## 1.4. Basis for the Presented Work

Exploiting the available instrumentation and technology introduced above, a variety of highly sophisticated automated analysis systems have been developed within the workgroup of Chemical Analysis and Vibrational Spectroscopy. The research on FIA-FT-IR and FIA-FT-Raman setups covered a wide range of analytical applications, from basic major compound analysis in complex matrices [14] across wine analysis [15,16] to flow analysis with SERS detection [17]. As can be seen, the development of different instrumental arrangements consisting of a limited set of components can already lead to numerous solutions for various scientific fields.

However, in order to meet the industry's and science's increasing demands on analytical instrumentation, also the setup components as well as the flexibility in combining them to form an effective and *satisfyingly* functional unit have become one of the key issues in the workgroup's ongoing research. The introduction of new components as well as the employment of novel interfaces is now the promising approach to overcome encountered limitations in detection power and to further extend the range of applicability.

## 2. NEW CONCEPTS AND STRATEGIES

### 2.1. Solvent Elimination using Flow-Through Microdispenser

As already mentioned before, IR spectroscopy of solutions is strongly limited by the absorbance features of the solvent itself. Therefore a lot of research is focusing on the promising approach of eliminating the intense background prior to measurement. So far, different kinds of *thermospray* [18], *particle beam* [19-23], *electrospray* [24], *pneumatic nebulizer* [25-28] and *ultrasonic nebulizer* [29,30] interfaces have been used to evaporate the solvent and minimise its effect on the analyte signal. However, most of the so far published approaches still do not allow full exploitation of the detection power of IR spectroscopy as they lack the crucial ability to *satisfyingly* concentrate the analyte into the cross section of the focused probing IR beam. Modern IR microscopes generally focus on spots with diameters as small as 100  $\mu\text{m}$  whereas the majority of solvent elimination procedures will not provide analyte deposits with diameters smaller than 300  $\mu\text{m}$  resulting in almost 90% of the analyte to be excluded from analysis. Moreover, considering *Lambert-Bouguer-Beer's law* (see chapter 1.2), it is more effective to concentrate a specific amount of sample in a small area to be probed rather than spreading the same amount on a larger surface using a larger sized IR beam, as the thickness of the sample (and hence the optical *pathlength*) will increase with decrease surface spreading.

A novel flow-through *microdispenser* developed by T. Laurell et al. [31] has already proven high precision and accuracy in dispensing small, defined droplets in the *picoliter* range on a drop on demand bases. This was already demonstrated in various publications on interface flow systems to MS detection devices and hence, presents a promising approach for the development of a possible new IR solvent elimination interface.

### 2.2. Surface Enhanced Raman Spectroscopy in Levitated Drops

Nowadays, there exists an increasing demand for miniaturised analysis systems due to technological advantages, such as integration of multiple process steps in chips (*lab-on-a-chip*) for enhanced mobility and efficiency, as well as for economical and ecological reasons, such as less reagent consumption and decreasing the volume of waste products.

However, also some problems have to be faced when downsizing processes which are of growing concern with decreasing scale.

The most obvious problem associated with this issue is the sensitivity of the detection method as the amount of analyte available for the measurement is significantly reduced. Surface enhanced Raman spectroscopy with its highly sensitive detection characteristics is therefore a predestined vibrational spectroscopic method for implementation in such systems.

Another problem which may be of minor importance in large scale analytical instrumentation is the non-specific analyte adsorption at container walls and tubings. However, modern trends in analytical chemistry towards miniaturised analysis systems require special awareness of this problem as the decreasing amount of analyte in combination with the growingly unfavourable ratio of surface to volume upon downsizing of instrumental components severely contribute to the dimension of the possible error of measurement. As a result the decreasing amount of sample to be investigated is increasingly altered as downscaling progresses. To tackle this effect it is necessary to reduce the contact with container walls to a minimum which can be achieved by using a levitator [32,33] to keep the reaction media levitated in the air.

To finally be able to inject the sample or possible reagents into the levitator, the flow-through microdispenser can be used which further solves the problem of reliable handling of minute amounts of samples, another concern related to miniaturised systems.

### 2.3. Laser Detection using Quantum Cascade Lasers

Solvent elimination is but one strategy to deal with the limited sensitivity of IR spectroscopy of analytes in solutions. Another approach takes advantage of quantum cascade lasers (QCLs) as new highly intensive mid-IR light sources [34-36]. As the QCLs emit IR radiation at the specific wavelength they are designed for with high power, this technology enables to determine the presence or absence of a certain IR absorption band at a level of sensitivity unmatched by conventional instrumentation using continuous light sources. The strong intensity of the emitted radiation allows longer optical pathlengths through the sample solution without facing total absorption and therefore lowers the detection limit. Moreover, the small spectral bandwidth of the generated IR beam eliminates the effect of saturation of the wavelength unspecific detectors by radiation from spectral regions of no interest, providing further improvement on the method's sensitivity.

Whereas solvent elimination focuses on the cause of the problem itself by implementation of novel IR interfaces with the requirement of process adaptation to meet the interfaces operation characteristics, the QCL concept concentrates on reducing the effect by replacing the common light source without significant changes in the design and operation of the sampling procedure. That way, already existing standard IR transmission cells can be used in the way they have already proven their simplicity in use and application.

## 3. SOFTWARE

### 3.1. Sagittarius V2

Sagittarius V2 is capable of controlling a basic of SIA system consisting of a Cavro XP 3000 syringe pump (Cavro, Sunnyvale, CA, USA) and a Valco selection valve (Valco, Houston, TX, USA) together with an Agilent 33120 A waveform generator (Agilent Technologies, Palo Alto, CA, USA) responsible for the operation of the microdispenser. Furthermore, it supports an xy-stage with an in-house built stepper motor controller that is needed for experimental setups aiming at the automated deposition of analytes onto any kind of support. The software was programmed in Microsoft Visual Basic 6.0 with the aim of an optimum in flexibility necessary to allow the user to run different instrumental configurations and manipulate the sequence and timing of events without detailed knowledge in software programming itself.

#### 3.1.1. Startup Window

The Sagittarius V2 *Startup* window provides the possibility to activate and/or deactivate devices in respect to their presence in the experimental setup (Figure 4). Quite commonly a certain configuration of instrument is used for the performance assessment of a system, however depending on state of the step by step development might be removed or reintroduced and can therefore be changed in their state of availability at the initialisation of the program. To confirm the configuration the *Settings Correct* button initialises the active devices and brings on the main screen (see below). In the case that more detailed setup adjustments need to be made the program has to be continued with the *Advanced Settings ...* button as described in the following.

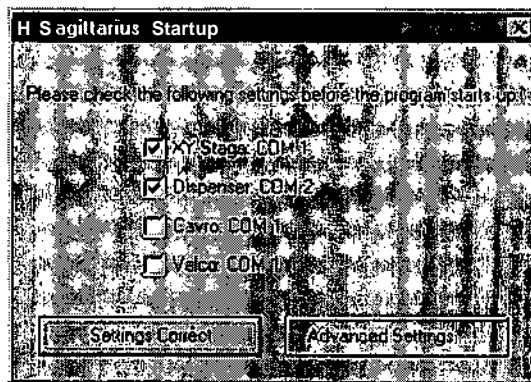


Figure 4: *Sagittarius V2 - Startup window*

### 3.1.2. Setup Dialog

A more advanced configuration of the components of the equipment in use is possible through the program's setup dialog. This option is accessible via the *Advanced Settings ...* button in the *Startup* window as well as by selecting *Setup* in the *Options* menu of *Sagittarius*' main screen after initialisation. Apart from their state of availability (*Device Active* check box) and the serial communication port they are connected to (*COM-Port* entry field), all instruments can be configured here in detail. In the following, short explanations from the presented software's point of view are given to the editable parameters, however for more details generally the instruments' manuals will need to be contacted. Attention has to be paid not to enter incorrect values as they might result in malfunction of the device concerned.

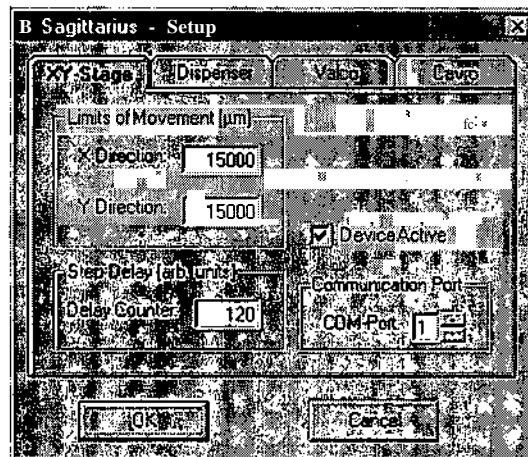


Figure 5: *Sagittarius V2 - XY-Stage Setup*

*XY-Stage:* (Figure 5)

*Limits of Movement:* These entry fields allow to specify the maximum movement of the stage in the two dimensions. As the in-house built controller has no possibility of detecting the end of the *xy-stage*, it is necessary to enter these values to protect the stage and motors from damage when exceeding the stages limits.

*Step Delay:* The value stated here relates to the speed of the stage's movement. The controller is only capable of moving a stepper motor by one step (2.5 urn in the case of the used *xy-stage*) for every command it receives from the computer. That way the speed at which the stage is displaced is defined by the speed of commands repeatedly received by the controller. In order to allow adjustment of the frequency of the stepper motors' steps, the step delay was implemented. Between every single step of the stage commanded by the software, the computer will count up to this stated value, resulting in faster stage movement at lower delay values. However, this is correlated with the power of the computer and the necessary step delay for a desired speed of movement needs to be determined every time the software and the stage are to be applied to a different PC. For a Pentium II 400 MHz processor the step delay will be around 850 for an *xy-stage* speed of around 350  $\mu\text{m}/\text{sec}$ .

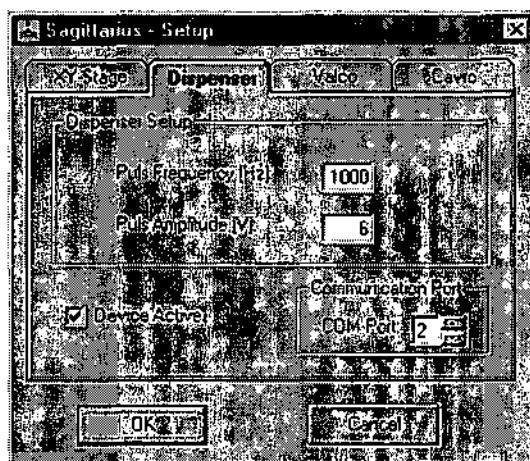


Figure 6: Sagittarius V2 - Dispenser Setup

*Dispenser* (Figure 6)

*Pulse Frequency:* This parameter defines the duration of the pulse used to drive the piezo element of the *microdispenser*. The resulting signal will keep the dispenser's membrane in the displaced position for half the time of the duration of a single period at the stated frequency. Generally, the entered value will generate a square wavefunction with 50% positive amplitude which displaces the piezo generating a droplet. However, during tests it

was found that the duration of the membrane displacement is not crucial for the droplet formation and can therefore remain at 1 kHz.

*Pulse Amplitude:* The pulse amplitude represents the amplitude of the rectangular wave passed on to the piezo driving electronics, which will modify the rising edge of the final pulse operating the piezo element. The higher this value, the shorter the rise time of the signal driving the piezo and hence, the faster the displacement of the membrane ejecting the droplets.

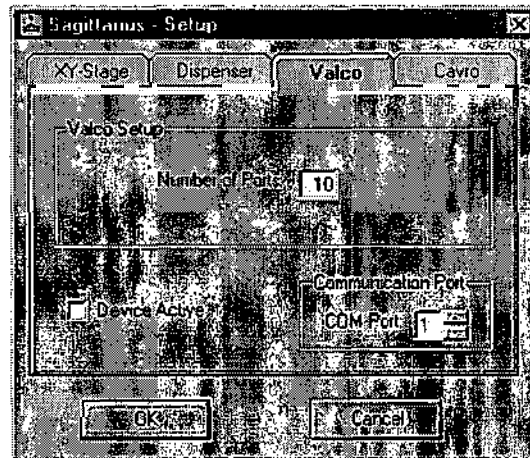


Figure 7: *Sagittarius V2- Valco Setup*

*Valco:* (Figure 7)

*Number of Ports:* Here the number of ports of the setup's selection valve have to be specified. This is necessary as the valve's electronics can not determine this parameter automatically, however are depending on this value to calculate the angular difference between each port and that way address each port accurately by the its degree of rotation.

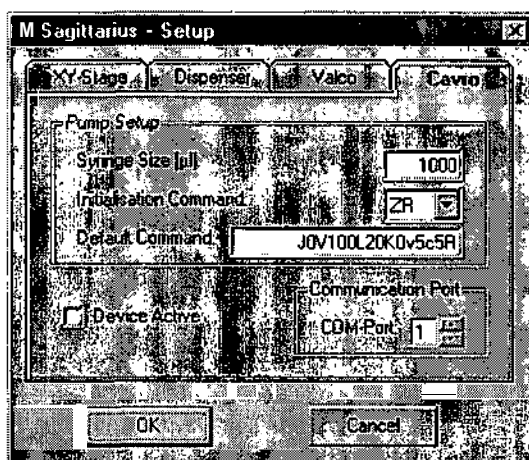


Figure 8: *Sagittarius V2 - Cavro Setup*

*Cavro*: (Figure 8)

*Syringe Size*: This entry has to be made in order to adapt the software to different syringe sizes used with the pump. The XP3000 pump itself determines its position in steps, where 3000 steps make a full stroke of the pump. To allow the user to work with the more useful unit of  $\mu\text{l}$ , the software will calculate the number of steps required by the pump's communication protocol into  $\mu\text{l}$  and vice versa.

*Initialisation command*: This is used to choose the command resetting the pump. The value ZR should not be changed! Using YR will swap the addressing of the pump's valve.

*Default Command*: Certain parameters of the pump can be set using this line. While speed, position, the pump's valve position as well as the pump's output signal are accessible through the main screen of the program, there are other parameters concerning the pump that can be set and might sometimes be useful to be changed. These values can be set here using the pump's command protocol. After pressing OK in the dialog, the pump will be set to the specified values.

### 3.1.3. Main Screen - Manual Control Window

The main screen (Figure 9) allows full manual control and status monitoring of all active devices.

The *Options* menu offers access to the *Setup* dialog described as well as performance of a reinitialisation of the system through the *Reset* option and termination of the program by selecting *Exit*.

All available status parameters for the supported hardware are displayed within the *Actual Values / System Status* frame. Devices are indicated as either *Ready*, *Bury* or *N/A* (not available) according to their status, together with their actual parameter values.

For active components the corresponding control frame is visible providing manual access to the instrument's functions. The control frame of an inactive device is hidden and will only become visible by activation through the Setup dialog.

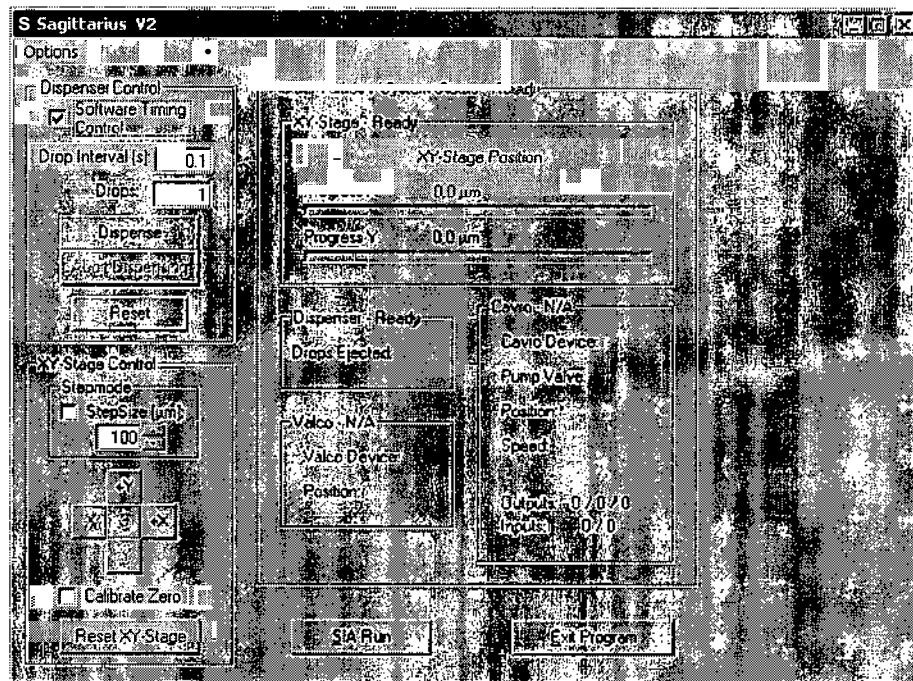


Figure 9: Sagittarius V2 - Manual Control

*Dispenser Control :*

*Software Timing Control:* If this option is selected, the software will trigger every single droplet to be generated. This however is only useful for drop intervals (see below) above 0.5 seconds. If faster dispensing is required, it is recommended to deselect this option, so that the waveform generator itself controls the timing, because the software does not provide enough accuracy and finally comes to its speed limit at 0.1 seconds. However, it is advised to select this option if possible, as otherwise, the software will not be able to track the dispensing process anymore. Sagittarius V2 will pass the drop interval and the number of droplets to be dispensed on to the waveform generator to process the desired operation, but it will not be able to determine the actual number of generated drops at a certain time as well as the end of the process. It will indicate the device as to be ready right after the command was

transmitted to the waveform generator regardless of the duration of the process. This is of special relevance in the case of automated SIA runs (see 3.1.5) when commands will be executed sequentially, each time waiting for the previous command to be finished.

*Drop Interval:* Specifies the time interval between subsequent droplets. See *Software Timing Control* above for limitation considerations.

*Drops:* Determines the number of drops that are to be dispensed. If the number zero is entered, the dispenser will start dispensing continuously until the operation is aborted.

*Dispense* button: Confirms entries for the dispenser and starts the dispensing process.

*Abort Dispensing* button: Will abort dispensing process immediately.

*Reset:* Aborts possible active process and sets the waveform generator back to its default values.

#### *XY-Stage Control:*

*Stepmode:* If this option is selected, the stage will move only for the specified distance. However, if the *Calibrate Zero* option (see below) is activated, the *Stepmode* will allow the stage only to move by single steps (2.5  $\mu\text{m}$ ) regardless of the stated step size. This is used for fine adjustment of the stage's origin.

*Calibrate Zero:* By activating this option, the stage will move without the software tracking its actual position. The *XY-Stage Status* frame will not change and the xy-stage movement limits will not be active! This option is intended to be used to set the xy-stage hardware to its 0/0 position. After finishing the calibration, the option should be deactivated and the actual xy-stage position indicated in the status frame set to 0/0 by pressing the *Reset* button in the XY-Stage Control.

*+X/-X/+Y/-Y/S* button: Pressing these button will cause the xy-stage to move into the indicated direction or to stop (S button). If neither *Stepmode* nor *Calibrate Zero* is activated, the stage will move until it reaches the limit of movement specified in the Setup dialog or position 0/0. For the effect of the activated *Stepmode* or *Calibrate Zero* mode see the corresponding paragraphs above.

*Reset XY-Stage* button: This resets the actual position indicated by the software to 0/0 and will not move the hardware back to zero.

*Cavro Control:*

*Device:* This entry field is not fully implemented in the current version of the program and must be set to 1. As it is possible to use multiple Cavro devices together, this option is present for future implementation of multiple device operation.

*Pump Valve:* Here it is possible to set the pump's valve position. With the initialisation command set to ZR (see Cavro Setup above), setting this parameter to I will move the valve to the left inlet while the letter O switches it to the right inlet. Changing the initialisation command results in the opposite behaviour, but will not be accounted by the software and is therefore not recommended to be changed.

*Speed:* The pump speed entered here refers to the command protocol of the pump's firmware. A pump speed of 100 causes the pump to execute a full stroke within 60 seconds. At a speed of 200 the full stroke will therefore be accomplished in 30 seconds. As full stroke is equivalent to the syringe size in use, the volumetric flow generated by the pump at a certain speed changes with the size of the syringe.

*Position:* This value represents the absolute position to which the pump fills or empties the syringe.

*Execute* button: Confirms entries for the pump and starts the pump.

*Abort* button: Will abort any pumping process immediately.

*Set Outputs* button: This brings on a dialog window to set the three possible output signals to zero or 1. These signals are TTL (transistor-transistor-logic) signals that can be used to trigger other devices with TTL compatible inputs.

*Reset* button: Reinitialises the pump and sets it back to its default values.

*Valco Control:*

*Device:* This entry field is not fully implemented in the current version of the program and must be set to 1. Also with Valco instruments it is possible to use multiple devices together and is therefore present for future implementation of multiple device operation.

*Position:* Refers to the port to which the selection valve is meant to switch to.

*Switch* button: Confirms entries for the valve and switches to the entered port.

*SLA Run* button: Switches to the section for automated operation of the supported devices (see below).

*Exit Program* button: Terminates the Sagittarius V2 program.

### 3.1.4. SIA Run Window

Automated command sequences for the co-ordination of the components supported by Sagittarius can be generated and modified within the programming environment provided by the *SIA Run* window (Figure 10).

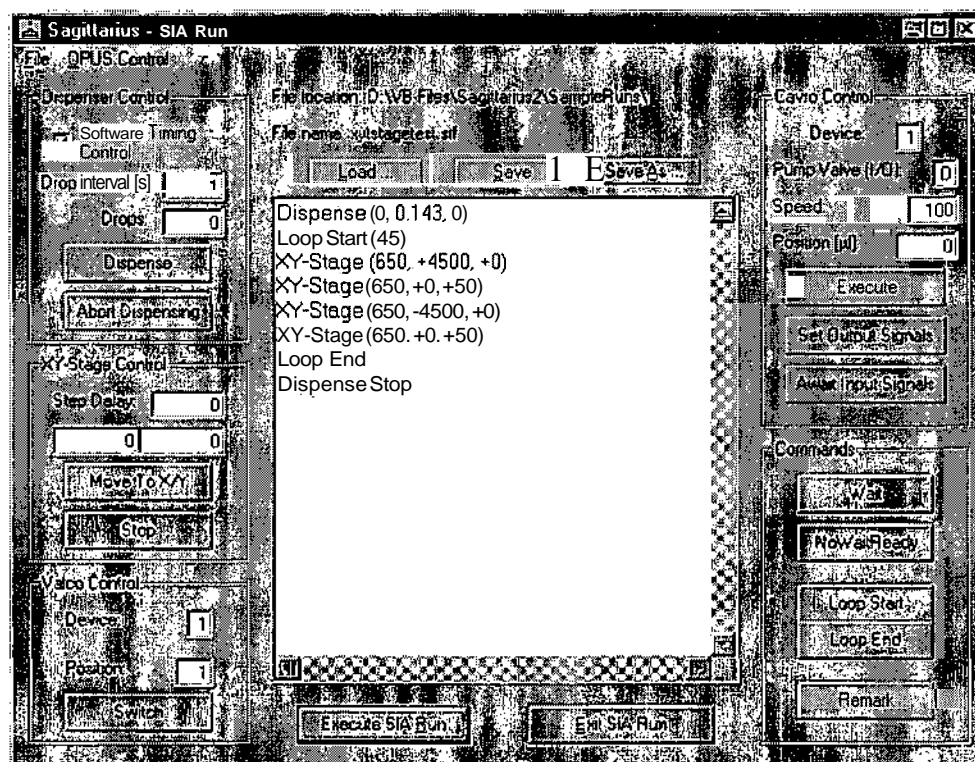


Figure 10: Sagittarius V2 - SIA Run

The list of events for the run automation is contained in the entry field in the centre and can either be modified by manually typing in possible commands according to the Sagittarius programming syntax or by choosing the desired command from the available options provided in the surrounding frames. The device control frames and buttons resemble the ones offered in the program's main window, however with the difference that the buttons do not directly execute a command but place the corresponding entry at marked position in the list of commands for the automated run. In general all commands will be executed sequentially with the program waiting every time for a command to be finished before continuing with the next event (see also list of commands below).

In the following only command buttons differing from the ones in the main window will be described and explained:

*XY-Stage Control:*

*Step Delay:* This parameter is equal to the entry in the Setup window, but is introduced again at this place so that it is possible to change the speed of movement as needed during an automated procedure.

Two entry fields below Step Delay entry: They represent the X and Y destination coordinates of the xy-stage.

*Move To X/Y* button: This will place the command in the command list that will make the stage move to the specified destination at the speed defined by the step delay.

*Stop* button: The added command will stop any movement of the stage.

*Cavro Control:*

*Await Input Signals* button: This command will cause the automated run to hold and wait for the two input lines of the Cavro pump to match the values specified. The entry for the expected values has to be entered through a dialog that will appear after pressing this button.

*Commands:* This frame contains options that only serve for automated run sequences and are **therefore** not available in the main window for manual device control.

*Wait* button: This button brings up an input box to specify the time Sagittarius V2 will wait, when encountering this event, until it continuously processes the command sequence. After confirming the wait time specified, the according entry will be added to the command list.

*NoWaitReady* button: The code inserted will cause Sagittarius V2 not to wait for the end of the next command in line, but will immediately continue with following one.

*Loop Start* button: Loop Start marks the beginning of a command section that is to be repeated multiple times and requires a Loop End statement to indicate the section's end. The appearing input box will ask for the number of repetitions the section should be repeated.

*Loop End* button: Loop End specifies the end of section of commands that are to be processed several times and needs to be preceded by a Loop Start command to mark the section's beginning.

*Remark* button: As long procedure codes can get confusing, this options allows the user to add remarks to the command list. When Sagittarius finally processes the command sequence, it will ignore all remarks.

*OPUS* menu: This menu with it's two options *Background* and *Sample* allow the implementation of automated background and sample measurements by any instrumentation controlled by the OPUS NT software from Bruker GmbH within the procedure. As a consequence of the choice of one of the menu items a dialog window will appear (Figure 11) which allows the specification of the OPUS macro that shall be executed and, in the case that *Sample* was chosen, also enables the specification of the name and data path of the resulting measurement file.

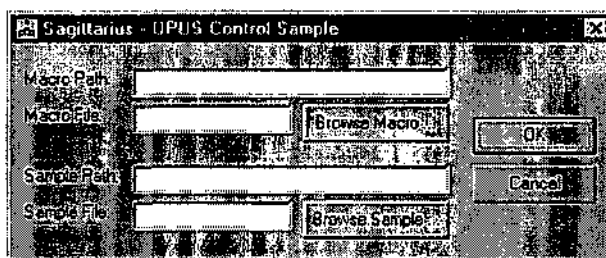


Figure 11: Sagittarius V2 - OPUS Control Dialog

To be able to make use of this feature, the OPUS NT software must be loaded and running on the same computer as Sagittarius V2. During the automated run Sagittarius V2 will then open a DDE (dynamic data exchange) communication channel to OPUS NT and arrange that the specified macro is being started. After the macro has been started, Sagittarius V2 passes the string "Sample" or "Bkg" depending on whether *Sample* or *Background* has been chosen to the macro. So only one macro is needed to record sample and background spectra, the macro only has to verify the content of the transmitted string. Furthermore in the case of a sample measurement, the strings *Sample Path* and *Sample File* are passed on to the OPUS macro to allow the remote specification of the desired file name and destination. The programming of the according OPUS macro is described in detail in the according software manual from Bruker GmbH.

After having programmed the automated run sequence the data has to be saved before intending to start the process, as otherwise changes will be discarded.

*Execute SLARun* button: This control button gets the user to the automated run control window (Figure 12). However, before the new window comes up, the software first checks

the syntax and validity of the listed commands and their parameters as well as the presence of all specified devices. Possible errors will be indicated with the request for them to be changed prior to the start of the process.

*Exit SLA Run* button: This option directs the user back to the Sagittarius V2 main window for manual device control (see above).

### 3.1.5. Automated Run Control Window

The *automated run control* window (Figure 12) supplies full control of the programmed process together with information on the status of the run sequence and the devices.

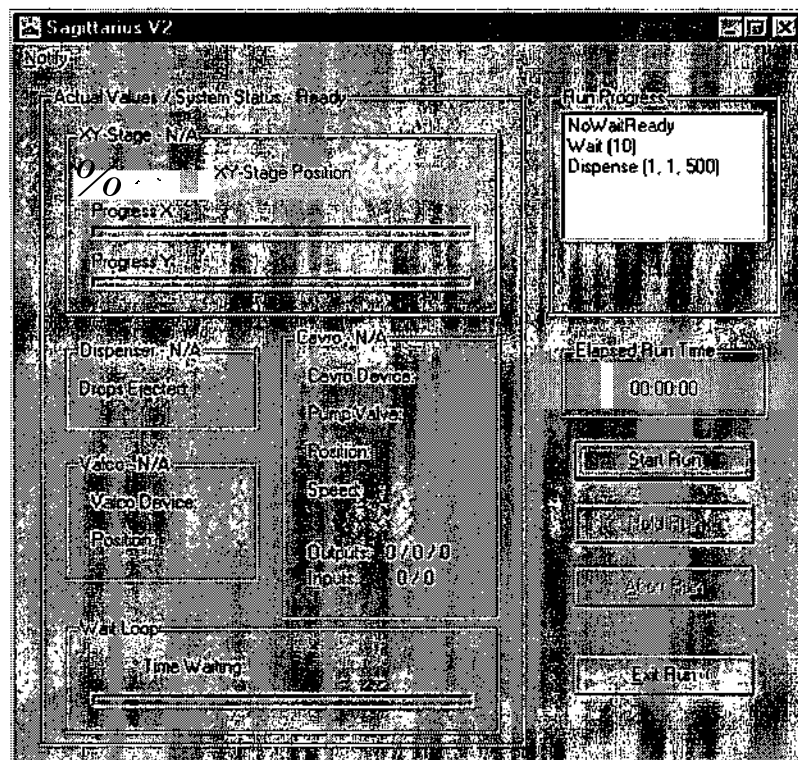


Figure 12: *Sagittarius V2—Automated Run Control window*

During long processes it is often desired to leave the laboratory in order to work on other tasks in the office located in a different room. However, to be able to quickly react on possible events (especially errors) occurring within the automated process, a notification option was implemented in the software. This feature is accessible through the *Notify* menu with its two options *Error Notify* and *Finish Notify*. Activating one or both options brings on a dialog where the name or the IP address of the computer to be informed of the chosen

event can be specified. If a name is entered, it is assumed that the remote computer is part of the same workgroup, whereas the specification of an IP address gives access to any computer in the network. It is also possible to notify multiple computers by separating their names and/or addresses by semicolon. The option however is limited to computers with Microsoft Windows operating systems featuring the "net send" command (e.g. Windows NT and Windows 2000)!

The big *Status* frame shows all device parameter similar to the manual control window described earlier, together with the status of any possible *Wait* operation delaying the progress of the subsequent process events.

The *Run Progress* frame further displays information on the command sequence highlighting the event currently being processed, whereas the *Elapsed Run Time* field informs the user about the overall time that elapsed since the start of the process.

The *Start Run* button is used to initiate the automated sequence, whereas *Hold Run* allows to temporarily stop the command execution and resume with the following event whenever desired. With *Abort Run* the sequence can be aborted and returning to the first line in the sequence of commands. Finally the *Exit Run* option will get the user back to the *SLA Run* programming window (see above).

### 3.1.6. Run Files and Log-Files

The files containing the command sequence all have the extension ".srf" (Sagittarius Run File) and are text files. They can be written and edited with standard text editors as long as they are finally named with the .srf extension. That way it is possible to create event sequences also on other computers or if the program itself is busy. Furthermore, it is not necessary to rely on the program to enter the commands in the sequence, as Sagittarius V2 will check the syntax and parameters of all commands prior to entering the run control window, hence reducing the possibility of mistakes.

Every execution of an automated sequence is logged in a text file named "LastRun.log" in the directory where Sagittarius V2 is located. It will be overwritten every time a new run is started and contains the times together with the commands in progress. If an error occurs during the execution of an programmed procedure, the software will furthermore create a copy of the log-file with the name "LastError.log" also located in the Sagittarius V2 home directory.

### 3.1.7. List of Commands

The program processes command by command, every time waiting until the command processed is completed successfully before continuing with the next command (exceptions: *NoWaitReady* and *Dispense (X, Y, 0)*).

*General command format:*

The program is case insensitive.

Command parameters are separated with comma.

Decimals are separated with a decimal point.

*NoWaitReady*

Refers to next command in program. Program will immediately continue after next command. The run doesn't hold until the next command was finished successfully.

*Wait (T)*

Holds Run for T seconds

$T: 0 \leq$

time to hold run in seconds

*Loop Start (C)*

Marks the start of a loop

$0 < C <$

number of cycles

*Loop End*

Marks the end of a loop

,

Indicates a user remark. The program will ignore this line.

*Valco (D, P)*

Switches Valco valve

$D: 1$

device number (more than 1 not featured)

*P: 1* — *Number of Ports* (see Setup dialog)

port number

*Cavro (D, V, S, P)*

Moves Cavro pump

*D: 1*

device number (more than 1 not featured)

*V: I, O, B*

position of pump valve

*I* ... In position (standard left)

*O* ... Out position (standard right)

*B* ... Bypass (connecting left-right, DO NOT MOVE PLUNGER in this position!!)

*P: 0* — *Syringe Size* (see Setup dialog)

absolut plunger position in  $\mu$ l

*CavroOutputs (X, Y, Z)*

Set Cavro Outputs (pins 13, 14, 15) of master device (#1)

*X, Y, Z: 0 or 1*

*0* ... low (0V)

*/* ... high (5V)

*AwaitCavroInputs (A, B)*

Holds Run until Cavro Inputs (pins 7, 8) of master device (#1) reach levels A and B

*A, B: 0 or 1*

*0* ... low (0V)

*/* ... high (> 2.5V)

*Dispense (X, Y, Z)*

*X: 0 or 1*

*0* ... waveform generator controls timing of **dropinterval**: necessary for **dropintervals** < 0.5 seconds and for highest precession

*I* ... software controls *dropinterval*: sufficient for *dropintervals*  $\geq 1$  second

*Y*:  $0 < Y < 60$

time interval between droplets

*Z*:  $0$  or  $<$

number of droplets

$0$  ... infinite number of droplets (program will continue with next command immediately)

*Dispense S fop*

Stops Dispenser operation

*XY-Stage (T, X, Y)*

Moves XY-Stage

*T*:  $> 0$

arbitrary value to adjust xy-stage speed (the lower the faster, usually around 850 for 300  $\mu\text{m}/\text{sec}$  on Pentium II 400 MHz PC)

*X*:  $0$  — *Limit X* (see Setup dialog)

x-value in microns

*Y*:  $0$  - *Limit Y* (see Setup dialog)

y-value in microns

*XY-Stage Stop*

Stops XY-Stage operation

*Opus Bkg (Macro)*

Start OPUS macro and passes on the string *Bkg*.

*Macro*: Complete name (path plus filename) of the macro to start

*Opus Sample (Macro, Path, File)*

Start OPUS macro and passes on the strings *Sample*, *Path* and *File*.

*Macro*: Complete name (path plus filename) of the macro to start

*Path, File*: Strings passed on to *Macro*

### 3.1.8. Fields of Application

Sagittarius V2 was developed to provide high flexibility especially in the automated operation of systems consisting of any of the four devices (Cavro XP 3000 pump, Valco selection valve, dispenser controlled via Agilent 33120A waveform generator and xy-stage with in-house built stepper motor controller). Furthermore, it supports the online data recording of OPUS NT operated measurement instrumentation to extend its automation power.

As the program does not require all devices to be present and implemented in the systems to be operated, it can be used for any set-up and application based on whatever combination of the supported equipment without restrictions, starting from standard automated flow systems for sample preparation and delivery to highly sophisticated analyte deposition units.

### 3.2. QCL-Control

The QCL-Control software (Figure 13) is a Microsoft Visual Basic 6.0 based program that was developed to provide control and data recording options of a quantum cascade laser set-up designed in the workgroup of Prof. Bernhard Lendl.

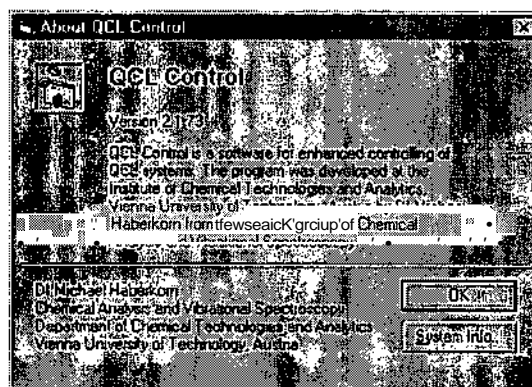


Figure 13: *QCL-Control software*

Basically it makes use of the SR245 computer interface from Stanford Research Systems (Sunnyvale, CA, USA), which provides the possibility to either generate -10 to +10 VDC signals or to read voltage levels in this range as digital values. It provides 8 analogue ports

(I/O ports) which can be configured as in- or output ports. With the help of the input ports signals from Boxcar integrators that process the laser pulses detected by the mid-IR detectors can be determined, as well as the temperature of the QCL device which can be monitored from the hardware as a DC voltage level. The output channels serve as control ports to set possible parameters of various hardware components via DC voltage levels at their according control inputs.

Furthermore, two digital I/O ports are available on the SR245 that allow the reading and setting of TTL compatible signals. The first of these ports can be used to synchronise the computer interface readout with the occurrence of laser pulses.

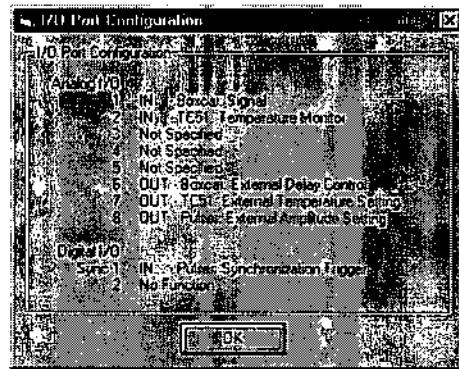


Figure 14: *QCL-Control – I/O Port Configuration*

The pre-set configuration of the mentioned I/O ports by the QCL-Control software is given in Figure 14. This window is also accessible through the main window's menu, via ? and submenu I/O Port Settings.

### 3.2.1. Setup Dialog

Parameters which are not commonly changed in the set-up are accessible through the *Setup* dialog (Figure 15).

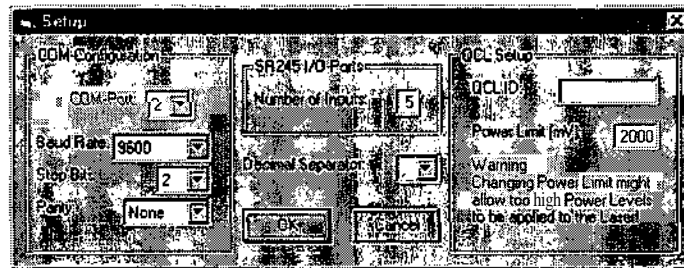


Figure 15: *QCL-Control – Setup Dialog*

The *COM-Configuration* frame offers adjustment of settings concerning the serial communication port through which the computer addresses the SR245 interface. The necessary parameter values for *Baud Rate*, *Stop Bits* and *Parity* are given the SR245 hardware whereas the *COM-Port* specifies the serial port of the computer which the computer SR245 is connected to.

The *Number of Inputs* entry declares how many analogue ports of the SR245 are used as input ports for reading data. The hardware will always consider the first ports up to the number specified as inputs and the remaining as outputs.

The field for setting the *Decimal Separator* allows the adaptation of the software to different regional settings concerning the treatment of numbers. Generally, the software will try to determine the decimal separation character through the system registry, however, this might not always be possible and therefore this option was implemented here. If QCL-Control uses a wrong character for decimal separation, the program is likely to create errors.

The *QCL Setup* frame is of special interest when an pulse generator with the possibility to externally control its pulse's amplitude via a DC input channel (as the AVL-2-C-N-EA AVTECH pulse generator) is used to drive the laser. If this input channel is linked to the analogue port 8 of the SR245 (see *I/O Port Settings* above), specifying the *Power Limit* within this frame as the allowed maximum for the QCL in use will then prevent the user from setting the amplitude of the pulses to too high values protecting the lasers from damage.

The *QCL ID* entry serves for documentary purposes only. Here the number identifying the laser in use should be entered and will later be written to any measurement file created.

### 3.2.2. Main window

The main window (Figure 16) offers full control of all possible features and settings necessary to conduct measurements with the newly developed set-up.

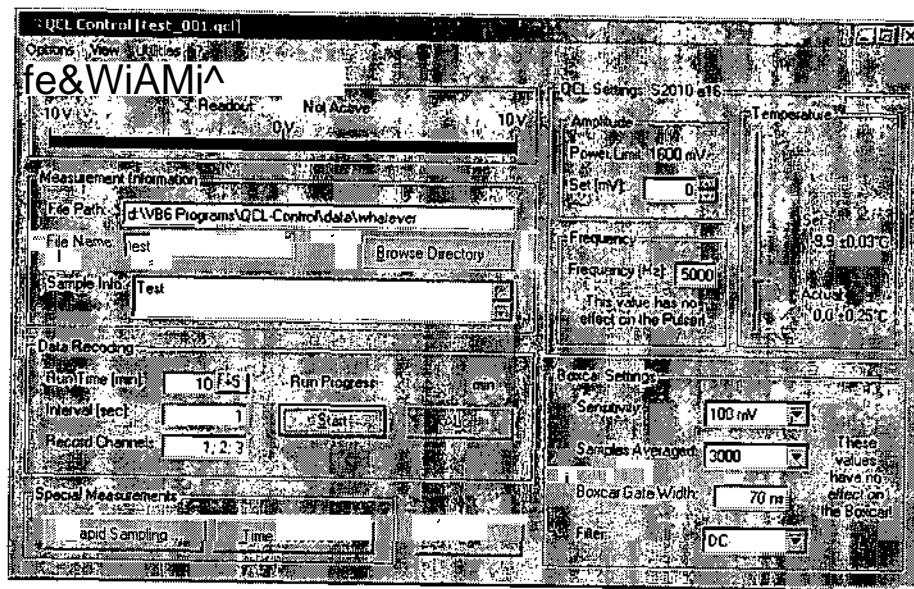


Figure 16: QCL-Control- Main Window

The *Options* menu allows the user to access the *Setup* dialog as well as to *Reset* the system or *Exit* the program.

Through the *View* menu it is possible to activate a *Readout Chart* window for the visualisation of the measurement data as a two dimensional graph and secondly to toggle the continuous display of the reading in the *Data Stream* frame via the *Data Stream* option. The input channel read by the *Data Stream* feature is indicated in the *Data Stream* frame title and is influenced by the entered *Record Channels* (see below).

The *Utilities* menu provides the possibility to *Notify* a remote computer about the progress and possible errors of the measurements. A *dialog* window will ask the user to either specify the name or the IP address of the computer to be notified. Stating a computer's name requires it to be part of the same workgroup as the measurement computer, whereas the IP address allows access to any computer in the network. This feature however only works with Windows NT based operating systems on both computers (measurement and remote computer).

Information about the program and its requirements in the configuration of the SR245 I/O port settings (see above) can be retrieved from the *?* menu.

The *Data Stream* frame displays the value of the indicated measurement channel in numbers and in the form of a readout bar. The content of this frame is being updated either during measurements or if the *Data Stream* option in the *View* menu is activated.

Specifications on the location and name of the file to store the data as well as information about the measured sample can be entered within the *Measurement Information* frame. The software uses automatic filename incrementation based on the specified filename followed by underscore, a changing three digit number and the extension “.qcl” (name\_XXX.qcl). The sample information stated here will be added to the generated measurement file.

Within the *QCL Settings* frame the amplitude of the pulse driving the laser and the operating temperature can be set.

In order to control the pulse amplitude via the QCL-Control software, the analogue output channel 8 of the SR245 computer interface has to be connect to the DC external amplitude control input of the pulse generator driving the laser (e.g. AVL-2-C-N-EA AVTECH pulser, Avtech Electrosystems, Ottawa, Canada). The specified amplitude value represents the exact voltage level that will be applied to the SR245 analogue output channel 8.

Concerning the temperature control panel, SR245 analogue output channel 7 has to be linked to the DC external temperature control input of the QCL temperature control unit TC51 from Alpes Lasers (Neuchâtel, Switzerland) to meet this feature's hardware requirements. The laser's operating temperature can then be set with the help of the vertical sliding bar. Furthermore, if the data stream option in the *View* menu is activated and the temperature monitor output of the TC51 unit is connected to the analogue input channel 2 of the SR245 computer interface, the actual temperature of the laser will be also be displayed. The mentioned amplitude and temperature control connections are optional and not required for measurements where these parameters are controlled manually by the operator. Finally, also the frequency at which the laser is operated can be specified within the QCL Settings section, however this value only serves as information that is added to the generated measurement data files.

All parameters stated within the *Boxcar Settings* frame do not effect the settings of possible Boxcar hardware integrated in the setup. Entries made here are merely added to the resulting measurement files as additional information. The values expected by the selection lists correspond to the available options of SR250 Boxcar Averagers from Stanford Research Systems (Sunnyvale, CA, USA).

The *Data Recording* frame allows recording of the voltage levels of different SR245 analogue input channels with time. This requires the specification of the duration of the recording (Run Time), the interval between subsequent readout cycle as well as the input channels that are to be recorded within one readout cycle. Using the +5 button the original

run time can be extended by increments of 5 minutes during a progressing run. If multiple channels are entered for the measurements, they have to be separated by semicolon and the first channel stated will be the one tracked in the *Data Stream* frame and plotted in the *Readout Chart* window.

The measurements are triggered with the help of the *Start* and *Abort* button.

More advanced analysis of signals is possible with the *Rapid Sampling* and *Time Resolved* options (see 3.2.4 and 3.2.5) featured in the Special Measurements frame.

### 3.2.3. Readout Chart window

For immediate visualisation of collected data a chart option (Figure 17) was implemented in the QCL-Control software.

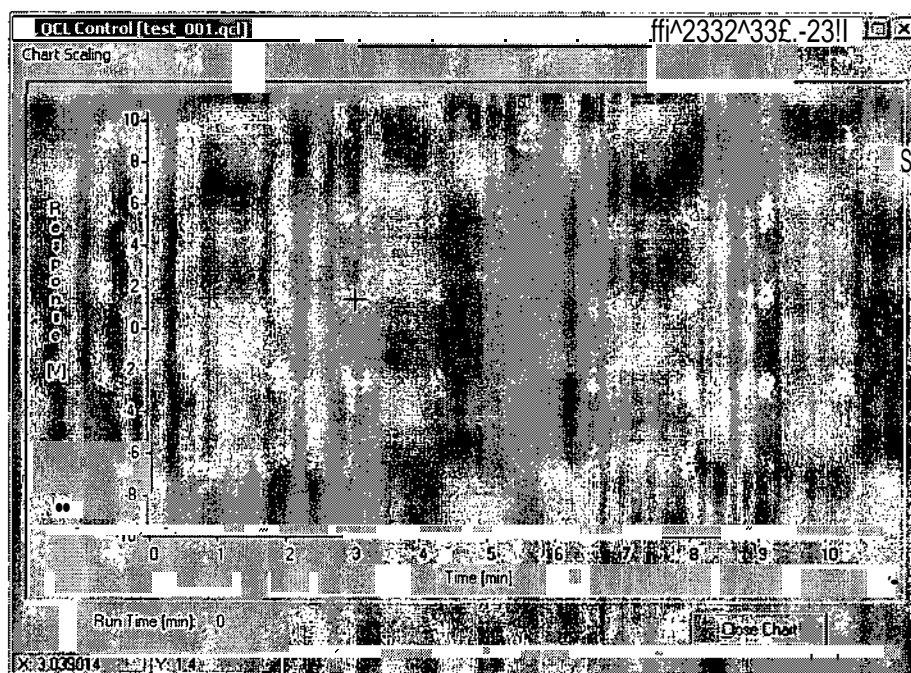


Figure 17: QCL-Control- Readout Chart window

In the *Readout Chart* window the graph of the data recorded for the first of the channels specified for recording will be displayed. During a measurement the chart will be updated with every new data point and in the case no data tracking is in progress, the window will show the last data set recorded.

At the bottom of the window the coordinates of the mouse cursor within the diagram are given for the ease of reading values within the plot.

The *Chart Scaling* menu contains options to adjust the range of values visible in the diagram. *Scale Axis* allows the specification of the axis ranges via a dialog window. *Full Scale* will minimise the range of the diagram for all values of a recorded graph (only available after recording is finished). If *Auto Scaling* is activated the scaling of the *ordinate* is dynamically adjusted during a measurement so that the graph will be fully visible in the diagram while the *abscissa* will be set from zero to the specified duration of the measurement.

This menu is also available by pressing the right mouse button when the cursor is placed over the diagram.

Finally, it is also possible to zoom in and out in the diagram using the left mouse button. Pressing and holding the left mouse button inside the chart area will draw a rectangle to which the program will zoom in to upon releasing the button. Executing the described action in combination with the SHIFT key will make the software zoom out instead.

#### 3.2.4. Rapid Sampling dialog

For tracking highly frequent laser signals, the rapid sampling option was implemented in the software. That way it is possible to read signals with the computer interface up to a frequency of 2 kHz. To gain access to this feature the SR245's digital channel 1 has to be connected to the trigger output of a device which provides TTL pulses to synchronise signal generation and reading.

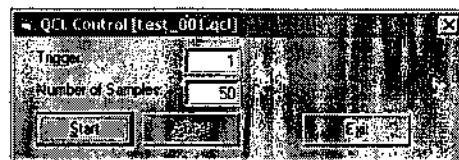


Figure 18: *QCL-Control* – *Rapid Sampling* dialog

The *Rapid Sampling* dialog (Figure 18) allows the specification of necessary parameters for this measurement option. The *Trigger* entry designates the  $n^{\text{th}}$  synchronisation pulse as a trigger for signal sampling and *Number of Samples* specifies how many samples to be measured.

### 3.2.5. Time Resolved Measurement dialog

For advanced detector response analysis, QCL-Control also supplies a feature to obtain time resolved information on signal profiles. This option only works in combination with SR250 boxcar averager and requires linking of the analogue output channel of the RS245 unit to the external delay control input of the SR250.

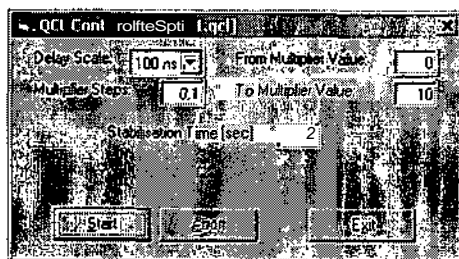


Figure 19: QCL-Control- Time Resolved Measurement dialog

The according measurement parameters have to be specified within the *Time Resolved Measurement* dialog. The *Delay Scale* selection list corresponds to the SR250 boxcar's front panel setting and is necessary for the software to determine the correct time scale for the measured response values. *From* and *To Multiplier Values* multiplied by the *Delay Scale* define the starting and end time of the time resolved measurement, relative to the trigger signal received by the boxcar module that indicates time zero of the experiment. *Multiplier Steps* times *Delay Scale* gives the time interval between subsequent points of data acquisition. To allow the boxcar averager to accumulate enough data to provide a representative result for each new data point a *Stabilisation Time* period is defined.

### 3.2.6. File format

The generated data files are standard text files with the extension “.qcl”. QCL-Control automatically increments the filenames based on the filename stated within the according field in the main window followed by underscore and a three digit number (name\_XXX). The first section is an introductory part which contains general information about the experiment, whereas the second part consists of the actual tabulator separated measurement data. The first column represents the time axis whereas the following column list the acquired signals for the according SR245 analogue input channels listed in the column header. See below for an example of a generated data file:

QCL ID:	S1839a21
QCL Driving Power:	0 mV
QCL Frequency:	16 K Hz
QCL Temperature:	0,0°C
Boxcar Sensitivity:	100 mV
Boxcar Averaging:	10000 Samples
Boxcar Gate Width:	460 ns
Boxcar Filter:	DC
Sample Info:	100um spacer; no BS, new detector (red); only 10,3 V on LDD
Measurement:	Standard Run
Start of Run:	Donnerstag, 3. April 2003 15:32:37
Time [sec]	Channel#1 [V]
0,0	-6,462
0,8	-6,462
2,0	-6,462
3,2	-6,462
4,5	-6,460

### 3.2.7. Fields of Application

QCL-Control is designed specifically for quantum cascade laser setups consisting of an SR245 Stanford Research Systems computer interface linked to an AVL-2-C-N-EA AVTECH pulse generator as well as a TC51 temperature controller from Alpes Lasers. Further implementation of a SR250 Stanford Research Systems boxcar averager provides access to all features offered by the software, making it a powerful tool for advanced studies of QCL signals.

However, for just recording and tracking of the signal at the analogue input channels of the SR245 computer interface, it is not necessary to establish any other connections than the ones from detection device to the desired analogue input channel. Ignoring the settings of the pulse amplitude and the temperature as well as the temperature readout, the software can record the time trace of signal of simply any detection unit, provided that it features an

analogous output delivering a voltage signal correlating with the detector response (e.g. refractive index and UV-Vis detectors, lock-in amplifiers, ...) which can be linked to one of the input channels of the SR245 unit. As these analogous signal outputs are very common for detection devices, the QCL-Control software in combination with the SR245 interface presents a universally applicable signal recording package.

## 4. FLOW-THROUGH MICRODISPENSER

### 4.1. Principle of Operation

The flow-through **microdispenser** was developed by T. **Laurell** et al.[31] as a device to highly reproducibly generate small droplets with exactly defined volumes in the **picoliter** range.

Reliably handling smallest amounts of liquid is of major interest in biochemical, pharmaceutical and medical research where usually availability of **analytes** and reagents is very limited. Furthermore, the possibility of the presented microdispenser to operate in flow-through mode is of significant advantage for the combination with automated flow systems for sample delivery and preparation as it simplifies cleaning and rinsing of the dispensing device. Common dispensing devices function as "dead end" devices **with** the necessity to dispense all your reagent through the *nozzle*, making cleaning steps very time consuming. Moreover, the **microdispenser's** flow-through capability makes the droplet dispensing frequency more or less independent of the system's flow rate and also allows additional detection devices to be implemented in the flow line after the dispenser.

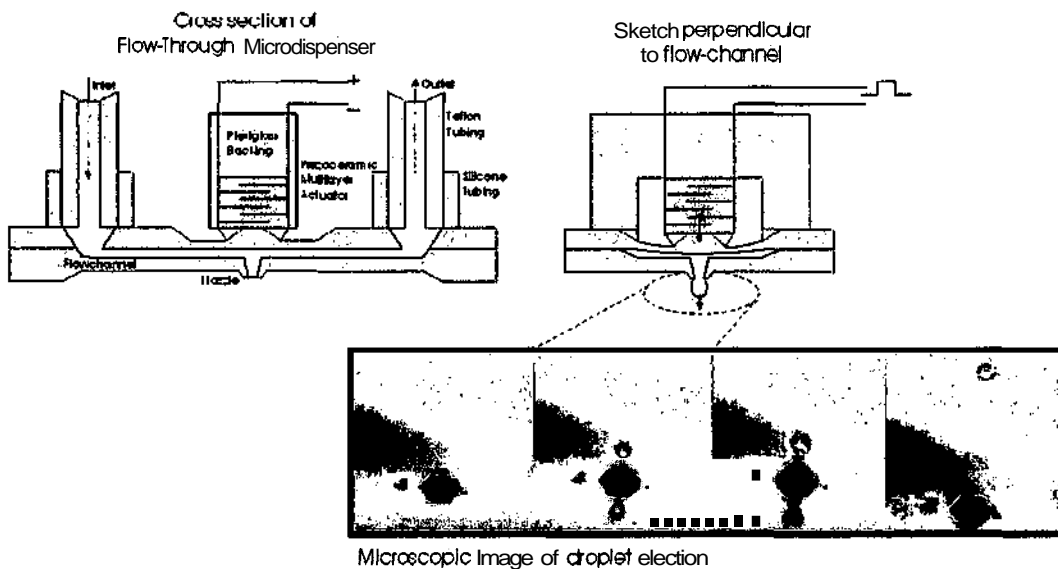


Figure 20: Scheme of flow-through microdispenser *with* microscopic images of droplet formation process

The **flow-through** microdispenser consists of two silicon structures created by conventional silicon **micromachining** processes. In order to generate the **microdrops**, a

**piezoceramic** element attached to a pushbar located on the thin membrane like upper wall of the flow-through channel creates a pressure pulse that forces the liquid out of the pyramid-shaped nozzle in the opposite wall (Figure 20). The pyramidal nozzle design ensures the high performance stability of the dispenser and makes this drop on demand device a high precision tool for microliquid handling.

The electronic pulses driving the piezo element are provided by a DC power supply together with a computer controlled arbitrary waveform generator. The electric signals from the two instruments are combined through dedicated piezo driving electronics in such a way that the DC signal defines the final pulse amplitude, and amplitude and the positive width of the rectangular wave from the waveform generator determine the pulses rising edge and width.

## 4.2. Fabrication

The processing of the silicon to gain the **microstructures** was done by **anisotropic** etching with KOH using 3 inch **p-type** (10 Ohm cm) **<100>-silicon** wafers [37].

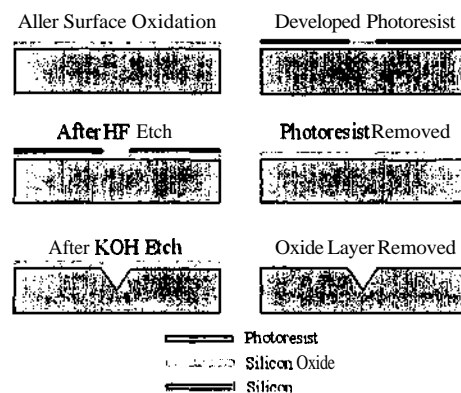


*Figure 21: Microstructuring process of silicon wafers*

For every structuring process (Figure 21), as a first step, the surface of the silicon wafer is oxidized **with** water steam for 5 hours in an oven at **1100°C** followed by spin coating with photoresist. The mask containing a 1:1 image of the desired **microstructure** is **then** placed on top of the photoresist and illuminated with UV light. With the help of a dedicated developer **solution**, the photoresist is then removed from surfaces to be etched. As a next step after covering the side of the wafer that is not to be processed with adhesive tape to prevent

contact with HF, the silicon wafer is dipped into an HF solution for a few tens of seconds to remove the oxidized layer at the places not covered by the photoresist. Taking off the tape and removing the photoresist with acetone and **ethanol**, results in a copy of the photoresist in the silicon oxide layer which serves as the mask for the **anisotropic** etching of the wafer in **KOH** at 90°C in an ultrasonic bath. It is not possible to directly use the photoresist structure as a mask for the anisotropic etch as it cannot withstand the etching conditions. Finally, the oxide layer is completely removed by a last treatment with HF solution as mentioned above to give the desired silicon structure.

To achieve the pyramidal shape of the **nozzle** of the **microdispenser**, pn-etch stop processing is used for this structure on the bottom wafer (Figure 22) [38,39]. For this electrochemical stop etch technique, the surface of the anisotropically etched nozzle cavity is phosphorous doped by placing a ceramic wafer loaded with phosphor next to the silicon wafer in the oven at 1000°C for 2 hours followed by oxidation. After this procedure, the **wafer's** outside is **anisotropically** etched with KOH to open the orifice. At last by applying an electrical potential of 1 V between the phosphorous doped silicon surface and the KOH solution, pn-**etching** is used to remove the outside silicon bulk material leaving the doped walls of the pyramidal nozzle untouched. In general, the phosphorous doped layer is n-doped silicon and forms a **pn-junction** with the p-doped bulk material. Applying a reverse bias to the **pn-junction** brings the phosphorous doped silicon surface to a positive potential whereas the p-doped silicon is not affected by the potential. Silicon is **oxidized** in the presence of an positive electric potential and with a high enough bias (passivation potential), the anodic oxidation protects the silicon from etching. In this case, the positive potential on the n-doped silicon prevents etching due to passivation by the anodic bias while the p-doped material is being etched unaffectedly.

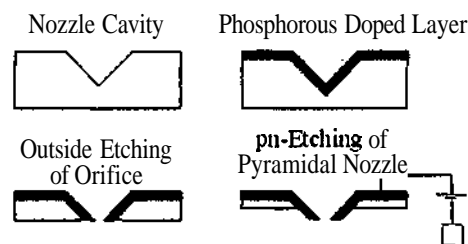


Figure 22: *Etching process for pyramidal nozzle*

Finally, to assemble the two silicon wafers to form the basic microdispenser structure, any silicon oxide is removed from one wafer using HF, whereas the other wafer is oxidized as

described above. After aligning and joining the two wafers with the help of a microscope with infrared illumination and an infrared sensitive camera, they are heated in an oven, where the clean silicon surface of the one wafer will chemically bond to the silicon oxide layer of the other wafer.

After dicing the wafer, the microdispenser structure is glued to the Plexiglas backing to which a piezoceramic element is attached using an epoxy glue. At last the silicon rubber tubing is fixed to the in- and outlet openings with the help of silicon glue.

### 4.3. Instrumental Setup

In order to fully exploit the benefits of the flow-through microdispenser as a drop on demand interface for automated and reproducible measurements, generally any flow system can be used to provide the compound of interest. On the simplest basis, a flow system with a peristaltic pump supplies the analyte solution for the dispenser as shown in Figure 23. Adaptation of the sample delivery system extends the applicability of the microdispenser to wide range of tasks. For limited sample availability, a problem commonly encountered in biomedical research, miniaturised flow systems could reduce the dead volume in the system giving access to the advantages of the microdispenser's characteristic high precision at liquid handling in the picoliter domain. In the case of analytes that cannot be detected in the way they are present in the sample matrix, flow and sequential injection systems can be implemented which serve as automated sample manipulation and chemical derivatisation equipment modifying the analyte of interest to provide detectable species. In the case of highly complex compound mixtures Chromatographic instrumentation (e.g. liquid chromatography, capillary electrophoresis) can extend the use of the microdispenser by adding further, detector independent selectivity to the analytical setup.

Finally, the treatment of the generated microdrops for the final measurement can further increase the analytical possibilities provided by the dispenser setup. As the volume of the droplets lies in the picoliter range, the aqueous solutions applied to a solid target will evaporate within less than a second at room temperature and atmospheric pressure which presents a valuable tool for solvent elimination and/or if subsequent drops are placed on top of each other highly effective analyte preconcentration prior to measurement becomes feasible. A different aspect can be added to the analysis system by implementation of a particle levitator which can confine ejected droplet in a dedicated place without necessity of solid boundaries. This can be of significant importance in analytical applications where for

example **analytes** have to be detected or chemical reactions need to be monitored without disturbing **unspecific** adsorption of compounds at solid surfaces causing errors due to possible memory effects.

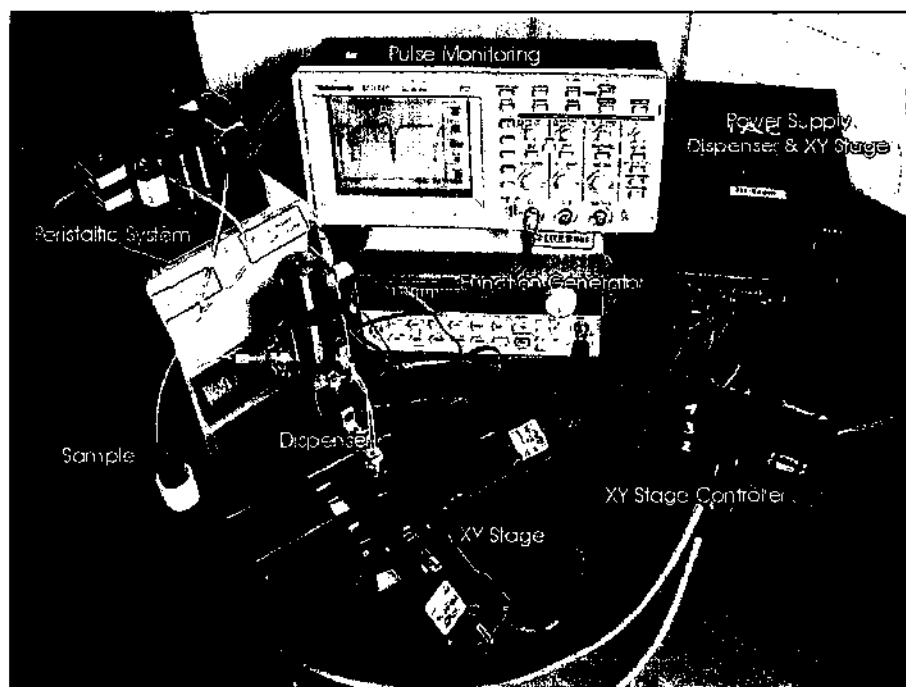


*Figure 23: Simple automated sampling system with microdispenser, driving electronics and xy-stage*

#### 4.4. Solvent Elimination Interface for FT-IR Spectroscopy (Publication I)

For mid-infrared Spectroscopy the aspect of solvent elimination in automated flow systems prior to measurement probably poses the most attractive advantage of the flow-through microdispenser. With its reproducible droplet generation and high lateral precession of deposition in combination with an computer controlled xy-stage, it presents a powerful tool for liquid handling of minute amounts of sample for accelerated solvent evaporation and sample **preconcentration** by deposition of multiple droplets within the spot of the probing IR beam.

During initial studies of the **microdrop** generation stability, a phase Doppler anemometer (Figure 24) provided as a demonstration instrument from TSI GmbH (Aachen, Germany) for the institute of Chemical Engineering at Vienna University of Technology was

used to determine droplet size distribution and ejection velocities. The phase Doppler **anemometry** (PDA) experiments showed droplet diameters of 46.7  $\mu\text{m}$  with a standard deviation below the detection limit of 0.1  $\mu\text{m}$  for water for the tested flow-through **microdispenser** which calculates to a volume of 53.3 **pl**. Slight variations of a few **picoliters** of the drop volume for different solvents (water, **methanol**, **acetonitrile**) could be found as a consequence of alteration of the solution's surface tension.

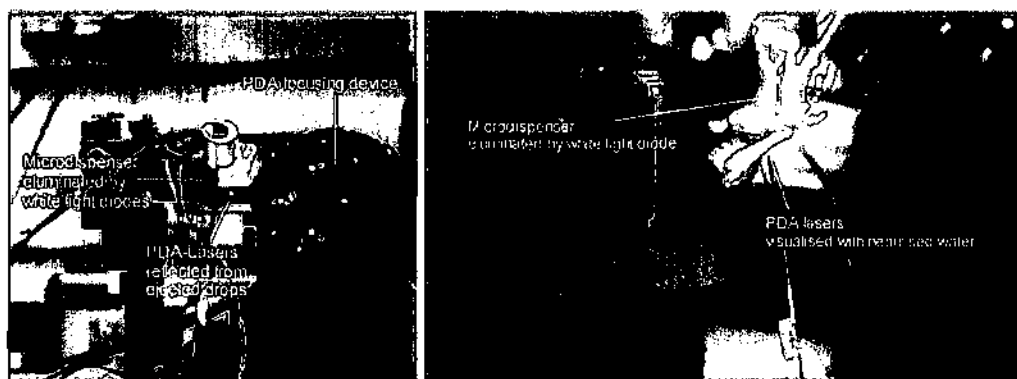


Figure 24: PDA experiment

In order to verify the capabilities and assess the performance of the developed solvent elimination interface for FT-IR spectroscopy, a versatile sequential injection system was used to prepare and provide the **analyte** solutions for the droplet dispensing stage (Figure 25). The fully automated computer controlled dispensing system was operated via the in-house written Microsoft Visual Basic 6.0 based software Sagittarius, the precursor of Sagittarius V2 (see chapter 3.1) with more limited control of the used Cavro XP3000 syringe pump, the **Valco** selection valve, the Agilent 33120A waveform generator for dispenser control and the in-house built **xy-stage** driving electronics.

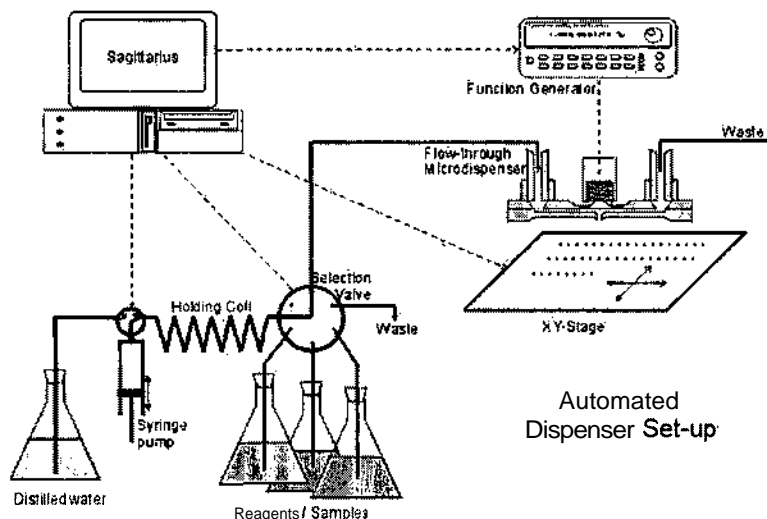


Figure 25: Instrumental setup for performance assessment of solvent elimination interface

Sucrose solutions were used as analytes to test the novel interface for its performance as it is a well investigated substance within the workgroup with extensive know-how in the interpretation of the FT-IR spectra. Droplets of solution of different sucrose concentration were deposited onto  $\text{CaF}_2$  crystals for mid-IR transmission measurements on an FT-IR microscope with an probing beam focused to  $100\ \mu\text{m}$  diameter. Generally, any IR transparent material can serve as a solid support for the deposition of an analyte given that it resists the chemical properties of the solution in use, however  $\text{CaF}_2$  was chosen in this case as it represents the cheapest crystal with sufficient IR transmission in the spectral region down to  $950\ \text{cm}^{-1}$ .

Based on the gained results, it could be verified that the developed solvent elimination interface is capable of quantitative analysis of down to around 50 picogram absolute amount of deposited sucrose which represents a 1000 times lower detection limit than commonly reported and furthermore allows sample preconcentration by deposition of multiple droplets on the same spot with high lateral precision.

Finally, to demonstrate the applicability of the novel system to liquid Chromatographic tasks, an experiment was designed with a high performance liquid chromatography (HPLC) manifold feeding the microdispenser (Figure 26).

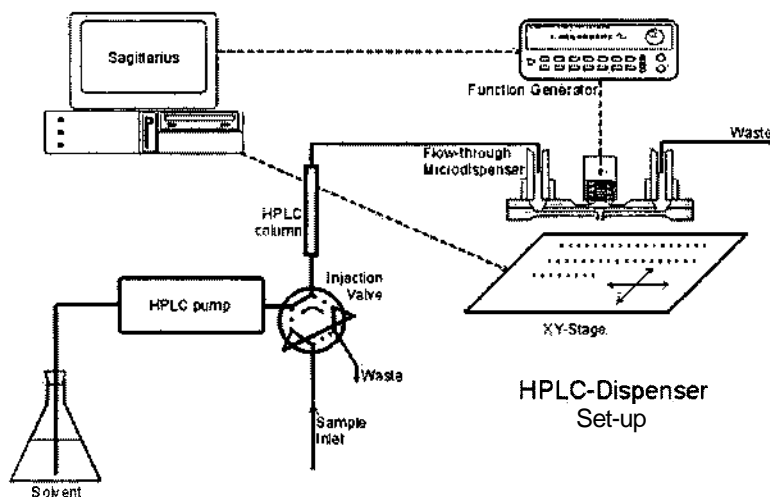


Figure 26: Scheme of HPLC solvent elimination interface

The experiment was conducted by dispensing one drop of eluting solution from the HPLC every second onto a  $\text{CaF}_2$  crystal at distances of 350  $\mu\text{m}$  so that each deposit was laterally separated from each other. As a test mixture an aqueous solution of 25 g/l of fructose and glucose was injected onto a separation column with water as a mobile phase. Analysing the trace of the crystallised compounds with the help of an infrared microscope in transmission mode showed effective separation of the analytes and allowed positive substance identification via the gained spectra.

#### 4.5. Airborne Surface Enhanced Raman Scattering (Publication II)

The concept of analysis without the influence of container walls is most relevant for miniaturised systems with limited amounts of sample and was therefore examined in combination with surface enhanced Raman scattering as it is a powerful method giving access to the detection of minute amounts of analyte.

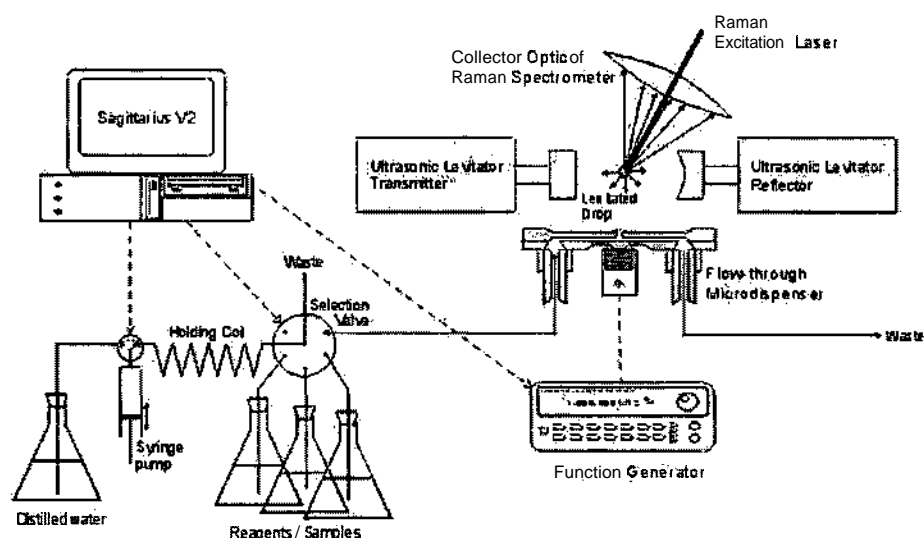


Figure 27: Setup for airborne surface enhanced Raman scattering measurements

Again the versatility of a sequential injection system providing the reagents and the precision and accuracy supplied by the flow-through microdispenser were combined to an efficient sample preparation unit injecting the desired solutions into an ultrasonic levitator representing the sample compartment free of walls for Raman analysis (Figure 27). To record the FT-SERS spectra the levitation unit was fixed in the focus of the Raman accessory of a FT-IR spectrometer adjusted in backscattering geometry with a 1064 nm Nd:YAG laser as a excitation source.

However, before the start of developing an automated airborne SERS setup the preparation procedure of a suitable SERS substrate had to be reconsidered. Most commonly used substrates [40] are silver colloids with synthesis procedures unsuitable for fast in-situ preparation in a levitated state as they usually require long reaction times and controlled temperature. Therefore, a new method providing silver sol at more favourable conditions was developed. Reduction of silver nitrate with hydroxylamine hydrochloride in alkaline solution at room temperature yielded a highly SERS active and stable silver colloid within a few seconds. The effectiveness of the that way prepared SERS substrate was verified via standard cuvette Raman measurements comparing analyte spectra gained from the commonly used Lee-Meisel silver sol (reduction of silver nitrate with sodium citrate) [41] with the ones from silver colloid synthesised following the new procedure.

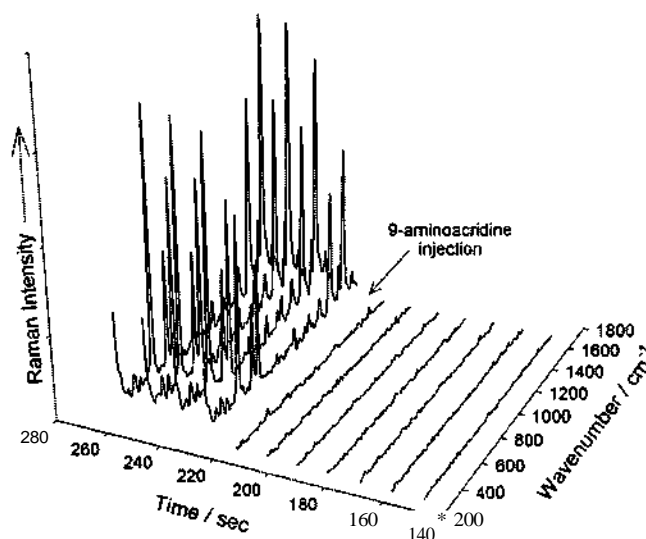


Figure 28: *In-situ monitoring of the analyte as injected onto airborne SEES substrate*

After finding similar enhanced in the Raman signal, the preparation was transferred to the levitated state within the above described automated setup. Sequential injection of the reagents silver nitrate and hydroxylamine via the flow-through microdispenser into the levitator resulted in an a levitated drop of silver sol. Subsequent injection of an analyte to the drop of airborne SERS substrate finally proofed the practical applicability of the concept and allowed detection limits down to femtogram amounts of 9-aminoacridine which was used as a test compound to verify the analytical performance. Moreover, the system allows in-situ monitoring of the process as shown in Figure 28 and to demonstrate its versatility also other compounds were tested with the developed airborne analysis setup demonstrating the wider range of detectable analytes.

#### 4.6. Conclusion and Outlook

Introducing the flow-through microdispenser as a novel tool for automated flow systems allowed the successful development of two novel interfaces with different focus of topic. Whereas one approach presents an efficient solvent elimination strategy for FT-IR spectroscopic detection, the other offers access to airborne in-situ SERS measurements of minute amounts of analyte.

Of course, it has to be said that there is still room for improvement and development. In the case of the LC-FT-IR interface only a very small fraction (0.01%) of the eluent flow was actually deposited and used for the FT-IR measurement. The relatively high flow rates of hundreds of  $\mu\text{l}/\text{min}$  in standard HPLC analysis result in a vast majority of the eluted fractions passing the dispenser into the waste. This excess of solution could either be subjected to a secondary detector retrieving further significant data from the "waste" or to generally decrease the amount of sample passing the interface undetected, a transfer of the presented interface to micro-liquid handling system, such as  $\mu$ -HPLC is planned to fully exploit to benefits of the flow-through microdispenser in that respect.

Considering the upcoming continuing research and developments on the topic of airborne Raman and SERS measurements, in-situ chemical reaction and interaction monitoring will be a promising field as droplet injection into the levitated microscale reaction vessel should offer a reliable and fast trigger for inducing chemical processes in the place of detection.

## 5 . QUANTUM CASCADE LASERS

### 5.1. Principle of Operation

Quantum cascade lasers (QCLs) represent a new generation of powerful miniature lasers covering the whole mid-IR spectral region. QCLs are usually operated in pulsed mode with an average emission powers in the tens of mW within a small spectral window of around a few wavenumbers. The brightness of these lasers at a given wavelength is significantly higher than the one of standard globars used as a light source in state-of-the-art FT-IR spectrometers.

The radiation emission process of standard semiconductor diode lasers is based on the conduction electrons drop to unoccupied states in the valence band across the band gap with the size of the band gap defining the emitted wavelength.

In contrast to this, quantum cascade lasers produce radiation by electronic transitions between conduction band states which formed by quantum confinement in ultrathin alternating layers (each several nm thick) of semiconducting heterostructures [42]. That way, the emission wavelength is determined by the thickness of the active layers rather than the chemical composition of the laser material which allows lasers of different wavelengths to be produced from one type of source material (e.g. AlInAs-GaInAs) significantly reducing the complexity and increasing efficiency of laser production. The use of cascades of alternating active layers allows the QCL to emit multiple photons (depending on the number of repetitions contributing to the cascade) per electron crossing the light source structure. The population inversion between the electronic states is obtained by controlled resonant tunnelling through the different heterostructures (Figure 29).

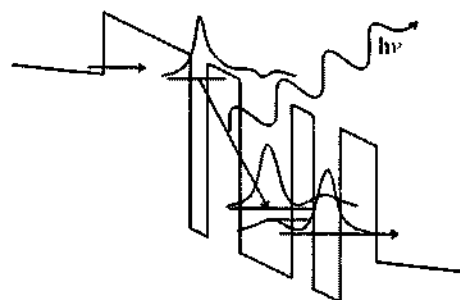


Figure 29: *Scheme of QCL light emission process by electronic transitions within ultrathin semiconductor layer*

The problem of reproducible growth of homogenous well defined nm layers of accurately mixed elements long delayed the practical realisation of quantum cascade lasers after the theoretical concept was proposed by Kazarinov and Suris [43] in 1971. Molecular beam epitaxy (MBE) finally gave access to growing the substrates for QCL production [34] and presents now a reliable manufacturing strategy in combination with a reflected high energy electron diffraction (RHEED) system to monitor the growth rate and surface structure.

## 5.2. Instrumental Setup

In general, the experimental setup for QCL measurements consists of laser driving electronics providing the pulses for the operation of the light source, a detector and data acquisition equipment to process the pulsed signal to give a digitalised response.

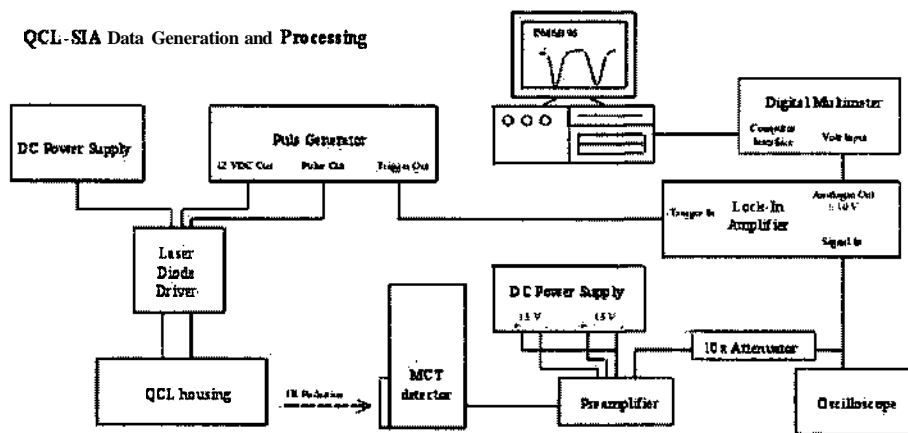


Figure 30: *QCL measurement setup*

In the case of the following conducted experiments, the laser driving electronics were purchased from Alpes Lasers (Neuchatel, Switzerland) who also provided the tested QCLs emitting at 1650 and 1080  $\text{cm}^{-1}$  wavenumbers. The dedicated equipment includes the laser housing in which to mount the QCL, a pulse generator and a pulse switching unit. The laser housing is contains a peltier element together with water connectors to allow electric and water cooling. The pulse witching unit is linked to the pulse generator defining the desired pulse shape as well as a commercial DC laboratory power supply to provide the necessary

current and voltage for laser Operation. The detection of the laser signal was done by a standard MCT (mercury cadmium telluride) detector whose response was acquired with a lock-in amplifier and passed on to a digital multi-meter serving as a computer interface to read the lock-in's analogue signal output. The data flow was recorded and visualised using the in-house written Microsoft Visual Basic 6.0 based software DMM196.

For the detection of analytes a fibre-optic flow transmission cell with adjustable optical path length (40-150  $\mu\text{m}$ ) for most flexible operation was designed and built in-house. A simple sequential injection manifold with a Cavro XP3000 syringe pump as well as a Valco Cheminert injection valve with a 10  $\mu\text{l}$  injection loop was used to provide the samples for testing the system performance.

### 5.3. Measurement of Aqueous Samples (Publication III)

The practical performance of the presented experimental setup was tested using adenine, a nucleic base without carbohydrate group and xanthosine, nucleoside with a carbohydrate unit as analytes. That way the functional group specific detection using QCLs emitting at different wavenumbers was examined. With the emission wavenumber of 1080  $\text{cm}^{-1}$  corresponding to the C-O stretching vibration of the carbohydrate group and 1650  $\text{cm}^{-1}$  representing the heteroaromatic ring structure of both species, adenine should be detected only by the second laser whereas xanthosine would generate a signal for both radiation sources.

With the positive differentiation between the two substances based on their difference in absorbance for the two wavelengths, the aspect of optical pathlength maximisation was studied. As described earlier in chapter 1.2 water absorbance poses a major problem in FT-IR measurements of aqueous samples where only pathlengths below 20  $\mu\text{m}$  are accessible with standard mid-IR light sources to get valuable information in the region of water's bending vibration at 1640  $\text{cm}^{-1}$ . The benefits of the QCL light source could be demonstrated as optical pathlengths of up to 59  $\mu\text{m}$  for the laser emitting at 1650  $\text{cm}^{-1}$  could be accessed, achieving a calculated detection limit of 70  $\text{mg/l}$  for xanthosine.

## 5.4. Conclusion and Outlook

Based on the promising results from publication III together with the experience of the workgroup's earlier work [44,45] a new instrumental setup was designed for more advanced studies in that field (Figure 31).

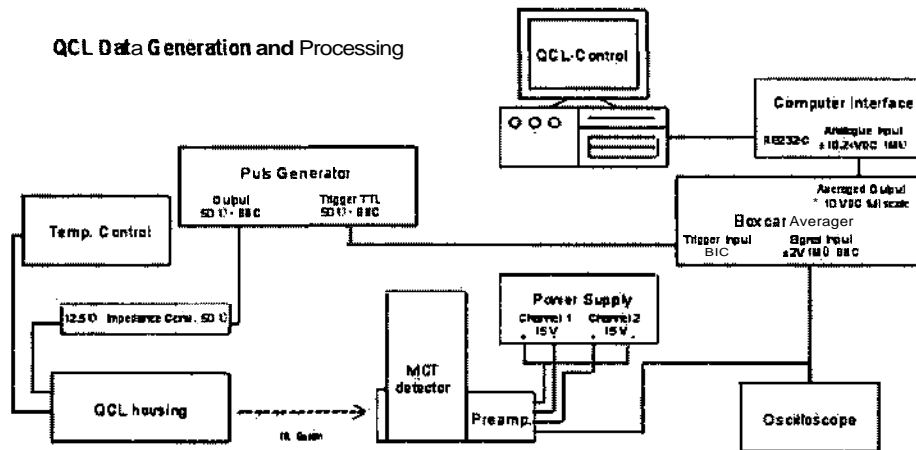


Figure 31: Improved setup for QCL detection

A special focus was set on minimising the systems background noise which was found to be resulting from general problems in the electronics such as insufficient shielding of components and non-matched impedances for connections carrying high frequency pulses. Moreover, new data acquisition equipment was implemented to replace the so far used lock-in amplifier as lock-in technology generally evaluates the detector signal of the whole time span between subsequent laser pulses. With the QCL pulse representing less than 1% of the repetition cycle this means that most of the signal is baseline noise and deteriorates the experimental readout. Therefore, the lock-in amplifier was exchanged against a boxcar averager only evaluates a defined time window of the pulse repetition cycle neglecting the unwanted baseline signal. To efficiently interface the equipment with a computer also a special computer interface was added to allow enhanced control of different parameters such as QCL temperature or pulse amplitude. The last step in this new setup development finally was the design of the dedicated Microsoft Visual Basic 6.0 based software QCL-Control as described earlier (chapter 3.2).

As by now, this more advanced QCL detection system is still being optimised for noise reduction and highest sensitivity for functional group specific analysis as part of the diploma

thesis of S. Schaden. Furthermore, an industrial cooperation with the company Anton Paar GmbH (Graz, Austria) was established for extended research on CO<sub>2</sub> in aqueous media.

## 6. REFERENCES

- 
- [1] Kellner, R.; Mermet, J.-M.; Otto, M.; Widmer, H. M. "Analytical Chemistry" WILEY-VCH: Weinheim, 1998
- [2] Ruzicka, J.; Hansen, E. H. "Flow Injection Analysis" John Wiley & Sons: New York, 1988 (2nd Ed.)
- [3] Valcárcel, M.; Luque de Castro, M. D. "Flow Injection Analysis, Principles and Applications" Ellis Horwood: Chichester, 1987
- [4] Ruzicka, J.; Hansen, E. H. "Flow Injection Analysis" Anal. Chem. **2000**, 72, 212A-217A
- [5] Ruzicka, J. "The Second Coming of Flow-Injection Analysis" Anal. Chim. Acta **1992**, 261, 3-10
- [6] Ruzicka, J.; Marshall, G. D. "Sequential Injection: A New Concept for Chemical Sensors, Process Analysis and Laboratory Assays" Anal. Chim. Acta **1990**, 237, 329-343
- [7] Griffiths, P. R.; de Haseth, J. "Fourier Transform Infrared Spectroscopy" John Wiley & Sons: New York, 1986
- [8] Chalmers, J. M.; Griffiths, P. R. "Handbook of Vibrational Spectroscopy" (Theory and Instrumentation, Vol. 1) John Wiley & Sons: New York, 2002
- [9] Adar, F.; Geiger, R.; Noonan, J. "Raman Spectroscopy for Process/Quality Control" Appl. Spectrosc. Reviews **1997**, 32, 45-101
- [10] Laserna, J. J. "Combining Fingerprinting Capability with Trace Analytical Detection: Surface-Enhanced Raman Spectrometry" Anal. Chim. Acta **1993**, 283, 607-622
- [11] Kneipp, K.; Kneipp, H.; Itzkan, L.; Dasari, R. R.; Feld, M. S. "Ultrasensitive Chemical Analysis by Raman Spectroscopy" Chem. Rev. **1999**, 99, 2957-2975
- [12] Fleischmann, M.; Hill, I. R. "Electrochemical Effect in Surface Enhanced Raman Scattering" Surf. Enhanced Raman Scattering **1982**, 275-292
- [13] Wu, D. Y.; Ren, B.; Tian, Z. Q. "Progress in the Theory of Surface Enhanced Raman Scattering" Internet J. Vib. Spectro. [www.ijvs.com] **2000**, 4, no pp. given
- [14] Lendl, B.; Kellner, R. "Determination of Sucrose by Flow Injection Analysis with Fourier Transform Infrared Detection" Mikrochim. Acta **1995**, 119, 73-79
- [15] Edelmann, A.; Diewok, J.; Schuster, K. C.; Lendl, B. "Rapid Method for the Discrimination of Red Wine Cultivars based on Mid-Infrared Spectroscopy of Phenolic Wine Extracts" J. Agric. Food Chem. **2001**, 49, 1139-1145
- [16] Edelmann, A.; Lendl, B. "Toward the Optical Tongue: Flow-Through Sensing of Tannin-Protein Interactions based on FTIR Spectroscopy" J. Am. Chem. Soc. **2002**, 124, 14741-14747

- 
- [17] Lendl, B.; Ehmoser, H.; Frank, J.; Schindler, R. "Flow Analysis based Surface Enhanced Raman Spectroscopy employing exchangeable Micro-Beads as SERS Active Surfaces" *Appl. Spectrosc.* 2000, *54*, 1012-1018
- [18] Robertson, A. M.; Littlejohn, D.; Brown, M.; Dowle, C. J. "Assessment of Thermospray Interface for the Coupling of High-Performance Liquid Chromatography and Fourier Transform Infrared Spectrometry" *J. Chromatogr.* 1991, *588*, 15-24
- [19] Robertson, R. M.; de Haset, J. A.; Kirk, J. D.; Browner, R. F. "MAGIC-LC/FT-IR Spectrometry: Preliminary Studies" *Appl. Spectrosc.* 1988, *42*, 1365-1368
- [20] Robertson, R. M.; de Haset, J. A.; Browner, R. F. "MAGIC-LC/FT-IR Spectrometry with Buffered Solvent Systems" *Appl. Spectrosc.* 1990, *44*, 8-13
- [21] Turula, V. E.; de Haset, J. A. "Evaluation of Particle Beam Fourier Transform Infrared Spectrometry for the Analysis of Globular Proteins: Conformation of  $\beta$ -Lactoglobulin and Lysozyme" *Appl. Spectrosc.* 1994, *48*, 1255-1264
- [22] Turula, V. E.; de Haset, J. A. "Particle Beam LC/FT-IR Spectrometry Studies of Biopolymer Conformations in Reversed-Phase HPLC Separations: Native Globular Proteins" *Anal. Chem.* 1996, *68*, 629-638
- [23] Venkateshwaran, T. G.; Stewart, J. T.; de Haset, J. A.; Bardett, M. G. "Solution Conformation of model Polypeptides with the use of Particle Beam LC/FT-IR Spectrometry and Electrospray Mass Spectrometry" *J. Pharm. Biomed. Anal.* 1999, *19*, 709-723
- [24] Raynor, M. W.; Bartle, K. D.; Cook, B. W. "Electrospray Micro Liquid Chromatography-Fourier Transform Infrared Micro Spectrometry" *J. High Resolut. Chromatogr.* 1992, *15*, 361-366
- [25] Somsen, G. W.; Hooijschuur, E. W. J.; Gooijer, C.; Brinkman, U. A. Th.; Veithorst, N. H.; Visser, T. "Coupling of Reversed-Phase Liquid Column Chromatography and Fourier Transform Infrared Spectrometry using Postcolumn On-Line Extraction and Solvent Elimination" *Anal. Chem.* 1996, *68*, 746-752
- [26] Somsen, G. W.; Jagt, L.; Gooijer, C.; Velthorst, N. H.; Brinkman, U. A. Th.; Visser, T. "Identification of Herbicides in River Water using On-Line Trace Enrichment combined with Column Liquid Chromatography-Fourier Transform Infrared Spectrometry" *J. Chromatogr. A* 1996, *756*, 145-157
- [27] Vredenburg, M. J.; ten Hove, G. J.; de Jong, A. P. M.; Visser, T.; Somsen, G. W. "Flexible Off-Line LC-IR Interfacing by Micro-Column Switching and Addition of a Make-Up Liquid" *Mikrochim. Acta* 1997, *14*, 725-727
- [28] Visser, T.; Vredenburg, M. J.; ten Hove, G. J.; de Jong, A. P. M.; Somsen, G. W. "Gradient Elution Liquid Chromatography-Infrared Spectrometry at  $\mu\text{g} \cdot \text{l}^{-1}$  level using Capillary Column Switching and Addition of a Make-Up Liquid. A Preliminary Study." *Anal. Chim. Acta* 1997, *342*, 151-158
- [29] Liu, M. X.; Dwyer, J. L. "Quantitative Analysis of Copolymers of GPC/FT-IR" *Appl. Spectrosc.* 1996, *50*, 349-356

- [30] Bourne, S. "An Online Direct-Deposition FTIR Detector for Chromatographs" Am. Lab. **1998**, *30*, 17F, 17H, 17J
- [31] Önerfjord, P.; Nilsson, J.; Wallman, L.; Laurell, T.; Marko-Varga, G. "Picoliter Sample Preparation in MALDI-TOF MS using a Micromachined Silicon Flow-Through Dispenser" Anal. Chem. **1998**, *70*, 4755-4760
- [32] Welter, E.; Neidhart, B. "Acoustically Levitated Droplets - A new tool for Micro and Trace Analysis" Fresenius J. Anal. Chem. **1997**, *357*, 345-350
- [33] Eberhardt, R.; Neidhart, B. "Acoustic Levitation Device for Sample Pretreatment in Microanalysis and Trace Analysis" Fresenius J. Anal. Chem. **1999**, *365*, 475-479
- [34] Faist, J.; Capasso, F.; Sivco, D. L.; Sirtori, C.; Hutchinson, A. L.; Cho, A. Y. "Quantum Cascade Laser" Science **1994**, *264*, 553-556
- [35] Namjou, K.; Cai, S.; Whittaker, E. A.; Faist, J.; Gmachl, C.; Capasso, F.; Sivco, D. L.; Cho, A. Y. "Sensitive Absorption Spectroscopy with Room-Temperature Distributed-Feedback Quantum-Cascade Laser" Optics Letters **1998**, *23*, 219-221
- [36] Gmachl, C.; Capasso, F.; Sivco, D. L.; Cho, A. Y. "Recent Progress in Quantum Cascade Lasers and Applications" Rep. Prog. Phys. **2001**, *64*, 1533-1601
- [37] Laurell, T.; Wallman, L.; Nilsson, J. "Design and Development of a Silicon Microfabricated Flow-Through Dispenser for On-line Picolitre Sample Handling" J. Micromech. Microeng. **1999**, *9*, 369-376
- [38] Lapadatu, D.; Kittiisland, G.; Nese, M.; Nilsen, S. M.; Jakobsen, H. "A Model for the etch-stop location on reverse-biased pn junctions" Sensors Actuators A **1998**, *66*, 259-267
- [39] Wallman, L.; Bengtsson, J.; Danielsen, N.; Laurell, T. "Electrochemical Etch-Stop Technique for Silicon Membranes with p- and n-type regions and its Application to neutral Sieve Electrodes" J. Micromech. Microeng. **2002**, *12*, 265-270
- [40] Creighton, J. A.; Blatchford, C. G.; Albrecht, M. G. "Plasma Resonance Enhancement of Raman Scattering by Pyridine adsorbed on Silver or Gold Sol Particles of Size comparable to the Excitation Wavelength" J. Chem. Soc., Faraday Trans. 2 **1979**, *75*, 790-798
- [41] Lee, P. C.; Meisel, D. "Adsorption and Surface-Enhanced Raman of Dyes on Silver and Gold Sols" J. Phys. Chem. **1982**, *86*, 3391-3395
- [42] Miller, D. A. B. "Optical Physics of Quantum Wells" Proc. of the Scottish Universities Summer School in Physics (1996), Volume Date 1994, 44<sup>th</sup> (Quantum Dynamics of Simple Systems), 239-266
- [43] Kazarinov, R. F.; Suris, R. A. "Possible Amplification of Electromagnetic Waves in a Semiconductor with a Superlattice" Fiz. Tekh. Poluprov. **1971**, *5*, 797-800 (Russian) English translation published in Sov. Phys. Semicond. **1971**, *5*, 707
- [44] Lendl, B.; Frank, J.; Schindler, R.; Müller, A.; Beck, M.; Faist, J. "Mid-Infrared Quantum Cascade Lasers for Flow Injection Analysis" Anal. Chem. **2000**, *72*, 1645-1648

- [45] Edelmann, A.; Ruzicka, C.; Frank, J.; Lendl, B.; Schrenk, W.; Gornik, E.; Strasser, G. "Towards functional group specific detection in High-Performance Liquid Chromatography using Mid Infrared Quantum Cascade Lasers" *J. Chromatogr. A* **2001**, *934*, 123-128

# I

Haberkorn, M.; Frank, J.; Harasek, M.; Nilsson, J.; Laurell, T.; Lendl, B.

*"Flow-Through Picoliter Dispenser  
A New Approach for Solvent Elimination in FT-IR Spectroscopy"*

Applied Spectroscopy **2002**, 56, 902-908

# Flow-Through Picoliter Dispenser: A New Approach for Solvent Elimination in FT-IR Spectroscopy

MICHAEL HABERKORN, JOHANNES FRANK, MICHAEL HARASEK,  
JOHAN NILSSON, THOMAS LAURELL, and BERNHARD LENDL\*

*Institute of Analytical Chemistry, Vienna University of Technology, Getreidemarkt 9/151, A-1060 Vienna, Austria (M. Haberkorn, B.L.); Institute of Physical Chemistry, Vienna University of Technology, Getreidemarkt 9/156, A-1060 Vienna, Austria (J.F.); Institute of Chemical Engineering, Fuel and Environmental Technology, Vienna University of Technology, Getreidemarkt 9/159, A-1060 Vienna, Austria (M. Harasek); and Department of Electrical Measurements, Lund University, P.O. Box 118, S-221 00 Lund, Sweden (J.N., T.L.)*

A new interface for FT-IR analysis of liquid samples on the basis of solvent elimination is presented. The approach is based on a piezoactuated flow-through microdispenser, a device built of two microstructured silicon wafers designed for micro-liquid handling. It could be verified during preliminary studies using a sequential injection (SI) system for automated liquid handling that the flow-through microdispenser as a possible interface for flow system-FT-IR analysis has the capability of meeting the demands of hyphenated miniaturized liquid handling systems (e.g.,  $\mu$ -HPLC, micro-high performance liquid chromatography), as it successfully provides highly stable, reliable and reproducible operating conditions for liquid handling in the picoliter range. Moreover, an increase in sensitivity for FT-IR measurements could be achieved, lowering the mass detection limit of sugars (such as the investigated sucrose) to 53 picograms. As is demonstrated on the example of an HPLC separation of a mixture of glucose and fructose, interfacing LC systems to FT-IR using a piezoactuated flow-through microdispenser is a feasible and promising approach.

Index Headings: Flow-through microdispenser; Solvent elimination; Fourier transform infrared spectroscopy; FT-IR; Micro-liquid handling.

## INTRODUCTION

Automated flow systems represent very versatile and robust tools for carrying out reactions, separations, and sample delivery functions.<sup>1</sup> In combination with these flow systems, a variety of detectors are available, of which IR spectroscopic detection is of special interest. As most organic compounds and also a wide range of inorganic substances have narrow absorption bands in the mid-infrared spectral region, the absorbing substance's IR spectrum represents a unique fingerprint. Hence, IR spectrometry generally would be an ideal detection method to identify dissolved analytes, as, for instance, in the case of fractions separated by liquid chromatography (LC).<sup>2</sup>

However, the fact that most substances are IR active implies that not only the analytes contribute to the recorded spectra, but also the carrier liquid of the flow systems contributes. Here, the solvent's spectral features dominate against absorbance bands resulting from the comparatively vanishing amount of analyte. As a consequence, several severe limitations have to be considered upon on-line IR detection of liquid samples using flow-

through cells.<sup>3,4</sup> One restriction is the range of spectral information that can be gained from the analyte in solution, which is limited by the absorbance features of the solvent leading to total extinction of radiation in some regions. Moreover, the maximum optical pathlength accessible with IR spectroscopy is limited to a certain value given by the detector requiring a minimum amount of energy in order to record data with a reasonable signal-to-noise ratio. This in turn significantly increases analyte detection limits. Novel intense IR sources, such as quantum cascade lasers (QCLs), promise to minimize these drawbacks.<sup>5-7</sup> However, the use of solvent gradients for liquid separation methods is also prohibited by the fact that the subtraction of changing eluent bands is hardly possible. Another problem arising from the restricted analysis time on-hand when measuring dynamic samples as in the case of Chromatographie techniques is the limited possibility of signal averaging to improve the signal-to-noise ratio.

In order to overcome the problems of significant solvent interference, much current research effort is focused on solvent elimination approaches. Different kinds of thermospray,<sup>8</sup> particle beam,<sup>9-13</sup> electrospray,<sup>14</sup> pneumatic nebulizer,<sup>15-18</sup> and ultrasonic nebulizer<sup>19,20</sup> interfaces are used for evaporation of carrier fluids and hence, to eliminate the effect of solvent absorbance on the signal generated by the analyte under investigation.<sup>21</sup> Still, not all approaches led to maximum exploitation of physical limits resulting from the nature of vibrational spectroscopic detection. Concentrating the deposited analyte into the IR beam probing the solid support significantly influences detection limits and therefore, is of major importance for successful improvement of sensitivity. Most of the published procedures, however, fail to provide deposits smaller than 200  $\mu\text{m}$  in diameter, but as modern FT-IR microscopes are capable of sampling spots as small as 100  $\mu\text{m}$ , there is further potential for performance enhancement focusing on optimization of sample deposition.

In this article a novel LC FT-IR interfacing approach based on drop-on-demand deposition is presented. A piezoactuated flow-through microdispenser, developed by T. Laurell et al.,<sup>22</sup> is used to dispense small, defined sample volumes (typically around 60 pL) with high precision and accuracy, generating solid deposits with diameters in the range of 40 to 80  $\mu\text{m}$ . So far the flow-through microdispenser has been successfully applied for various inter-

Received 20 November 2001; accepted 20 February 2002.

\* Author to whom correspondence should be sent.

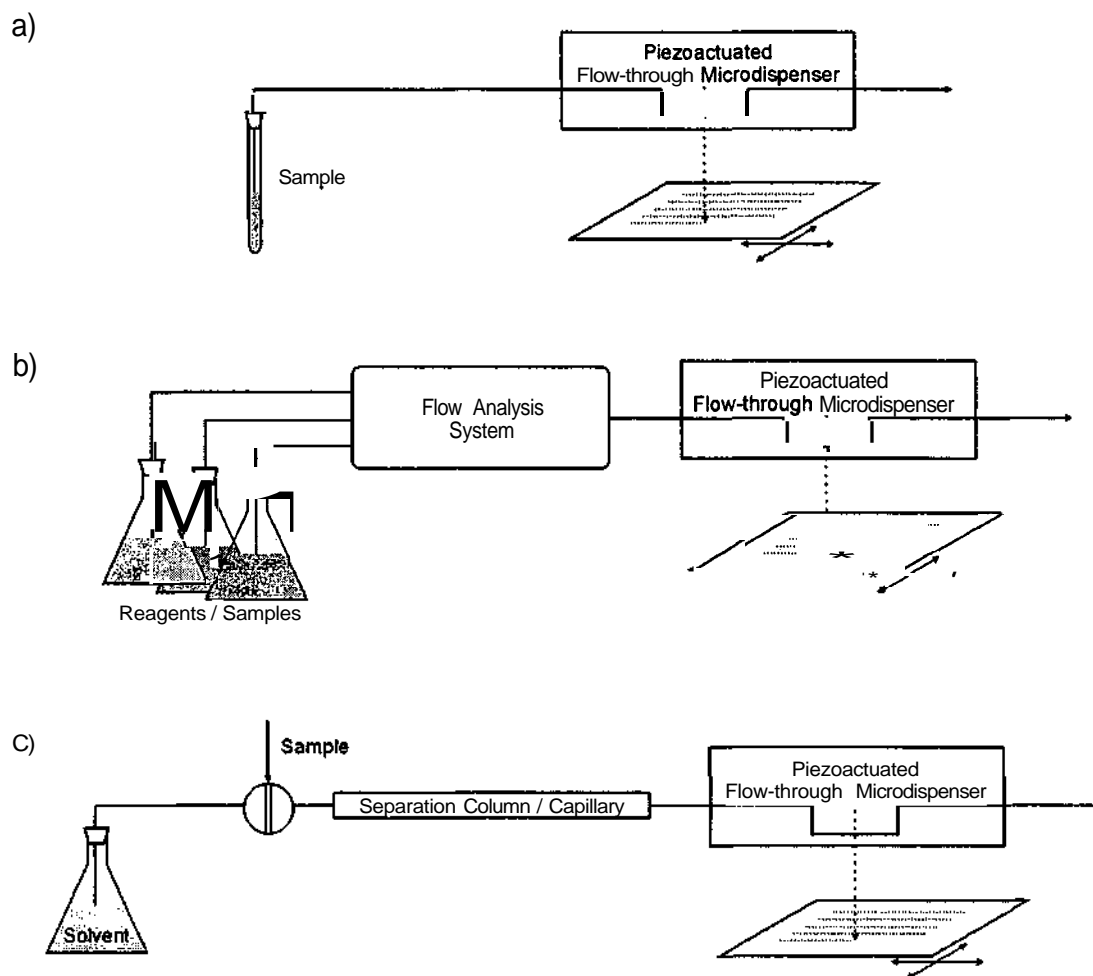


FIG. 1. Main set-ups for possible FT-IR interfacing implementing the flow-through microdispenser.

face developments in the field of mass spectrometry,<sup>23-29</sup> cell analysis with fluorescence imaging detection,<sup>30</sup> as a tool for sample enrichment prior to capillary electrophoresis,<sup>31</sup> for the fabrication of enzyme microstructures on gold surfaces,<sup>32</sup> and to study diffusion coefficients of redox species.<sup>33</sup> In general, the microdispensing device is based on the principle applied for inkjet printing, which is an already well established technique for micro-liquid handling systems,<sup>34,35</sup> with the one significant difference that the dispenser is designed for flow-through operation. This special characteristic provides high flexibility in the choice of solvent flow rates as there is no necessity to deposit the whole amount of liquid eluting from the separation system. Moreover, it allows implementation of auxiliary detection devices for collection of further information on the sample under investigation, which is not possible in other sophisticated solvent elimination approaches.<sup>36-39</sup>

As possible applications of the presented micro-liquid handling FT-IR interface, three different setups are imaginable for future methodological development: in the case of minimum amounts of sample available for analysis (Fig. 1a), such as in biomedical research objectives, the microdispenser represents a valuable sample delivery tool enabling accurate and precise handling of liquids in the picoliter range; for applications

where high throughput sampling and increased sensitivity is of importance (Fig. 1b), e.g., in the case of automated flow analysis systems such as solid phase extraction (SPE) systems for analysis of phenols in wine,<sup>40</sup> the automated combination of the computer controlled x,y-stage with the microdispenser provides the possibility of creating high density microarrays of the smallest dry analyte deposits (around 50  $\mu\text{m}$  in diameter); and finally, to interface liquid separation techniques (capillary electro chromatography (CEC), capillary electrophoresis (CE),  $\mu$ -HPLC) to FT-IR spectrometry where usually the mobile phase or solvent is the major concern limiting the performance of the spectroscopic detection method (Fig. 1c), the presented dispenser can be of high benefit considering the fast evaporation of picoliter amounts of solvent (below 1 s at room temperature and atmospheric pressure with water as a solvent). This article focuses on the two latter aspects of implementing the flow-through microdispenser for highly sensitive measurements of sample solutions with FT-IR in a solvent elimination approach.

## EXPERIMENTAL

**Flow-Through Microdispenser Setup.** The flow-through microdispenser is a micro-liquid handling de-

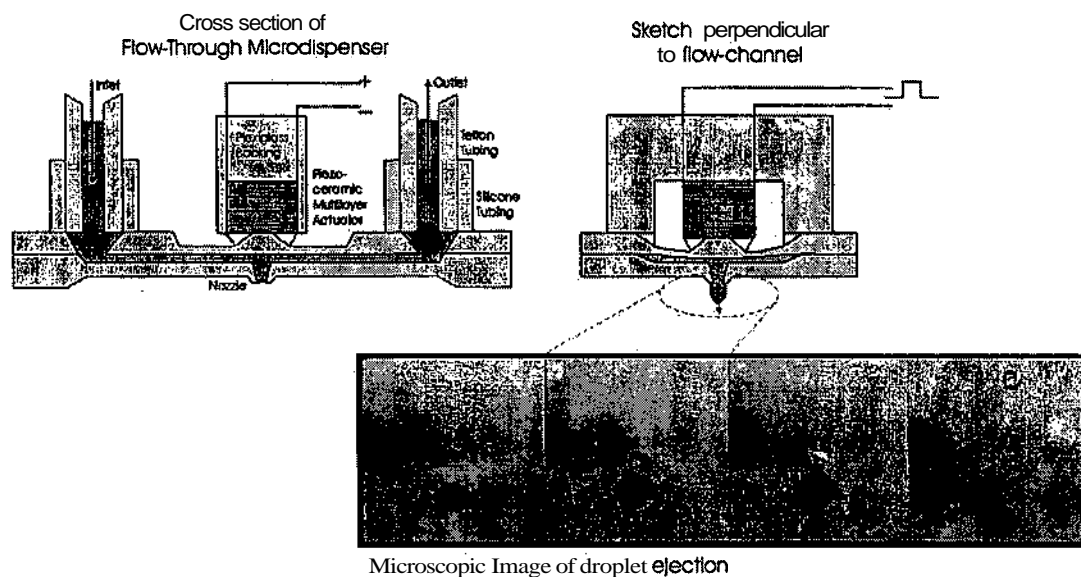


FIG. 2. Cross-section of the piezoactuated flow-through microdispenser with microscopic image of droplet formation.

vice formed by two silicon structures by conventional micromachining (Fig. 2). A piezoceramic element generates a pressure pulse in the flow-through channel, which forces droplets in the range of around 60 pL to be dispensed through the nozzle. The pyramid-shaped nozzle ensures high stability in operating the dispenser and makes this **drop-on-demand** device a high precision tool, especially focusing towards capillary chromatography FT-IR systems. To drive the piezoceramic element, a dc power supply (Votcraft® DIGI 35) together with a computer controlled arbitrary waveform generator (Agilent 33120 A, Agilent Technologies, Palo Alto, CA) was used to provide an electronic pulse with defined amplitude (9 V), width (500  $\mu$ s), rise (20  $\mu$ s), and decay time (3 ms).

The droplet sizes generated by the dispensing device were analyzed with the help of a phase Doppler anemometer (PDA, TSI GmbH, Aachen, Germany).

To enable lateral location of the deposits on the solid support with a precision of  $\pm 5 \mu$ m, a computer controlled x,y-stage (Applied Motion Products Inc.) with step sizes of 2.5  $\mu$ m and a maximum distance of 15 mm was implemented in the dispensing unit.

All computer controlled components of the microdispensing unit and the sequential injection (SI) system described below were operated with the help of an in-house-written MS Visual Basic 6.0 (Microsoft) based software program (Sagittarius, Version 3.5.0.567) installed on a Pentium 90 PC with 64 MB RAM and Windows 95 operating system.

**Liquid Handling Components—SI and HPLC Equipment.** For performance assessment of the flow-through microdispenser unit, a sequential injection system was set up to simplify studies of the microdispenser characteristics by simulation of sample elution peaks (see Fig. 3). The SI system featured a Cavro XP 3000 syringe pump (CAVRO Scientific Instruments, Sunnyvale, CA) equipped with a 500  $\mu$ L syringe and a Cavro XL Series Smart Valve, a 6 port selection valve. The PTFE tubing

(i.d. 750  $\mu$ m) and the fittings of the flow system were purchased from Global FIA Inc. (Gig Harbor, WA). In all experiments based on the sequential injection system, 200  $\mu$ L of the sample under investigation were passed through the microdispenser at a flow rate of 400  $\mu$ L/min with distilled water as the carrier solvent.

In the case of HPLC measurements, the SI system was replaced by an HPLC system consisting of a Merck/Hitachi L-7100 pump with a Rheodyne 7725 injection valve featuring a 50- $\mu$ L sample loop, a 4 X 3 mm guard column (Phenomenex Carbo-Ca<sup>2+</sup>) and a 300 X 7.8 mm separation column (Phenomenex Rezex 8% Ca. Monos.). The stationary phase of the guard as well as the separation column was composed of sulfonated styrene divinylbenzene anionic exchange resins with calcium counter ions with a particle size of 8  $\mu$ m and a cross linkage of 8%. In order to maintain an optimum separation temperature of 80 °C, the column was placed in a thermostated water bath and the experiments were performed at flow rates of 400  $\mu$ L/min, as in the case of the SI system.

**FT-IR Measurement.** For FT-IR measurements the analyte solutions were deposited on calcium fluoride supports (38 X 19 X 2 mm) and analyzed with a Vector 22 Fourier transform spectrometer (Bruker GmbH, Germany) equipped with an IR microscope (IR Plan®, Spectra Tech, Shelton, CT) operated in transmission mode.

The spectra were recorded by coaddition of 100 scans collected at a mirror velocity of 20 kHz HeNe frequency using an aperture narrowing the IR beam down to 100  $\mu$ m in diameter and a high sensitivity, liquid nitrogen cooled mercury cadmium telluride (MCT) detector (Graseby Infrared, Newmarket, UK). For each deposit a new background spectrum was collected in close vicinity to the sample spot in order to keep background instabilities due to surface irregularities of the CaF<sub>2</sub> support at a minimum. CaF<sub>2</sub> is a robust and comparatively inexpensive IR transparent sub-

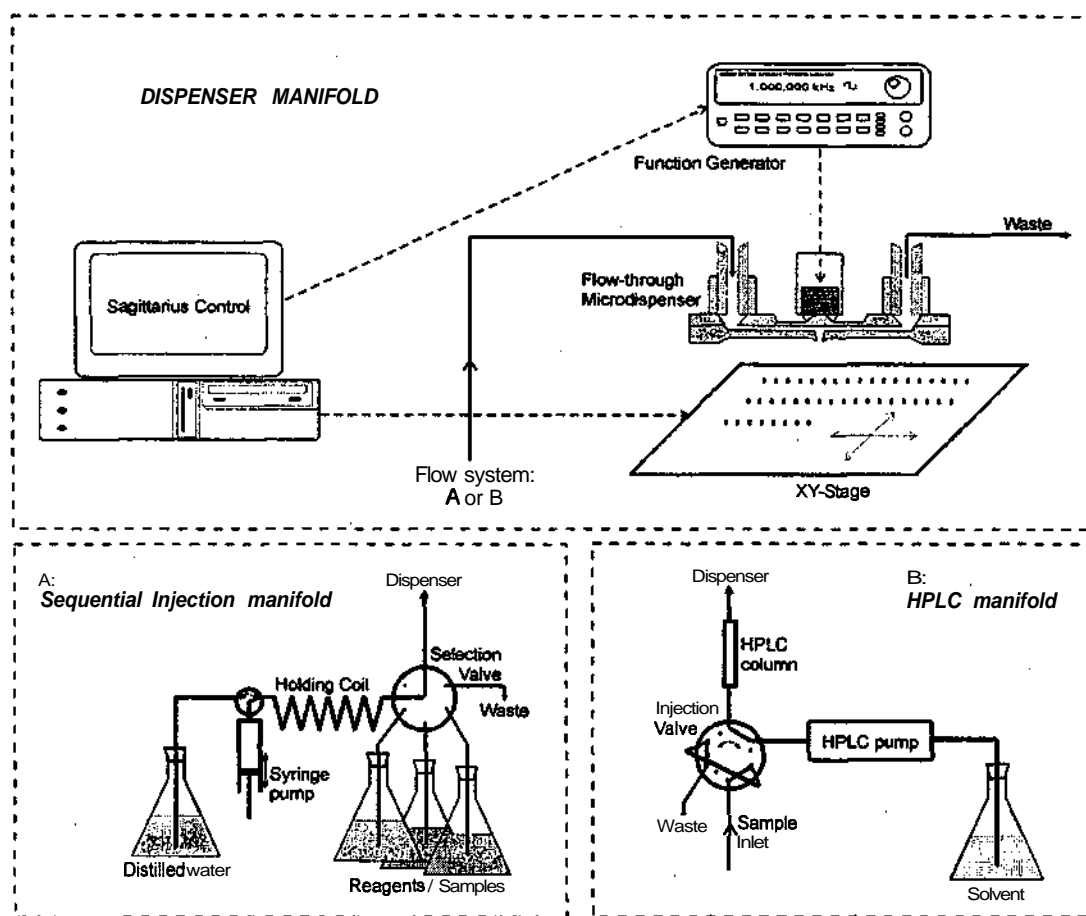


FIG. 3. Scheme of the dispenser setup. Dispenser stage with optional (A) sequential injection or (B) HPLC manifold.

strate, which is only attacked by very acidic solutions, but in general any IR transparent material can be used as a solid support for the dispenser. Care, however, must be taken that the surface is clean and smooth, as this will effect the crystallization behavior of the analyte, causing artifacts in the gained IR spectra.

**Reagents.** All chemicals were of analytical grade. D(-)-fructose and sucrose were both purchased from Merck (Darmstadt, Germany), whereas D(+)-glucose monohydrate was obtained from Fluka (Buchs, Switzerland). The laboratory's deionized water served as an eluent for the HPLC separation procedure.

## RESULTS AND DISCUSSION

**Flow-Through Microdispenser Performance Assessment.** Analyzing the microdispenser droplets with a phase Doppler anemometer showed that the drops generated from water have a diameter of  $46.7 \mu\text{m}$  (with a standard deviation below the detection limit of  $0.1 \mu\text{m}$ ), representing a respective volume of  $53.3 \text{ pL}$ . Slight changes in the droplet volume (a few picoliters) due to differences in surface tension of different solutions can be controlled by modification of the applied electrical pulse driving the piezoceramic element. During further initial performance studies of the flow-through microdispenser analyte deposition approach, it could be verified that by exploitation of the highly stable dispensing

conditions offered by the piezoactuated dispenser, absolute amounts of sucrose down to  $53 \text{ pg}$  became accessible to quantitative evaluation in the mid-infrared region. The spectrum of such a low amount of analyte was still clearly interpretable, and by performing a linear regression on the MIR transmission data gained from different standards of sucrose, a linear correlation between the peak area from  $1080$  to  $1027 \text{ cm}^{-1}$  with a horizontal baseline set at  $1174 \text{ cm}^{-1}$  and the absolute amount deposited in the range between  $53$  and  $5300 \text{ pg}$  could be found with a correlation coefficient of  $0.9946$  (Fig. 4).

With the help of co-deposition experiments, the dispenser's precision and the effect of drop accumulation on the recorded spectra were investigated. As can be seen in Fig. 5, deposition of multiple droplets of a  $10 \text{ g/L}$  sucrose standard solution at the same spot at rates of  $1 \text{ Hz}$  results in regular, circular-shaped sample deposits. The spot diameters vary, depending on the amount of sucrose deposited on the  $\text{CaF}_2$  support, between  $30$  and  $60 \mu\text{m}$ . This again means that the whole sample is being probed by the IR beam, which has a diameter of  $100 \mu\text{m}$ . Also, the resulting spectra can be calibrated against the number of co-deposited droplets. However, the best reasonable regression is achieved applying a second-order polynomial function to correlate the peak area from  $1080$  to  $1027 \text{ cm}^{-1}$  with a horizontal baseline point at  $1174 \text{ cm}^{-1}$  with the number of drops

Different amounts of sucrose (53 - 5300 pg)  
by co-deposition of 10 drops (53 pL each)

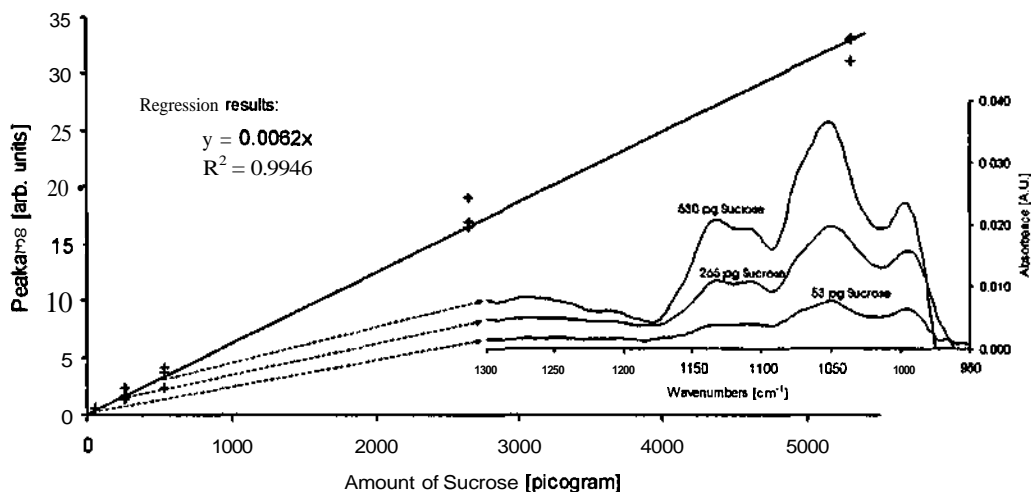


FIG. 4. Linear calibration of spectra collected from sucrose deposits gained by co-deposition of 10 drops (53 pL each) of different concentrated solutions (0.1, 0.5, 1, 5, and 10 g/L), plus according spectra of 53, 265, and 530 pg sucrose.

deposited on top of each other. In the tested calibration set from 1 to 10 drop co-deposition, a correlation coefficient of 0.9722 was determined for a second-order polynomial regression function.

**HPLC-Microdispenser-FT-IR.** To demonstrate the applicability of the flow-through microdispenser as an interface for LC and FT-IR, a mixture of glucose and fructose (concentrations: 25 g/L each) was separated and the eluting solution was passed through the dispenser. Upon dispensing 53 pL fractions per second, the solvent was evaporated at room temperature and atmospheric pressure with a droplet evaporation time below one second, leaving behind a solidified trace of the chromatogram. The liquid volume required for this deposition procedure (3.2 nL/min) represents 0.01‰ of the eluent flow passing through the dispenser, which results in a major waste flow. Considering future objectives of interfacing miniaturized liquid sample handling systems in which the amount of analyte available for analysis is the crucial limitation, this minimum volume requirement of the flow-through microdispenser will be of high benefit. Figure 6a gives the 3D plot of the collected mid-infrared spectra of the HPLC-separated sugars, each spectrum representing the IR absorbance information of one deposited spot on the  $\text{CaF}_2$  support. As already mentioned in the experimental section, 100 scans collected at 20 kHz HeNe frequency mirror velocity were coadded in order to keep noise level in the spectra low. At this scanning speed, however, it takes approximately 60 s to gain a single

spectrum, which would have limited the resolution of the sample peaks to a maximum of about 2 spectra if measured on-line in a flow cell under dynamic conditions. In the presented case, the time resolution is 2 s for spectra gained from 100 coadded scans at 20 kHz HeNe frequency. This can be considered one of the significant advantages of the proposed LC FT-IR approach applied to a relatively large scale separation technique like standard HPLC.

Plotting the absorbance at the  $1060 \text{ cm}^{-1}$  wavenumber, which is representative for both sugars, against time gives the typical Chromatographic peaks that one would expect from a nonselective detector reacting on both compounds (Fig. 6b) not capable of substance identification.

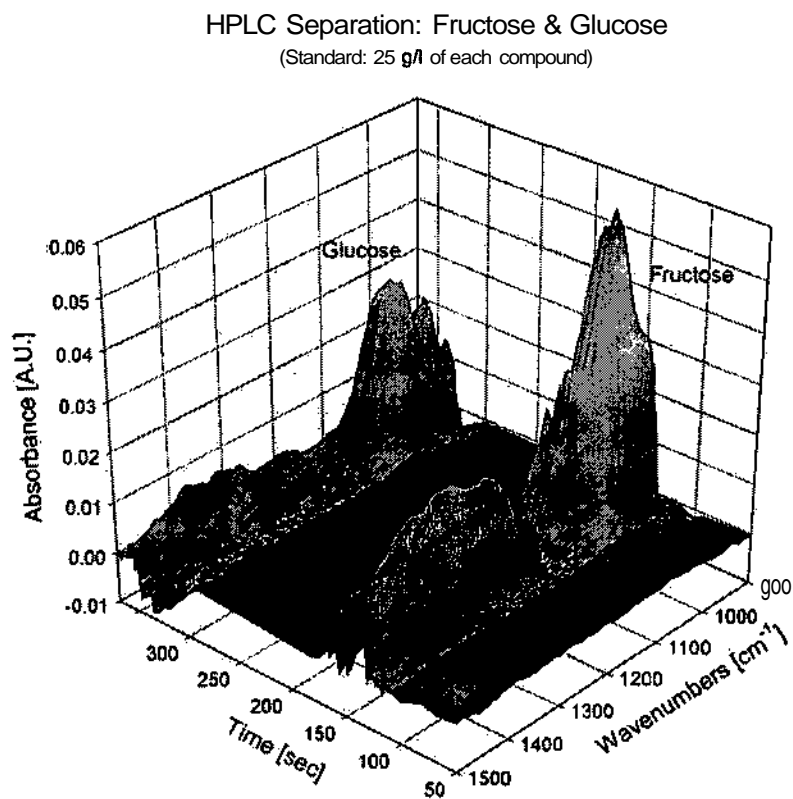
## CONCLUSION

We have demonstrated the feasible application of a piezoactuated flow-through microdispenser as a solvent elimination FT-IR interface. The presented interface has provided a significant enhancement to analyte detection by solvent elimination already at room temperature and atmospheric pressure. The new approach also proved reliable liquid handling in the picoliter range and droplet deposition with high lateral resolution, which opens access to further improvement in sensitivity by possible droplet co-deposition in order to preconcentrate analytes on a spot prior to measurement.



FIG. 5. Microscopic image of co-deposition experiments with a 10 g/L sucrose standard solution.

a)



b)

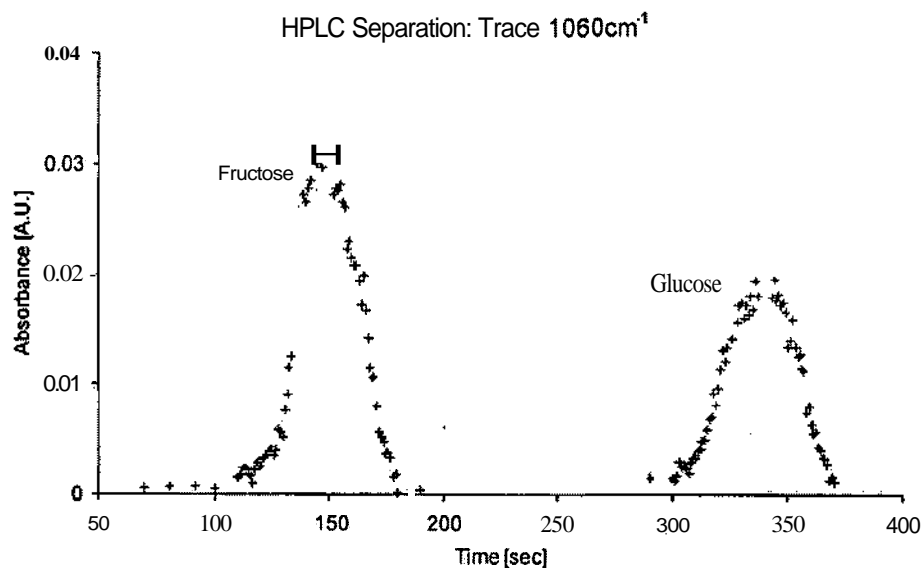


FIG. 6. Chromatogram of HPLC separation of 25 g/L standard mixture of fructose and glucose; (a) 3D plot of gained spectra; (b) time trace of absorbance at  $1060\text{cm}^{-1}$  wavenumbers.

The microdispenser's stability and precision in handling of small liquid volumes makes this interfacing approach match the demands of flow systems serving as reaction, separation, and sample delivery tools.

Future research work will be focused on the optimization of the target surface in order to further enhance sensitivity and reproducibility of the presented flow-through microdispenser interface.

## ACKNOWLEDGMENT

The authors thankfully acknowledge **DI Axel Breuer** from **TSI GmbH** (Aachen, Germany) for providing the phase Doppler anemometer as a demonstration instrument. Further grateful acknowledgment is given for the financial support received from the Austrian Science Fund within project **P13686 ÖCH**.

1. J. Ruzicka, *Anal. Chim. Acta* 261, 3 (1992).
2. G. W. Somsen, C. Gooijer, and U. A. Th. **Brinkman**, *J. Chromatogr., A* 856, 213 (1999).
3. R. Vonach, B. Lendl, and R. Kellner, *Anal. Chem.* 69, 4286 (1997).
4. R. **Vonach**, B. Lendl, and R. Kellner, *J. Chromatogr., A* 824, 159 (1999).
5. B. Lendl, J. Frank, R. Schindler, A. Müller, M. Beck, and J. Faist, *Anal. Chem.* 72, 1645 (2000).
6. A. Edlmann, C. Ruzicka, J. Frank, W. Schrenk, E. Gornik, G. Strasser, and B. Lendl, *J. Chromatogr., A* 934, 123 (2001).
7. **M. Kölhed**, V. Pustogov, B. Mizaikoff, M. Haberkorn, J. Frank, B. Karlberg, and B. Lendl, *Vib. Spectrosc.*, paper in press (2002).
8. A. M. Robertson, D. Littlejohn, M. Brown, and C. J. **Dowle**, *J. Chromatogr.* 588, 15 (1991).
9. R. M. Robertson, J. A. de **Haseth**, J. D. Kirk, and R. F. Browner, *Appl. Spectrosc.* 42, 1365 (1988).
10. R. M. Robertson, J. A. de Haseth, and R. F. Browner, *Appl. Spectrosc.* 44, 8 (1990).
11. V. E. Turula and J. A. de Haseth, *Appl. Spectrosc.* 48, 1255 (1994).
12. V. E. Turula and J. A. de Haseth, *Anal. Chem.* 68, 629 (1996).
13. T. G. Venkateshwaran, J. T. Stewart, J. A. de Haseth, and M. G. **Bartlett**, *J. Pharm. Biomed. Anal.* 19, 709 (1999).
14. M. W. Raynor, K. D. **Bartle**, and B. W. Cook, *J. High Resolut. Chromatogr.* 15, 361 (1992).
15. G. W. Somsen, E. W. J. Hooijschuur, C. Gooijer, U. A. Th. Brinkman, N. H. Velthorst, and T. Visser, *Anal. Chem.* 68, 746 (1996).
16. G. W. Somsen, I. Jagt, C. Gooijer, N. H. Velthorst, U. A. Th. Brinkman, and T. Visser, *J. Chromatogr., A* 756, 145 (1996).
17. M. J. Vredenburg, G. J. ten Hove, A. P. M. Jong, T. Visser, and G. W. Somsen, *Mikrochim. Acta* 14, 725 (1997).
18. T. Visser, M. J. Vredenburg, G. J. ten Hove, A. P. M. Jong, and G. W. Somsen, *Anal. Chim. Acta* 342, 151 (1997).
19. M. X. Liu and J. L. Dwyer, *Appl. Spectrosc.* 50, 349 (1996).
20. S. Bourne, *Am. Lab.* 30, F17 (1998).
21. J. C. Jones, D. Littlejohn, and P. R. Griffiths, *Appl. Spectrosc.* 53, 792 (1999).
22. T. Laurell, L. Wallman, and J. Nilsson, *J. Micromech. Microeng.* 9, 369 (1999).
23. P. Önerfjord, S. Ekström, J. Bergquist, J. Nilsson, T. Laurell, and G. **Marko-Varga**, *Rapid Commun. Mass Spectrom.* 13, 315 (1999).
24. T. Miliotis, S. Kjellström, J. Nilsson, T. Laurell, L.-E. Edholm, and G. Marko-Varga, *J. Mass Spectrom.* 35, 369 (2000).
25. T. Miliotis, S. Kjellström, P. Önerfjord, J. Nilsson, T. Laurell, L.-E. Edholm, and G. Marko-Varga, *J. Chromatogr., A* 886, 99 (2000).
26. S. Ekström, P. Önerfjord, J. Nilsson, M. Bengtsson, T. Laurell, and G. Marko-Varga, *Anal. Chem.* 72, 286 (2000).
27. S. Ekström, D. Ericsson, P. Önerfjord, M. Bengtsson, J. Nilsson, G. Marko-Varga, and T. Laurell, *Anal. Chem.* 73, 214 (2001).
28. T. Laurell, J. Nilsson, and G. Marko-Varga, *J. Chromatogr., B* 752, 217 (2001).
29. T. Miliotis, P.-O. Ericsson, G. Marko-Varga, R. Svensson, J. Nilsson, T. Laurell, and R. Bischoff, *J. Chromatogr., B* 752, 323 (2001).
30. S. Santesson, M. Andersson, E. Degerman, T. Johansson, J. Nilsson, and S. Nilsson, *Anal. Chem.* 72, 3412 (2000).
31. M. Petersson, J. Nilsson, L. Wallman, T. Laurell, J. Johansson, and S. Nilsson, *J. Chromatogr., B* 714, 39 (1998).
32. S. **Gáspár**, M. Mosbach, L. Wallman, T. Laurell, E. Csöregi, and W. Schuhmann, *Anal. Chem.* 73, 4254 (2001).
33. M. Mosbach, T. Laurell, J. Nilsson, E. Csöregi, and W. Schuhmann, *Anal. Chem.* 73, 2468 (2001).
34. A. Koide, Y. Sasaki, Y. Yoshimura, R. Miyake, and T. Terayama, *Proceedings on the 13th Annual International Conference on Micro Electro Mechanical Systems*, Tsuchiura, Japan (2000).
35. M. Döring, *GIT Labor-Fachz.* 43, No. 3, 596 (1999).
36. O. Yogi, T. Kawakami, M. Yamauchi, J. Y. Ye, and M. Ishikawa, *Anal. Chem.* 73, 1896 (2001).
37. M. Moini, *Anal. Chem.* 73, 3497 (2001).
38. R. Moerman, J. Frank, J. C. M. Marijnissen, T. G. M. Schalkhamer, and G. W. K. van **Dedem**, *Anal. Chem.* 73, 2183 (2001).
39. V. N. Morozov and T. Y. Morozova, *Anal. Chem.* 71, 1415 (1999).
40. A. Edlmann, J. Diewok, K. C. Schuster, and B. Lendl, *J. Agric. Food Chem.* 49, 1139 (2001).

## II

Leopold, N.; Haberkorn, M.; Laurell, T.; Nilsson, J.; Baena, J.R.;  
Frank, J.; Lendl, B.

*"On-Line Monitoring of Airborne Chemistry in Levitated Nanodroplets:  
In Situ Synthesis and Application of SERS-Active Ag-Sols  
for Trace Analysis by FT-Raman Spectroscopy"*

Analytical Chemistry **2003**, 75, 2166-2171

# On-Line Monitoring of Airborne Chemistry in Levitated Nanodroplets: In Situ Synthesis and Application of SERS-Active Ag-Sols for Trace Analysis by FT-Raman Spectroscopy

Nicolae Leopold,<sup>†</sup> Michael Haberkom,<sup>‡</sup> Thomas Laurell,<sup>§</sup> Johan Nilsson,<sup>§</sup> Josefa R. Baena,<sup>‡</sup> Johannes Frank,<sup>‡</sup> and Bernhard Lendl<sup>\*‡</sup>

Faculty of Physics, Babes-Bolyai University, Kogalniceanu 1, 3400 Cluj-Napoca, Romania, Institute of Chemical Technology and Analytics, TU Vienna, Getreidemarkt 9-164/AC, 1060 Vienna, Austria, and Department of Electrical Measurements, Lund University, P.O. Box 118, 221 00 Lund, Sweden.

We report a new strategy for on-line monitoring of chemical reactions in ultrasonically levitated, nanoliter-sized droplets by Raman spectroscopy. A flow-through microdispenser connected to an automated flow injection system was used to dose picoliter droplets into the node of an ultrasonic trap. Taking advantage of the flow-through characteristics of the microdispenser and the versatility of the automated flow system, a well-defined sequence of reagents could be injected via the microdispenser into the levitated droplet placed in the focus of the collection optics of the Fourier transform Raman spectrometer. In that way, chemical reactions could be carried out and monitored on-line. The developed system was used for fast, reproducible, in situ synthesis of a highly active surface enhanced Raman scattering (SERS) sol resulting from the reduction of silver nitrate with hydroxylamine hydrochloride in basic conditions. With this chemical system, SERS substrate preparation could be achieved at room temperature and in short time. The in situ prepared silver sol was used for trace analysis of several organic test molecules that were injected into the levitated SERS-active droplet again using the microdispenser. The concentration dependence of the SERS spectra was studied using 9-aminoacridine, revealing that down to the femtogram region high-quality SERS spectra could be obtained. Additionally, SERS spectra of 6-mercaptopurine, thiamine, and acridine were recorded in the levitated drop as well.

Improvement of the problem-solving capability of analytical chemical instrumentation is an important goal of many researchers active in that area. This general aim brings about a lot of interesting new concepts and ideas whose success and impact may be judged over the years by their implementation in commercial instrumentation. In this respect, the concept of

miniaturization of key parts in analytical instruments can clearly be identified as a very successful strategy of the recent past.<sup>1-5</sup> The reason for many advantages related to miniaturization results from the significant increase of the surface-to-volume ratio in miniaturized analytical instrumentation when compared to their standard counterparts.<sup>1</sup> This fact allows for more efficient heating and cooling of liquids and in turn for faster separations as well as reaction cycles.<sup>6</sup> A second general advantage of miniaturization can be seen in simple and efficient integration of several steps of the overall analytical process in close proximity to each other, which makes automated and effective handling of minute amounts of samples possible.<sup>7</sup> Despite the clear positive impact of miniaturization on analytical chemical instrumentation there are also problems related to it. An important difficulty resulting from miniaturization is the reliable detection of the reduced amounts of analytes present in the microsystems, specially for detection principles whose magnitude of response is dependent on the available sample volume.<sup>8,9</sup> This is the case for optical methods which either measure absorption or the intensity of frequency-shifted light such as fluorescence and inelastically scattered (Raman) light. A possible way out of this problem is to consider surface enhanced Raman scattering (SERS) for highly sensitive and molecular-specific detection. In SERS spectroscopy, a rough noble metal surface in combination with an excitation laser wavelength appropriate to excite the surface plasmon resonance is required to achieve high-sensitivity Raman scattering of

- (1) Reyes, D. R.; Iossifidis, D.; Auroux, P. A.; Manz, A. *Anal. Chem.* **2002**, *74*, 2623-2636.
- (2) Auroux, P. A.; Iossifidis, D.; Reyes, D. R.; Manz, A. *Anal. Chem.* **2002**, *74*, 2637-2652.
- (3) Jakeway, S. C.; de Mello, A. J.; Russell, E. L. *Fresenius J. Anal. Chem.* **2000**, *366* (6-7), 525-539.
- (4) Mouradian, S. *Curr. Opin. Chem. Biol.* **2002**, *6* (1), 51-56.
- (5) Craston, D.; Cowen, S. *Prog.* **1998**, *81* (3), 225-244.
- (6) Northrup, M. A.; Mariella, R. P., Jr.; Carrano, A. V.; Balch, J. W. Silicon-based sleeve microreactors for chemical reactions involving temperature cycling, especially PCR. U.S. Patent 5589136, 1996.
- (7) Ekstroem, S.; Oennerfjord, P.; Nilsson, J.; Bengtsson, M.; Laurell, T.; Marko-Varga, G. *Anal. Chem.* **2000**, *72* (2), 286-293.
- (8) Manz, A.; Harrison, D. J.; Verpoorte, E.; Widmer, H. M. *Adv. Chromatogr.* **1993**, *33*, 1-66.
- (9) Taylor, J.; Wang, C.; Harrison, D. J. In *Micro Total Analysis Systems 2002*. Baba, Y., et al., Eds.; Kluwer Academic Publishers: Dordrecht, The Netherlands, 2002; Vol. 1, pp 344-346.

\* Corresponding author. Tel.: +43-1-58801-15140. Fax: +43-1-58801-15199. E-mail: blendl@mail.zserv.tuwien.ac.at; http://www.iac.tuwien.ac.at/cavs/.

<sup>†</sup>Babes-Bolyai University.

<sup>‡</sup>TU Vienna.

<sup>§</sup>Lund University.

molecules close to the surface.<sup>10</sup> The reason for the significant increase in Raman scattering is seen predominantly in the increased electrical field strength that decays rapidly into the adjacent solution.<sup>10,11,29</sup> As a consequence, basically only the first molecular layers contribute to the observed SERS signal, thus making the measured signal strength practically independent of the available volume.

However, there are also important practical problems related to the use of SERS spectroscopy for analytical chemical applications. The main drawback is the difficulty associated with the production of reproducible SERS substrates. Furthermore, an additional important problem is degradation of the SERS surfaces upon multiple use together with memory effects, which make the use of SERS in analytical chemical applications troublesome. To solve these inconveniences, several approaches have been developed, such as covering of the active surface with organic monolayers to avoid the degradation and memory effects<sup>12</sup> or the preparation of fresh colloids to be employed as SERS substrates. For the latter case, flow systems have also been employed to improve reproducibility of the resulting colloid, either for the synthesis of batches of stabilized silver colloids<sup>13</sup> or for the on-line generation and use of the substrates. Here, problems concerning adsorption of the analytes on the tubings and memory effects were detected.<sup>14</sup> Another option is the use of anion exchanger microbeads, which have proven to be suitable as a carrier for in situ synthesis of colloidal silver, which can be used as a stable and sensitive SERS substrate. In this way, SERS beads could be prepared fresh for every experiment so that a new unused substrate was available for every experiment.<sup>15</sup> Recently, the development of a microflow cell for SERS analysis where the silver colloid is prepared using the lab-on-a-chip concept and applied to semiquantitative measurements has been reported.<sup>16</sup>

In the present paper, a new and versatile setup for carrying out on-line Raman monitoring of chemical reactions in acoustically levitated nanodroplets is described. The setup is used for trace analysis of organic substances using SERS. In the presented approach, an acoustic levitator is attached to the Raman spectrometer in such a way that one of the nodes is aligned with the collecting optics of the spectrometer. Picoliter sized droplets are dosed into this node of the acoustic trap using a flow-through microdispenser to form the levitated drop, which serves as the reaction vessel. The microdispenser is fed by a versatile sequential injection (SI) system, which allows us to dose a sequence of reagents into the levitated drop. This feature is used to in situ synthesize a SERS-active silver colloid in the levitated drop. After synthesis, the analyte is also dosed via the microdispenser into the drop to record its SERS spectrum. For subsequent measurements, the whole procedure including SERS sol synthesis and sample addition is repeated. In doing so, fresh SERS-active drops are available for each analysis, thus efficiently avoiding problems

related to analyte carryover and SERS sol instability. A further important issue of the presented method is the use of hydroxylamine-reduced silver sol. This new silver sol can be prepared in the drop within a few seconds at room temperature, which is a decisive advantage over the commonly used Lee Meisel colloid<sup>17</sup> that requires time-consuming refluxing for silver sol synthesis.

## EXPERIMENTAL SECTION

**Chemicals.** All the chemicals employed were reagent grade or better. Stock solutions of  $1.1 \times 10^{-3}$  M silver nitrate (Merck, Darmstadt, Germany),  $3 \times 10^{-2}$  M hydroxylamine hydrochloride (Fluka, Vienna, Austria), and 0.1 M NaOH (Sigma-Aldrich, Vienna, Austria) were prepared by dissolving the proper amounts of the reagents in distilled water. Solutions of  $10^{-4}$  M 9-aminoacridine (Merck),  $10^{-3}$  M acridine (Fluka),  $10^{-4}$  M 6-mercaptopurine (Fluka), and  $10^{-2}$  M thiamine (Fluka) were prepared in distilled water containing NaCl in increasing concentrations (0.2, 0.4, 0.6, and 0.8 M, respectively).

**Apparatus.** The automated flow system was built with a Cavo XP 3000 syringe pump (Sunnyvale, CA) equipped with a 1-mL syringe. A Valco six-port selection valve (Houston, TX) was also employed. PTFE tubings (Global FIA, Gig Harbor, WA) with inner diameters of 0.25 and 0.75 mm were used for the flow system. The pump and the valve of the SI system as well as the driving electronics of the microdispenser were controlled via the in-house written MS Visual Basic 6.0 based software Sagittarius V2 (1.2.0003).

The flow-through microdispenser developed in-house using silicon micromachining methods consisted of two microstructured silicon plates that are joined to form a channel with a pyramidal nozzle in the middle. A piezoelectric element is connected to the channel wall opposing the nozzle, in such a way that when a voltage pulse is applied, the droplets are ejected.<sup>18</sup> The used ultrasonic levitator (Dantec/invent Measurement Technology, Erlangen, Germany) is based on a piezoelectric vibrator that generates a standing acoustic wave in air with several nodes into which liquid or solid samples may be placed and held in a levitated position.<sup>19</sup> The drop thus obtained is levitated in the focus of the collector objective of an FT-Raman spectrometer. The FT-SERS spectra from the drop were recorded in backscattering geometry with a Bruker IFA 106 Raman accessory attached to a Bruker IFS 66 FT-IR spectrometer equipped with a liquid nitrogen cooled Ge detector. The 1064-nm Nd:YAG laser was used as excitation source, and the laser power was set to 100 mW. All FT-SERS spectra were recorded with a resolution of  $8 \text{ cm}^{-1}$  by co-adding 32 scans.

Reference FT-SERS measurements were recorded using a 2-mL quartz cuvette in backscattering geometry with the same spectrometer in order to compare information obtained from measurements of analytes in levitated droplets with the spectra obtained using the standard Lee–Meisel procedure for silver colloid preparation.

A UV–visible diode array spectrometer (HP 8452A, Hewlett-Packard) was also employed to record the UV–visible spectra of the silver colloids.

(10) Laserna, J. J. *Anal. Chim. Acta* **1993**, *283*, 607–622.

(11) Weiss, A.; Haran, G. *J. Phys. Chem. B* **2001**, *105* (49), 12348–12354.

(12) Weissenbacher, N.; Lendl, B.; Frank, J.; Wanzelböck, H. D.; Mizaikoff, B.; Kellner, R. *J. Mol. Struct.* **1997**, *410*, 539.

(13) Keir, R.; Sadler, D.; Smith, W. E. *Appl. Spectrosc.* **2002**, *56*, 551–559.

(14) Cabalin, L. M.; Ruperez, A.; Laserna, J. J. *Talanta* **1993**, *40*, 1741–1747.

(15) Ayora Cañada, M. J.; Ruiz Medina, A.; Frank, J.; Lendl, B. *Analyst* **2002**, *127*, 1365–1369.

(16) Keir, R.; Igata, E.; Arundell, M.; Smith, W. E.; Graham, D.; McHugh, C.; Cooper, J. M. *Anal. Chem.* **2002**, *74*, 1503–1508.

(17) Lee, P. C.; Meisel, D. *J. Phys. Chem.* **1982**, *86*, 3391–3395.

(18) Laurell, T.; Wallman, L.; Nilsson, J. *J. Micromech. Microeng.* **1999**, *3*, 369–376.

(19) Welter, E.; Neidhart, B. *Fresenius J. Anal. Chem.* **1997**, *357*, 345–350.

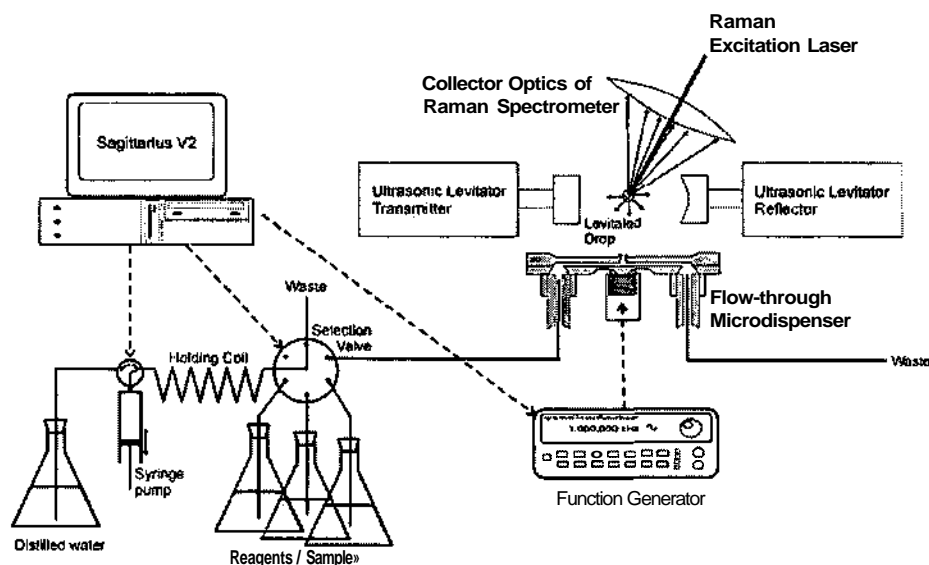


**Figure 1.** Experimental setup comprising a flow-through microdispenser coupled to an automated flow system, an ultrasonic levitator, and a FT-Raman spectrometer.

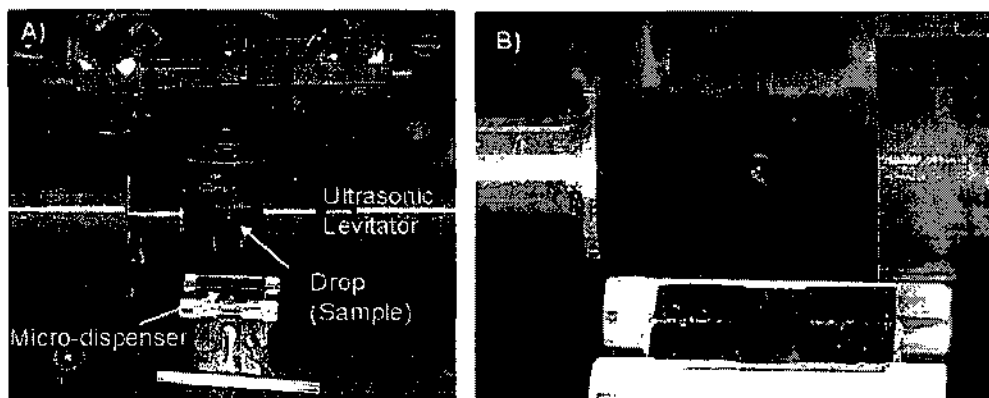


**Figure 2.** (A) Image of the ultrasonic levitator holding a drop in a node that is aligned with the collection optics of the Raman spectrometer. (B) Detail showing the microdispenser sending a stream of droplets (60 pL each) to the levitated nanodrop.

**Experimental Setup.** Figure 1 shows the experimental setup used for in situ preparation of a SERS substrate in levitated nanodroplets and on-line monitoring by FT-Raman spectroscopy. As can be seen in the figure, the computer controlled flow system enabled sequential introduction of the different solutions (reagents and analytes) into the microdispenser, to dose the proper amounts, in streams of 60-pL droplets, into the node of the acoustic trap. A picture of the optics of the Raman spectrometer including the acoustic trap, as well as a closeup of the microdispenser can be seen in Figure 2.

## RESULTS AND DISCUSSION

### Preparation and Characterization of the Silver Colloid.

The possibility of utilizing colloidal dispersions of Ag or Au in aqueous solutions as a method for enhancing Raman scattering was first demonstrated by Creighton and co-workers in 1979.<sup>20</sup> For SERS, the most frequently used silver colloids are those

produced by reduction of silver nitrate with sodium citrate, the so-called Lee–Meisel<sup>17</sup> method, or by reduction of silver nitrate with sodium borohydride, following the Creighton procedure.<sup>20</sup> Apart from these, other Ag<sup>+</sup>-reducing methods have been reported.<sup>21–25</sup> Despite the apparent simplicity of the published procedures for preparing sols, the preparation of a highly active SERS colloid is not routine and the in situ synthesis is difficult, as the procedures usually involve long reaction times and controlled temperature. For this reason, we have employed a new simple and fast method for preparing stable, highly SERS-active silver colloids by reduction of silver nitrate with hydroxylamine hydrochloride under basic conditions at room temperature. Hydroxylamine as reducing agent is widely known,<sup>26,27</sup> but its

(20) Creighton, J. A.; Blatchford, C. G.; Albrecht, M. G. *J. Chem. Soc., Faraday Trans.* **1979**, *75* (2), 790.

(21) Li, Y.-S.; Cheng, J.; Coons, L. B. *Spectrochim. Acta A* **1999**, *55*, 1197–1207.

(22) Nickel, U.; Castell, A. Z.; Pöppel, K.; Schneider, S. *Langmuir* **2000**, *16*, 9087–9091.

(23) Kim, H. S.; Ryu, J. H.; Jose, B.; Lee, B. G.; Ahn, B. S.; Kang, Y. S. *Langmuir* **2001**, *17*, 5817–5820.

(24) Ahern, A. M.; Garell, R. L. *Anal. Chem.* **1987**, *59*, 2816.

(25) Kneipp, K. *Spectrochim. Acta A* **1994**, *50*, 1023–1030.

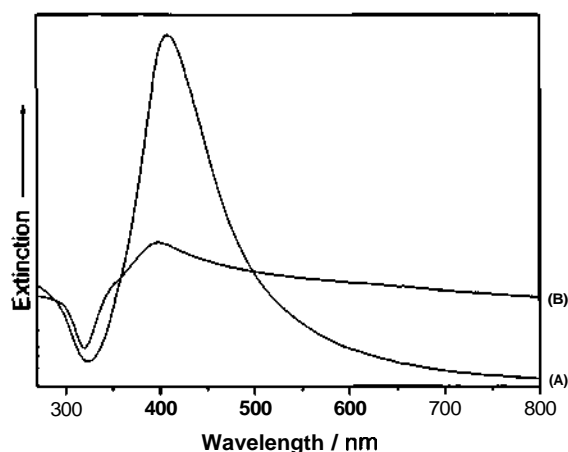


**Figure 3.** Extinction spectrum of (A) hydroxylamine-reduced silver sol and (B) hydroxylamine-reduced silver sol after the addition of NaCl.

application for the reduction of silver to obtain a SERS colloidal substrate has not been reported yet.

For comparison purposes, and in order to test the properties of the hydroxylamine-reduced silver sol, it was initially prepared in batch according to the following procedure: 0.017 g of silver nitrate was dissolved in 90 mL of distilled water. Then 0.021 g of hydroxylamine hydrochloride was dissolved in 5 mL of distilled water to which a volume of 5 mL of 0.1 M sodium hydroxide was added. This mixture was then quickly added to the silver nitrate solution. Within a few seconds, a silver colloid solution was obtained (pH  $\sim$ 8.3) that was found to be stable for more than 90 days. The extinction spectrum of the hydroxylamine-reduced silver colloid showed an extinction maximum at  $\sim$ 412 nm and a full width at half-maximum (fwhm) of  $\sim$ 115 nm, as shown in Figure 3 A, indicating a narrow size distribution of the particles. For comparison purposes, SERS spectra of 9-aminoacridine were recorded with both Lee–Meisel- and hydroxylamine-reduced silver sol in a cuvette.<sup>28</sup> The hydroxylamine-reduced silver colloid properties were found to be comparable in terms of sensitivity with those obtained when the Lee–Meisel method was used, with the advantage of a fast and easy preparation at room temperature and high reproducibility and preparation success rate. These features allow in situ synthesis and on-line measurements.

To obtain a better extinction at the wavelength of the Raman excitation laser employed (1064 nm), NaCl was chosen as an aggregating agent. The effect of the addition of NaCl is observed in Figure 3B. It is well known that the aggregation of the particles leads to a wider particle size distribution, thus providing a higher SERS activity at longer wavelengths. As a consequence, in all subsequent SERS experiments, NaCl was added to the silver sol to enhance the sensitivity of the method.

**Airborne SERS Spectroscopy.** Once the simple and fast preparation of the new active SERS substrate was demonstrated, an automated flow system was employed for the continuous supply

(26) Turkevich, J.; Stevenson, P. C.; Hiller, J. *Discuss. Faraday Soc.* **1951**, *11*, 55.

(27) Brown, K. R.; Walter, D. G.; Natan, M. J. *Chem. Mater.* **2000**, *12*, 306–313.

(28) Leopold, N.; Lendl, B. Silver Colloids for Surface-Enhanced Raman Spectroscopy Produced by Reduction with Hydroxylamine. Manuscript in preparation

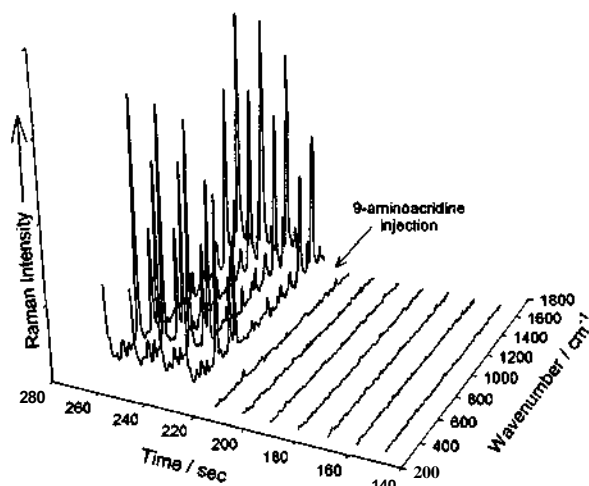


**Figure 4.** Time evolution of the processes in the droplet as monitored by FT-Raman spectroscopy, comprising silver sol synthesis followed by injection of the analyte 9-aminoacridine.

of the different reagents in order to obtain a levitated droplet for SERS measurements. First, 432 nL of  $1.1 \times 10^{-3}$  M silver nitrate was dosed by the microdispenser into the acoustic node of the ultrasonic levitator, followed by 48 nL of a solution of  $3 \times 10^{-2}$  M hydroxylamine containing 0.1 M NaOH. Both reagents were dispensed at a rate of 200 droplets (60 pL each) per second. In this way, the silver ions are reduced in the levitated drop yielding a silver sol, which serves as an airborne SERS substrate. To the obtained colloid, 12 nL of a  $10^{-5}$  M 9-aminoacridine solution containing 0.2 M NaCl was added. The evolution of the system with time is presented in Figure 4. The different processes in the droplet do not produce any significant signal in the recorded spectra due to the low concentration ( $10^{-3}$  M range) of the reagents employed for the synthesis of the silver sol and the extremely small cross section for Raman scattering.<sup>29</sup> However, after the addition of 9-aminoacridine ( $\sim$ 220 s), well-defined SERS spectra were obtained. The whole process, comprising synthesis of the SERS substrate and recording of the SERS spectra, took  $\sim$ 4 min. During this time, the levitated droplet is exposed to the action of the laser and evaporation of the solvent takes place if the laser power is too high. To avoid this effect, the laser power was set to 100 mW.

The analytical performance of the SERS substrate was tested using 9-aminoacridine as the model compound. As the microdispenser allows for highly accurate dosing of the amount of analyte, different concentrations of 9-aminoacridine up to  $4 \times 10^{-7}$  M were dosed into the levitated droplet by following the procedure described above. The obtained spectra are presented in Figure 5 and clearly show the dependence of the SERS signals on the concentration of the analyte. The usual range of linear response of SERS covers 2–3 orders of magnitude. Higher concentrations lead to saturation of analyte molecules on the limited number of silver particles, yielding a flat response.<sup>9,29</sup> In the present case, the lowest concentration of analyte in the droplet resulting in an acceptable spectrum was  $\sim$  $10^{-10}$  M, corresponding to an absolute

(29) Kneipp, K.; Kneipp, H.; Itzkan, I.; Dasari, R. R.; Feld, M. S. *Chem. Rev.* **1999**, *99*, 2957–2975.

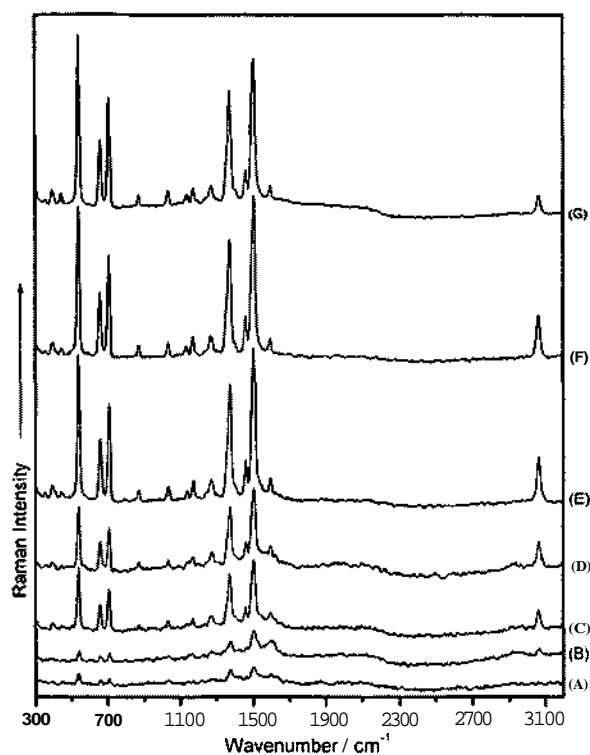


**Figure 5.** FT-SERS spectra of different amounts/approximated concentration of 9-aminoacridine in a levitated drop containing silver colloids: (A)  $23 \times 10^{-15} \text{g}/2 \times 10^{-10} \text{ M}$ , (B)  $46 \times 10^{-15} \text{g}/4 \times 10^{-10} \text{ M}$ , (C)  $230 \times 10^{-15} \text{g}/2 \times 10^{-9} \text{ M}$ , (D)  $460 \times 10^{-15} \text{g}/4 \times 10^{-9} \text{ M}$ , (E)  $4.6 \times 10^{-12} \text{g}/4 \times 10^{-8} \text{ M}$ , and (F)  $46 \times 10^{-12} \text{g}/4 \times 10^{-7} \text{ M}$ . (G) FT-SERS spectrum from  $4 \times 10^{-7} \text{ M}$  9-aminoacridine obtained with a Lee–Meisel silver sol measured in a cuvette.

amount as small as 23 fg. Figure 5G presents the FT-SERS spectrum of 9-aminoacridine measured in a cuvette with a Lee–Meisel silver sol. Independently of the two different silver sols used, for each analyte, the peak positions and relative intensities in the recorded spectra were found to be not dependent on the preparation method of the silver colloids.<sup>28</sup>

The versatility of the developed experimental setup was tested using several analytes, namely, acridine, 6-mercaptopurine, and thiamine, whose SERS spectra were later compared with those obtained using the Lee–Meisel silver sol in a cuvette as a reference.<sup>28</sup> Owing to the great differences in the enhancement of the SERS signals observed for each compound, different concentrations were employed to obtain SERS spectra with a good signal-to-noise ratio. A preliminary study was also performed in order to optimize the concentration of the aggregating reagent (NaCl) for each one of the analytes. The airborne silver sol was prepared in the same way as given above, followed by the addition of the analyte. Thus, a solution of  $10^{-3} \text{ M}$  acridine in 0.4 M NaCl was dosed to the drop using the microdispenser to give a final concentration of  $\sim 4 \times 10^{-5} \text{ M}$  acridine in the levitated droplet. In the same way,  $10^{-4} \text{ M}$  6 mercaptopurine in 0.6 M NaCl and  $10^{-2} \text{ M}$  thiamine in 0.8 M NaCl were dispensed into different droplets to yield a final concentration of  $2 \times 10^{-6} \text{ M}$  mercaptopurine and  $4 \times 10^{-4} \text{ M}$  thiamine in the drop. The spectra of acridine, 6-mercaptopurine and thiamine obtained from levitated droplets with a laser power of 100 mW as well as the corresponding Lee–

2170 *Analytical Chemistry*, Vol. 75, No. 9, May 1, 2003

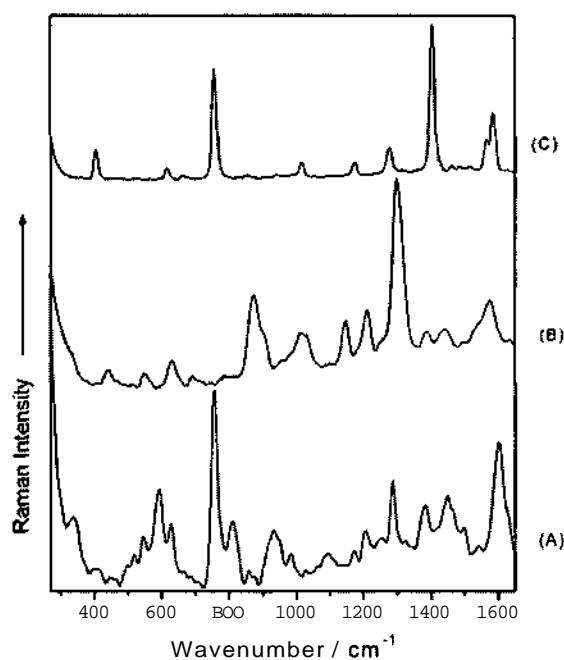


**Figure 6.** FT-SERS spectra of (A)  $4 \times 10^{-4} \text{ M}$  thiamine, (B)  $2 \times 10^{-6} \text{ M}$  6-mercaptopurine, and (C)  $4 \times 10^{-5} \text{ M}$  acridine recorded from the levitated drop.

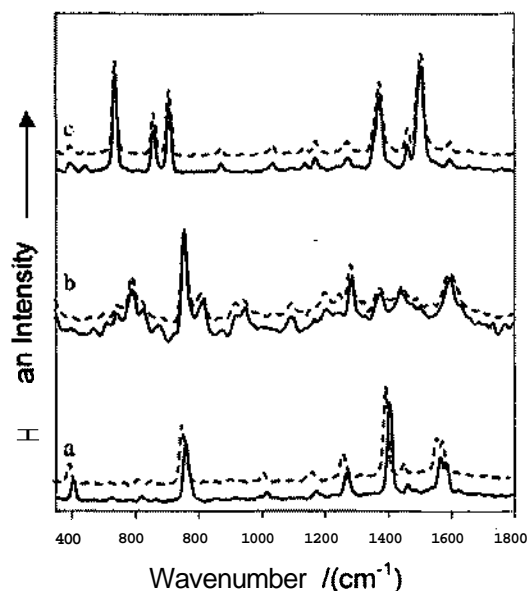


**Figure 7.** FT-SERS spectra recorded from different injections of (a)  $10^{-4} \text{ M}$  acridine in 0.4 M NaCl, (b)  $10^{-5} \text{ M}$  thiamine in 0.2 M NaCl, and (c)  $10^{-5} \text{ M}$  aminoacridine in 0.2 M NaCl.

Meisel spectra are presented in Figure 6. It can be seen that the spectra obtained from the differently prepared silver sols are very similar.

It was also observed that the SERS intensity changes with time, probably due to an ongoing adsorption of the analyte molecules to the silver particles or to an aggregation and sedimentation of the metal. However, owing to the computer control of the developed system, the time sequence of SERS sol synthesis and measurement could be controlled accurately. This allowed repro-

ducible SERS sol synthesis and spectrum acquisition always at the same time. In doing so, reproducible spectra could be obtained, as can be seen in the SERS spectra of dual injections of several analytes shown in Figure 7. The reproducibility of the whole system, including synthesis of the SERS substrate, injection of the analyte, and measurement of the SERS spectra, was assessed using  $15 \times 10^{-12}$  g of 9-aminoacridine in a concentration of  $10^{-5}$  M as a model compound. Three different experiments were run, and the intensity of the peaks measured at characteristic wavenumbers for the selected analyte (viz. 538.6, 658.0  $\text{cm}^{-1}$ ) was employed as analytical signal without further treatment. In such conditions, the relative standard deviation of the system ranged from 3.1 to 3.2%. Therefore, we can conclude that the new proposed method of in situ synthesis and application of SERS-active silver sols in the levitated drop allows for SERS spectra comparable to the reference method but with the significant advantage of a fast overall procedure free of carryover effects and high long-term stability with good reproducibility.

## CONCLUSION

The versatility of the presented approach allows addressing different application areas in chemistry. For instance, the pre-

sented system for generation of SERS-active droplets can in principle be combined with liquid Chromatographic techniques using a second microdispenser. Furthermore, when a dispersive, more sensitive Raman spectrometer is used, direct monitoring of arbitrary chemical reactions in liquids can be easily achieved in the presented format. Therefore, applications in different fields including combinatorial chemistry can be envisioned too.

## ACKNOWLEDGMENT

N.L. thankfully acknowledges the financial support received from a Marie Curie fellowship from the European Union (HPMT-CT-2000-00059). Furthermore B.L, M.H., and J.R.B. acknowledge financial support received from the Austrian Science Foundation within Project 13686. J.R.B. also acknowledges a postdoctoral grant held by the Spanish Secretaría de Estado de Educación y Universidades and cofinanced by the European Social Foundation.

Received for review November 12, 2002. Accepted February 19, 2003.

AC026308L

### III

Kölhed, M.; Haberkorn, M.; Pustogov, V.; Mizaikoff, B.; Frank, J.;  
Karlberg, B.; Lendl, B.

*“Assessment of Quantum Cascade Lasers as Mid Infrared Light Sources  
for Measurement of Aqueous Samples”*

Vibrational Spectroscopy **2002**, 29, 283-289

## Assessment of quantum cascade lasers as mid infrared light sources for measurement of aqueous samples

Malin Kölhed<sup>a</sup>, Michael Haberkorn<sup>b</sup>, Viktor Pustogov<sup>b</sup>, Boris Mizaikoff<sup>b,1</sup>,  
Johannes Frank<sup>b</sup>, Bo Karlberg<sup>a</sup>, Bernhard Lendl<sup>b,\*</sup>

<sup>a</sup>Department of Analytical Chemistry, Stockholm University, SE 10691 Stockholm, Sweden

<sup>b</sup>Institute of Analytical Chemistry, Vienna University of Technology, A 1060 Vienna, Austria

Received 15 September 2001; received in revised form 29 November 2001; accepted 29 November 2001

### Abstract

The potential of Fabry Perot Quantum Cascade (QC) lasers for transmission measurements of aqueous samples was assessed. For this purpose two lasers, one lasing in the region of the bending vibration of water at  $1650\text{ cm}^{-1}$ , and the other in the water window at  $1080\text{ cm}^{-1}$ , were used in a flow injection system comprising a dedicated fibre-optic flow cell with an adjustable path length. As test analytes a nucleic base (adenine) and a nucleoside (xanthosine) were used. Compound-specific information was obtained as the nucleoside contained a carbohydrate unit in addition to the heteroaromatic ring structure. With the laser emitting at  $1650\text{ cm}^{-1}$  the heteroaromatic ring structure of both compounds gave rise to flow injection peaks, whereas, only the nucleoside, containing the C–O stretching vibrations of the carbohydrate unit, produced peaks also with the laser emitting at  $1080\text{ cm}^{-1}$ . The path length limitations were investigated for both lasers. For the  $1650\text{ cm}^{-1}$  laser, path lengths up to  $59\text{ }\mu\text{m}$  could be used, despite the strong absorption of water. For xanthosine analysis, the limit of detection ( $S/N = 3$ ) at this path length was determined to be  $0.07\text{ g l}^{-1}$ . Optical path lengths of up to  $150\text{ }\mu\text{m}$  could be used for the laser emitting at  $1080\text{ cm}^{-1}$ . © 2002 Elsevier Science B.V. All rights reserved.

**Keywords:** Quantum cascade lasers; Mid-IR; Aqueous solution; Flow injection analysis

### 1. Introduction

Mid-IR spectroscopy is a universally applicable, non-destructive spectroscopic technique that can provide important molecule-specific information about samples with a wide range of constituents: from small, simple molecules to complex biochemical systems.

However, application of mid-IR spectroscopy to aqueous solutions is difficult due to the strong absorption of water. The bending vibration of water causes particular problems, since it overlaps with the region of the information-rich amide-I band of proteins, implying that optical paths below  $10\text{ }\mu\text{m}$  are required for successful measurement in this spectral region when state-of-the-art FTIR spectrometers are used. Such short optical paths can be deployed using dedicated transmission cells, or when an attenuated total reflection (ATR) technique is used for measurements. However, both of these approaches have poor sensitivity as a result of the short optical path and there are

\* Corresponding author. Tel.: +43-1-5880115140;  
fax: +43-1-5880115199.

E-mail address: blendl@mail.zserv.tuwien.ac.at (B. Lendl).

<sup>1</sup> Present address: Department of Chemistry, Georgia Institute of Technology, Atlanta, GA, USA.

also practical problems since narrow transmission cells are difficult to fill reproducibly. In the case of ATR measurements great cleanliness of the ATR surface must also be maintained to avoid spectral artefacts.

To overcome these shortcomings, technical advances are needed. In this respect new developments in IR light sources, especially the development of Quantum Cascade (QC) lasers, are of great interest. QC lasers are unipolar lasers based on intersubband transitions between excited states of coupled quantum wells. Because of their cascade structure, QC lasers have slope efficiencies that are correlated with the number of stages. Resonant tunnelling acts as a pumping mechanism to achieve the population inversion. Unlike other laser sources, the wavelength is determined by quantum confinement, i.e. by the thickness of the active layer rather than by the chemical properties of the material, giving the flexibility to design lasers emitting in the region of interest [1-3]. These lasers are commonly operated in pulsed mode at room temperature, providing spectral densities in the milliwatt per wavenumber range. So far most spectroscopic applications of QC lasers have been involved with gas phase measurements using wavelength modulated absorption [4], cavity ringdown [5], photo-acoustic spectroscopy [6,7] and, most recently, trace sensors suitable for routine field deployment have been described [8,9]. QC lasers were first used for IR detection in condensed phase in conjunction with flow injection analysis [10] and high performance liquid chromatography [11] systems.

In this paper, we assess the possibility of using QC lasers for transmission measurements in aqueous solutions at extended path lengths, focusing especially on the spectral region of the bending vibration of water. The investigated laser wavelengths were 1650 and 1080  $\text{cm}^{-1}$  and the corresponding molar extinction coefficients of water at these wavenumbers are  $22.2 \times 10^3$  and  $4.5 \times 10^3 \text{ cm}^2 \text{ mol}^{-1}$ , respectively [12]. It is believed that the possibility of performing transmission measurements in the amide-I region with convenient path lengths will significantly facilitate the IR-spectroscopic investigation of biological samples and, consequently, motivate further research and technical advances in these fields of research.

## 2. Experimental

### 2.1. Sample solutions

The nucleoside investigated was xanthosine (99%) from Sigma and the nucleic base was adenine (99%) from Aldrich (Sigma-Aldrich). Stock solutions,  $1 \text{ g l}^{-1}$ , were prepared by dissolving each analyte in distilled water using an ultrasonic bath. These solutions were then diluted as required.

### 2.2. The flow injection manifold

The flow injection system consisted of a Cavro XP 3000 syringe pump (Sunnyvale, CA, USA) with a syringe size of 1000  $\mu\text{l}$  and a Valco Cheminert injection valve (Houston, TX, USA) equipped with a 10  $\mu\text{l}$  sample loop. The polytetrafluoroethane (PTFE) tubing, purchased from Global FIA (Gig Harbour, WA, USA), had an inner diameter of 250  $\mu\text{m}$  and a length of 20 cm from the injection to the detection point. The pump speed was 200  $\mu\text{l min}^{-1}$  allowing 3-4 repeated injections to be performed during one pump stroke.

The fibre-optic flow cell, built in-house, is depicted in Fig. 1. It consists of two hollow wave-guides (each with 1.2 mm o.d., 1.0 mm i.d. and 20 mm length) with diamond windows (0.16 mm) at the ends extending into the flow channel. The wave-guides were flexibly mounted in the flow cell in order to allow adjustment of the optical path length in the range 40-150  $\mu\text{m}$ . The emitted radiation from the laser was focused with a ZnSe lens (0.10 mm, focal distance 10 mm) on the first hollow wave-guide, thus, directing the light through the flow channel. The other hollow wave-guide then collected the light and a second ZnSe lens, identical to the first, focused the light onto the Mercury-Cadmium-Telluride (MCT) element of an FTIR-22-2.0 detector (InfraRed Associates, Stuart, FL, USA). The optical path length could easily be adjusted, and the actual distance was verified with a light microscope (Reichert, Austria). The cell volume was 0.1-0.3  $\mu\text{l}$ , depending on the path length. The volume of the PTFE conduit connecting the valve and the flow cell was about 10  $\mu\text{l}$ , i.e. of the same order as the injected sample volume. The residence time observed for the sample in the system was about 3-4 s at the applied flow rate, indicating that laminar flow

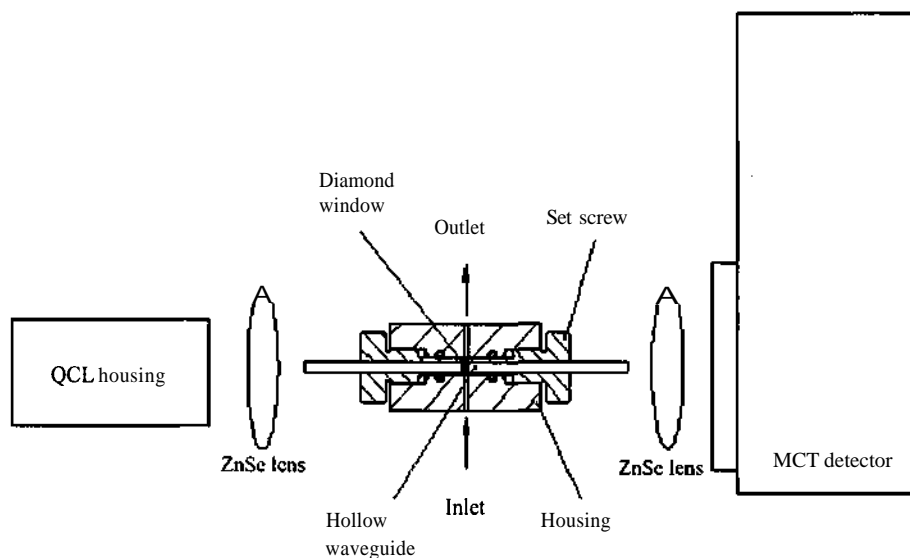


Fig. 1. Schematic diagram of the fibre optic flow cell (built in-house).

conditions prevailed throughout. Thus, a dispersion coefficient of 1 could be maintained for the central part of the sample plug, preventing undesired sample dilution.

### 2.3. Quantum cascade laser set-up

Two different Fabry Perot QC lasers were used, one emitting at  $1650\text{ cm}^{-1}$  (S2011 Al 1) and the other at  $1080\text{ cm}^{-1}$  (S1839 A16 down). Both have SB mounting and were purchased from Alpes Lasers (Neuchâtel, Switzerland). These lasers could only be used one at a time due to restrictions imposed by the laser housing (Alpes Lasers, Neuchâtel, Switzerland), which provided space for only one laser. The laser was easily mounted in the laser housing which was filled with dry nitrogen and closed. The housing was also provided with a Peltier element, silica gel pads, and a compartment allowing water- or air-cooling.

An oscilloscope (TDS 210, Tektronix UK Ltd., Berkshire, UK) was used to verify the detector output, which was acquired by a lock-in amplifier (Model 124A, Princeton Applied Research, Perkin-Elmer) using a time constant of 1 s. The analog lock-in output signal was digitalised by measuring the output voltage with a digital multi-meter (KEITHLEY Model 196 System DMM, KEITHLEY, Cleveland, OH, USA) featuring an IEEE 488 interface.

Both lasers were operated in pulsed mode with pulses generated by a QCL pulser-switching unit (a TPG 128-TTL Pulse Generator), which was controlled, in turn, by a QCL pulser-timing unit (both from Alpes Lasers, Neuchâtel, Switzerland). The duty cycle of the pulses driving the lasers was 1% at a 100 ns pulse width and the temperature was set to  $0\text{ }^{\circ}\text{C}$  using the Peltier element and water-cooling. The Peltier element was powered by a Voltcraft® 240 W dc power supply and the temperature was monitored by a Deltron AG device (Kirchberg, Switzerland). The entire set-up is shown in Fig. 2.

An MS Visual Basic 6.0 program was written in-house (DMM196, Version 3.02.0016) to enable time-dependent data recording during the sample runs. A chemometric Matlab 5.3 based program applying a Savitzky-Golay smoothing filter was finally used to smooth the recorded data.

### 2.4. Registration of reference spectra

The lasers emission spectra were registered using an MCT E-4793 (InfraRed Associates, Stuart, FL, USA) in a MIDAC Illuminator (MIDAC corporation, Irvine, CA, USA). A Bruker IFS 66 (Leipzig, Germany) equipped with a horizontal nine-bounce ATR crystal (Dura Samp11R, SensIR Technologies) was used to record the spectra of the analytes.

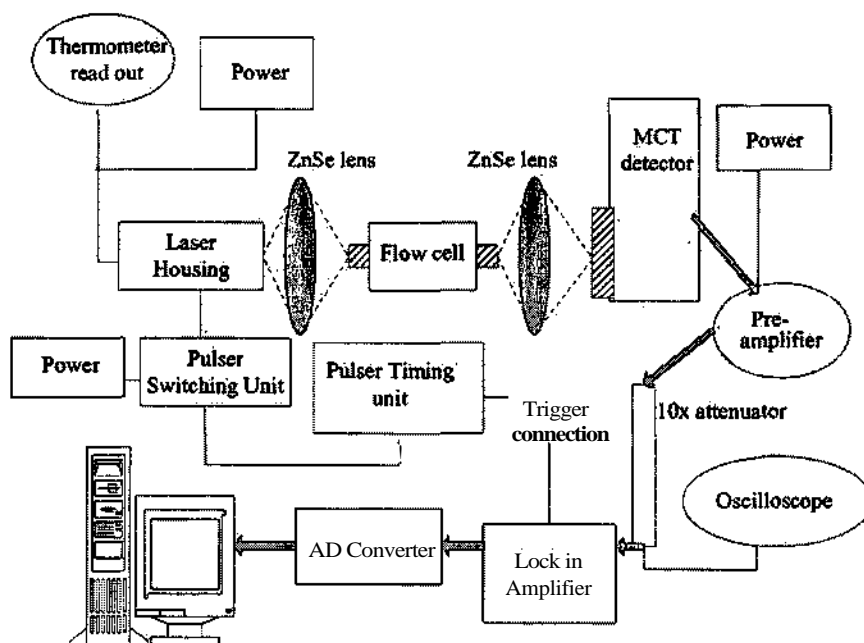


Fig. 2. Schematic diagram of the entire optical and electrical apparatus.

### 3. Results and discussion

#### 3.1. Characterisation of the lasers and operating conditions

The QC lasers are capable of emitting radiation at room temperature (up to 60 °C). However, the heat generated by the lasers at high duty cycles and

temperature-related effects on the quality of the laser limit the utility of this feature. Fig. 3 shows the increase in the laser emission output that occurred as the temperature was lowered. A temperature reduction of 0.1 °C changed the signal from the lock-in amplifier. This change was of the same magnitude as the total sample signal, demonstrating the necessity of precise temperature control. The emission modes of

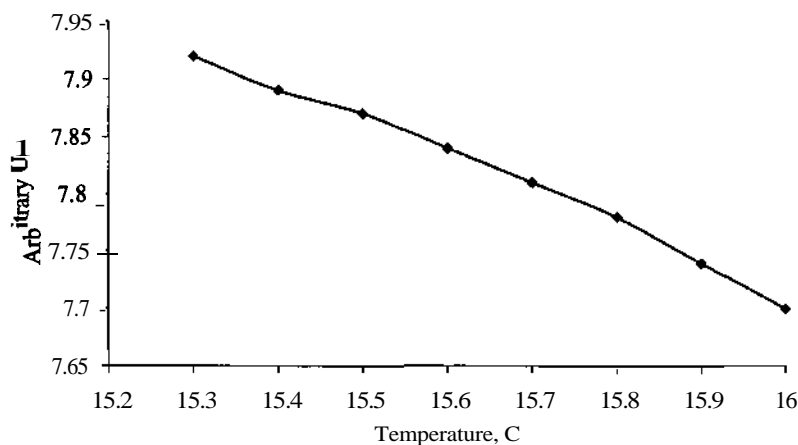


Fig. 3. Temperature dependence of the 1080  $\text{cm}^{-1}$  laser output, using an applied voltage of 9.6 V and water-cooling.

the lasers were robust only negligibly shifting with temperature. However, a temperature change of the laser's environment by 10 °C affected the intensity distribution within the modes, resulting in a shift of the center of emission by 1  $\text{cm}^{-1}$ . The emission peaks were broad, extending across 30–40  $\text{cm}^{-1}$ , and by decreasing the temperature or the voltage the lasers changed from multi to single modes.

The 1650  $\text{cm}^{-1}$  laser had a threshold value of 20.9 V, while the 1080  $\text{cm}^{-1}$  laser started to emit radiation at 7.8 V. The threshold value was measured at the power supply for the laser controller. When driving the 1080  $\text{cm}^{-1}$  laser with a duty cycle of 1% at 100 kHz, water-cooling was sufficient to remove all the heat generated by the laser in the laser housing (the temperature in the housing was typically 6–7 °C when applying a laser voltage of 9–11 V). The 1650  $\text{cm}^{-1}$  laser generated more heat, requiring the use of Peltier element cooling in addition to water-cooling. The temperature was then lowered to 0 °C, and at that temperature a stable laser signal was maintained during all the measurements.

### 3.2. Functional group specific detection

Fig. 4 shows a spectrum of an aqueous adenine solution and the emission spectrum of the 1650  $\text{cm}^{-1}$  laser. The vibration of the C=N–C bond gives rise to a broad and relatively intense absorption band at about 1640  $\text{cm}^{-1}$ , which overlaps with the emission spectrum of the QC laser. Adenine is a nucleic base, with

no carbohydrate group and no C–O stretching vibration at 1080  $\text{cm}^{-1}$ . Hence, it shows negligible absorbance at this wavenumber using the 1080  $\text{cm}^{-1}$  laser. The nucleoside xanthosine, in contrast, absorbs at both the 1080 and the 1640  $\text{cm}^{-1}$  regions. This difference can be utilised for analytical purposes and for specific discrimination between nucleosides and nucleic bases, for instance after separation in a Chromatographic system. To evaluate this latter possibility pure, single analyte solutions of adenine and xanthosine were injected into the developed system using the two QC lasers, one at a time. Fig. 5A shows recordings of the output voltage versus time when injecting 4 x 10  $\mu\text{l}$  of 1 g l<sup>-1</sup> adenine. The results clearly show that a decrease in voltage only occurs when the compound has a functional group that can absorb at the emitted wavenumber. Fig. 5B shows corresponding response curves for xanthosine registered under similar conditions. Xanthosine exhibits absorbance in both laser regions, as predicted by its chemical structure.

### 3.3. Maximum path length determination

When analysing aqueous solutions by state-of-the-art Fourier-transform transmission spectrometry in the spectral region around 1640  $\text{cm}^{-1}$ , optical path lengths must be less than 10 urn. This often causes problems when measuring biological samples where concentrations are low. It is, therefore, of interest to investigate the maximum optical path in this region when employing QC laser light sources.

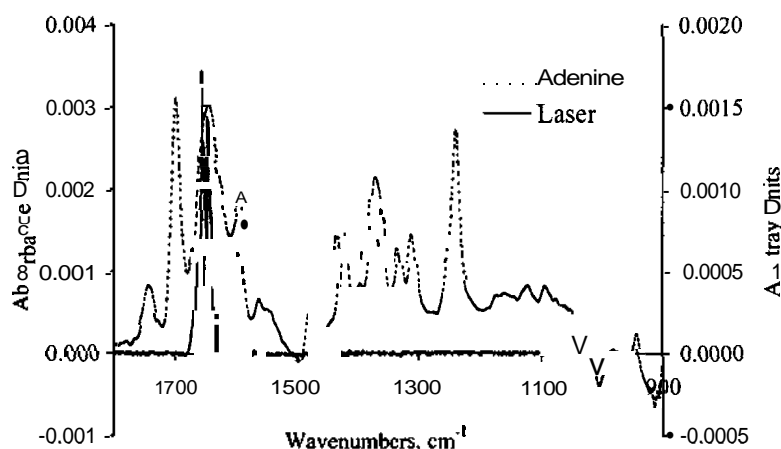


Fig. 4. Laser emission spectrum and absorbance spectrum of an aqueous adenine solution.

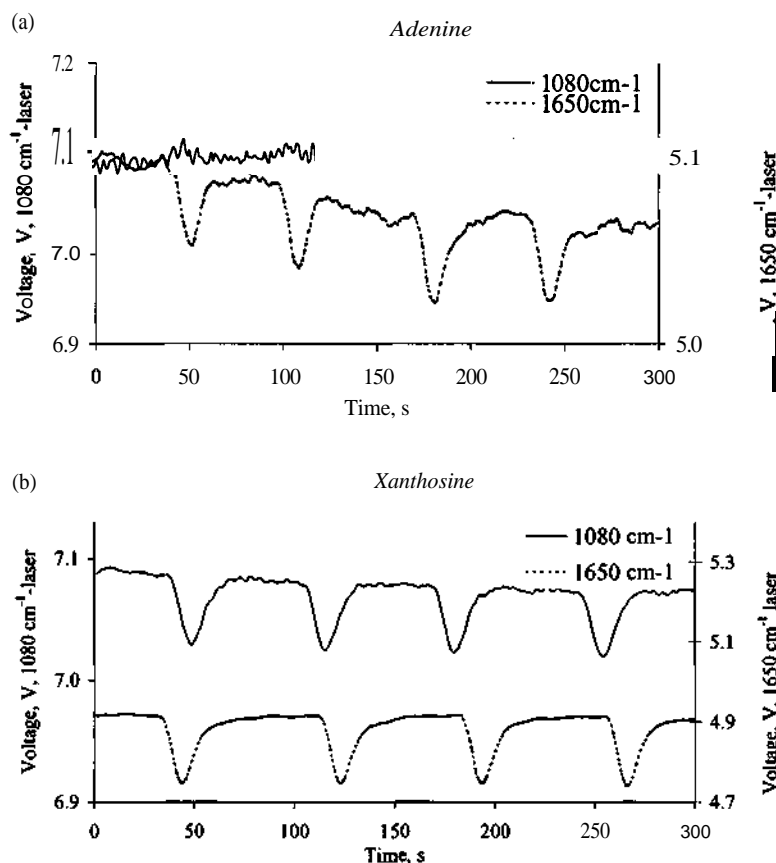


Fig. 5. Recordings following injections of aqueous solutions of (a) adenine and (b) xanthosine.

Using the more powerful QC laser emitting at  $1650\text{ cm}^{-1}$  in combination with the fibre-optic flow cell (built in-house), an optical path length as long as  $59\text{ }\mu\text{m}$  could be used. Table 1 shows the relative standard deviation (R.S.D.) of the readout over time when recording baseline as a function of the optical path length for the  $1650\text{ cm}^{-1}$  laser. Further, in Table 1,

Table 1  
R.S.D. and the  $S/N$  ratio as a function of optical path length for the  $1650\text{ cm}^{-1}$  laser for  $0.8\text{ g l}^{-1}$  xanthosine

Path length ( $\mu\text{m}$ )	R.S.D.	$S/N$ ( $0.8\text{ g l}^{-1}$ xanthosine)
50	0.04	21.5
59	0.11	36.1
67	0.27	32.5

the signal to noise ( $S/N$ ) ratio is presented for an analyte comprising  $0.8\text{ g l}^{-1}$  xanthosine. The calibration curve for this laser, using a path length of  $59\text{ }\mu\text{m}$ , is a straight line ( $y = 0.0224x + 0.0002$ ) with a regression coefficient of 0.998. The limit of detection ( $3S/N$ ) of xanthosine was calculated to be  $0.07\text{ g l}^{-1}$ . A similar study was also performed for the laser emitting at  $1080\text{ cm}^{-1}$ , for which quantitatively interpretable information could be gained up to the maximum optical path length possible with the flow cell detailed here, i.e.  $150\text{ }\mu\text{m}$ .

#### 4. Conclusions

The study described in this paper shows that the problem of the strong water absorbance in the MIR

region, which complicates the MIR analysis of biological samples, can be reduced by using a quantum cascade laser emitting in this spectral region. QC lasers are promising new light sources that might replace standard IR globars for certain applications due to their high emitting power and small size. Their powerful emission characteristics allow both the sensitivity and the exploitable optical path length to be increased, giving access to spectral regions where solvent interference is usually too high to allow acquisition of useful information about the analyte under investigation. To capitalise on their small size, further work is focusing on the development of QC laser arrays covering the entire mid-IR region. Another potentially valuable approach is to use these lasers as selective detectors in flow systems such as flow injection, liquid chromatography and capillary electrophoresis systems.

#### Acknowledgements

European Union Marie Curie Training Site on Advanced and Applied Vibrational Spectroscopy (Contract no.: HPMT-CT-2000-00059) and Foss Tecator are gratefully acknowledged for providing financial support. Furthermore B.L. acknowledges financial support from the Hochschuljubiläumsstiftung der Stadt Wien H-125/99.

#### References

- [1] F. Capasso, J. Faist, C. Sirtori, *Physica Scripta* T66 (1996) 57-59.
- [2] F. Capasso, C. Gmachl, R. Paiella, A. Tredicucci, A.L. Hutchinson, D.L. Sivco, J.N. Baillargeon, A.Y. Cho, H.C. Liu, *IEEE J. Sel. Top. Quantum Electron.* 6 (6) (2000) 931-947.
- [3] J. Faist, F. Capasso, D.L. Sivco, C. Sirtori, A.L. Hutchinson, A.Y. Cho, *Science* 264 (1994) 553-556.
- [4] K. Namjou, S. Cai, E.A. Whittaker, J. Faist, C. Gmachl, F. Capasso, D.L. Sivco, A.Y. Cho, *Opt. Lett.* 23 (3) (1998) 219-221.
- [5] B.A. Paldus, C.C. Harb, T.G. Spence, R.N. Zare, C. Gmachl, F. Capasso, D.L. Sivco, J.N. Baillargeon, A.L. Hutchinson, A.Y. Cho, *Opt. Lett.* 25 (9) (2000) 666-668.
- [6] D. Hofstetter, M. Beck, J. Faist, M. Nagele, M.W. Sigrist, *Opt. Lett.* 26 (12) (2001) 887-889.
- [7] B.A. Paldus, T.G. Spence, R.N. Zare, J. Oomens, F.J.M. Harren, D.H. Parker, C. Gmachl, F. Capasso, D.L. Sivco, J.N. Baillargeon, A.L. Hutchinson, A.Y. Cho, *Opt. Lett.* 24 (3) (1999) 178-180.
- [8] D.M. Sonnenfroh, T.W. Rawlins, M.G. Allen, C. Gmachl, F. Capasso, A.L. Hutchinson, D.L. Sivco, J.N. Baillargeon, A.Y. Cho, *Appl. Opt.* 40 (6) (2001) 812-820.
- [9] L. Hvozďara, S. Gianordoli, G. Strasser, W. Schrenk, K. Unterrainer, E. Gornik, S.S.S. Chavali, M. Kraft, V. Pustogow, B. Mizaikoff, A. Inberg, N. Croitoru, *Appl. Opt.* 39 (36) (2000) 6926-6930.
- [10] B. Lendl, J. Frank, R. Schindler, A. Muller, M. Beck, J. Faist, *Anal. Chem.* 72 (2000) 1645-1648.
- [11] A. Edelmann, C. Ruzicka, J. Frank, B. Lendl, W. Schrenk, E. Gornik, G. Strasser, *J. Chromatogr. A* 934 (2001) 123-128.
- [12] J.E. Bertie, Z. Lan, *Appl. Spectrosc.* 50 (1996) 1047-1057.

**Curriculum Vitae**  
**DI Michael HABERKORN**

**Address:**

Kegelgasse 40/1/15  
A-1030 Vienna  
AUSTRIA  
Mobile: +43-676-7084979

**Personal:**

Date of birth: 29<sup>th</sup> May 1975  
Place of birth: London, GB  
Nationality: Austrian  
Marital status: single

**Linguistic abilities:**

German: mother tongue  
English: 2<sup>nd</sup> mother tongue  
French: basic knowledge

**Education:**

***Elementary school:***

Zeppelin-schule in Linz, Austria 1981-1983  
Volksschule in Hinterbrühl, Austria 1983-1985

***High school:***

Bundesrealgymnasium Keimgasse in Mödling, Austria 1985-1993  
(Austrian High School with university preparatory track in technical studies)  
Matura (school leaving certificate) awarded in June 1993

***University:***

University of Technology in Vienna, Austria  
Registered Sept. 1993, subject: Technical Chemistry  
1. *Diplomprüfung* (equivalent to Bachelor Degree) awarded March 1997  
2. *Diplomprüfung* (equivalent to Master of Science) awarded July 2000  
Major area: Physical & Analytical Chemistry  
Diploma thesis: Development of an Enzymatic mid-IR Flow-Through Sensor for  
Sugar Analysis in Beer

***Current: PhD thesis:***

Development and Implementation of Novel Interfaces for Miniaturized Analysis Systems  
with Vibrational Spectroscopic Detection July 2000 - June 2003

University of Reading, GB May - July 1998  
Determination of PAHs and PCBs in marine sediment cores with GC-MS (soxhlet  
extraction for sample preparation)

University of Lund, Sweden

Training on Flow-Through Microdispenser operation 19<sup>th</sup> - 26<sup>th</sup> August 2000  
Production of Microdispensers 7<sup>th</sup> January - 1<sup>st</sup> February 2002

### Publications in Reviewed Journals:

- „Time-Resolved FT-IR Spectroscopy of Chemical Reactions in Solution by Fast Diffusion-Based Mixing in a Micromachined Flow Cell"  
P. Hinsmann, M. Haberkorn, J. Frank, P. Svasek, M. Harasek and B. Lendl *Appl. Spectrosc.* 55 (2001) 241-251
- "A Mid-IR Flow-Through Sensor for Direct Monitoring of Enzyme Catalysed Reactions. Case Study: Measurement of Carbohydrates in Beer"  
M. Haberkorn, P. Hinsmann and B. Lendl *Analyst* 127 (2002) 109-113
- "Assessment of Quantum Cascade Lasers as Mid Infrared Light Sources for Measurement of Aqueous Samples"  
M. Kölhed, M. Haberkorn, V. Pustogov, B. Mizaikoff, J. Frank, B. Karlberg and B. Lendl *Vib. Spectrosc.* 29 (2002) 283-289
- "Flow Through Picoliter Dispenser: A New Approach for Solvent Elimination in FTIR Spectroscopy"  
M. Haberkorn, J. Frank, M. Harasek, J. Nilsson, T. Laurell and B. Lendl *Appl. Spectrosc.* 56 (2002) 902-908
- "On-line Monitoring of Airborne Chemistry in Levitated Nanodroplets: In Situ Synthesis and Application of SERS-Active Ag-Sols for Trace Analysis by FT-Raman Spectroscopy"  
N. Leopold, M. Haberkorn, T. Laurell, J. Nilsson, J.R. Baena, J. Frank and B. Lendl *Anal. Chem.* 75 (2003) 2166-2171

### Reviewed Conference Proceedings:

- „On-line monitoring of airborne chemistry in levitated droplets: In-situ synthesis and application of SERS active Ag-sols for trace analysis by Raman spectrometry"  
N. Leopold, M. Haberkorn, T. Laurell, J. Nilsson, J.R. Baena and B. Lendl in Baba, Y. et al. (eds) *Micro Total Analysis Systems 2002*; Kluwer Academic Publishers: Dordrecht, The Netherlands, 2002; Vol. 1, pp 58-61
- „On-line mid-IR (quantum cascade laser and FTIR spectrometric) detection in capillary based separation systems"  
B. Lendl, M. Kölhed, P. Hinsmann, M. Haberkorn, P. Svasek and B. Karlberg in Baba, Y. et al. (eds) *Micro Total Analysis Systems 2002*; Kluwer Academic Publishers: Dordrecht, The Netherlands, 2002; Vol. J, pp 599-601

### Posters & Lectures:

*ICFIA99, June 1999, Prague, Czech Republic:*

- **Monitoring Enzyme Reactions In-Situ using SIA-FTIR**  
M. Haberkorn, R. Schindler and B. Lendl

*ASCOS 99, September 1999, Neusiedl am See, Austria:*

- **Mid-IR Flow-Through Sensors for Chemical Analysis**  
M. Haberkorn

*Flow Analysis VIII, June 2000, Warsaw, Poland:*

- **A Micro-Machined Multi-Sheath-Flow Mixer for Time Resolved FTIR Spectroscopy of Chemical Reactions in Solution**  
B. Lendl, P. Hinsmann, M. Haberkorn, J. Frank and P. Svasek
- **FTIR Flow-Through Sensors for Organic Acids, Metal Cations and Enzyme Substrates**  
M. Haberkorn, R. Schindler, A. Perez-Ponce and B. Lendl
- **Analysis of Methylmalonic Acid in Urine with Sequential Injection Analysis (SLA) - FTIR Spectroscopy**  
A.P.J.A. Markus, M. Haberkorn, B. Lendl and H.L. Williams

*ICAVS-1, August 2001, Turku, Finland:*

- **Quantum Cascade Laser as a Powerful Mid-IR Light Source for Sequential Flow Analysis**  
M. Kölhed, V. Pustogov, M. Haberkorn, J. Frank, B. Mizaikoff, B. Karlberg and B. Lendl
- **Interfacing HPLC to FTIR using a Piezoactuated Flow-Through Microdispenser**  
(Poster & Presentation)  
M. Haberkorn  
*Awarded "Best Young Scientist Presentation"*

*Advances in Analytical Separation Science, June 2002, Pörtlach, Austria:*

- **A novel HPLC-FTIR Interface based on a Piezoactuated Flow-Through Microdispenser**  
M. Haberkorn, J. Frank, J. Nilsson, T. Laurell and B. Lendl

*6<sup>th</sup> Euroconference on Environmental Analytical Chemistry, October 2002, Erperheide, Belgium:*

- **A new experimental setup for monitoring acoustically levitated sample droplets using FT-Raman spectroscopy**  
N. Leopold, M. Haberkorn, T. Laurell, J. Nilsson, J.R. Baena and B. Lendl

*6<sup>th</sup> International Symposium on Micro Total Analysis Systems, November 2002, Nara, Japan:*

- **On-line mid-IR (quantum cascade laser and FTIR spectrometric) detection in capillary based separation systems**  
B. Lendl, M. Kölhed, P. Hinsmann, M. Haberkorn, P. Svasek and B. Karlberg

### **Industrial Experience:**

<i>Coca-Cola Computer Services</i> (Vienna, Austria): Programming	Aug. 1991
<i>Billa</i> (Wiener Neudorf, Austria): Finance Administration	Aug. 1992
<i>Coca-Cola Company</i> (Vienna, Austria): Facilities Management	Aug. 1993 - Apr. 1999

### **Additional Assets:**

Experienced in clean room work: Lithography, microstructuring of silicon and quantum cascade laser material (AlGaAs)

Experienced in designing electronics and programming software for Computer Controlled Device Operation.

Experienced in Computer Installation and Maintenance, as well as in working with MS Windows based software (especially MS Office applications) and OS/2.

Experienced in programming MS Visual Basic 6.0.

Experience with AutoCAD.